Non-Stoichiometric Curing Effects on Mechanical Behaviors of Nano-Silica Particulate-Reinforced Epoxy Composites

June, 2014

DOCTOR OF ENGINEERING

Markus Karamoy Umboh

TOYOHASHI UNIVERSITY OF TECHNOLIOGY

ABSTRACT

The non-stoichiometric curing effects on mechanical properties of nano-silica particulate-reinforced epoxy composites were clarified experimentally to consider the interaction effects between nano-particles and network structures in matrix resin. The matrixes were prepared by curing with an excessive mixture of diglycidyl ether of bisphenol A type epoxy resin as the curing agent for the stoichiometric condition. The volume fraction of the silica particles with a median diameter of 240 nm was constantly 0.2 for every composite. The crosslinking densities and glass transition temperatures of the neat epoxy resins were identified from thermo-viscoelastic properties measured by dynamic mechanical analysis. The glass transition temperatures, the bending strengths, and the fracture toughnesses were found to sensitive to the crosslinking densities but the compressive yield stresses approximately did not affect to the crosslinking densities. The interactions between the nano-particles and the network structures reduce the glass transition temperatures and improve the compressive yield stresses, the bending strengths and the fracture toughnesses in high crosslinking densities. The bending strengths, the compressive yield stresses and the fracture toughnesses were higher for composites than those of the neat epoxy resins, because existence of the nano-silica particles encumbered the entanglements of the molecular chains and the deformations in the matrix resins having fine network structures with high crosslinking densities.

Keywords

Mechanical properties, Nanocomposite, Epoxy resin, Crosslinking density, Bending strength, Glass transition temperature, Thermo-viscoelastic properties, Fracture toughness, Compressive yield stress.

ACKNOWLEDGEMENTS

I would like to express my gratitude to my advisor, Professor Tadaharu Adachi for his guidance and encouragement throughout this study. Without his patience and support, this study would be a great deal more difficult. He is like a Father for me. He gave me an advice: “Actually what you get after getting the degree is not the degree but mental toughness”. Many thanks go to Professor Shozo Kawamura and Professor Masakazu Kobayashi for serving as my committee.

I would like to thank Dr. Masahiro Higuchi, Mr. Kouzo Oishi and Mr. Takeo Kyohei who gave me a helpful advice not only in research problems but also in lots of experiments. Furthermore, my study and life in Toyohashi-Japan will never be warm, enjoyable and memorable without guys who are undergraduate and graduate students in the ADACHI KEN.

I should like to thank The Lighthouse Christian Church-Toyohashi Church in Japan for warm heart that I never expected away from home and family, and my daughters Claisty Marsha Umboh and Haimi Elizabeth Umboh and also my wife for continued love and support. Also, I should not miss to mention several friends at Indonesia whose care and support are overwhelmed.

Finally, I am indebted to my mother and my sister, who love and care me unconditionally. Their prayers and faith to God in the name of Jesus Christ pushed me through all the difficult times, and inspired me to pursue not my dream but God’s glory.

“Blessed is the man who endures temptation; for when he has been approved, he will receive the crown of life which the God has promised to those who love Him “– James 1:12

TABLE OF CONTENTS

CHAPTER 1 INTRODUCTION

CHAPTER 2 THERMO-VISCOELASTIC AND BENDING BEHAVIORS

CHAPTER 3 COMPRESSION BEHAVIOR

CHAPTER 4 FRACTURE BEHAVIOR

CHAPTER 5 CONCLUSIONS

APPENDIXES

LIST OF TABLES

LIST OF FIGURES

NOTATION

E_B	Bending elastic modulus
E'	Storage modulus
E''	Loss modulus
$EEWR$	Epoxy equivalent weigh ratio
ε	Strain
$\dot{\varepsilon}(t)$	Strain rate
K_{IC}	Fracture toughness
n	Crosslinking density
T	Temperature
T_{g}	Glass transition temperature
σ	Stress
σ_B	Bending strength
φ_{max}	Maximum packing fraction
$\tan\,\delta$	Loss tan (Damping factor)

CHAPTER 1
INTRODUCTION

1.1 Epoxy Resins

Epoxy resins as a class of thermoset materials are one of the most versatile polymers under today. Epoxy resin was discovered in 1938 by Pierre Castan, a chemist in Switzerland. Since the first commercial production of epoxy resin occurred simultaneously in Europe and in the United States in the late 1930s and early 1940s, the consumption of epoxy resins has grown gradually almost every year [1.1].

Epoxy resins are used extensively in structural and special composites applications because of better performances such as excellent chemical resistance, excellent adhesion to various substrates, good heat and electrical resistances, low shrinkage, and good mechanical properties. These desirable properties result in epoxy resins having wide markets in industry, packaging, aerospace, construction, etc. Remarkable applications are bonding and adhesives, protective coatings, electrical laminates, apparel finishes, fibre reinforced plastics, flooring and paving, and composite pipes. Recently, the application of fibre reinforced epoxy composites can also be found in biomedical engineering. [1.2–1.4].

In general, epoxy resin contains one or more oxirane structures, three-membered rings containing two carbon atoms and one oxygen atom, namely the epoxide group or epoxy ring at the end(s) of the molecule and a few repeated units in the middle of the molecule. The epoxide group or epoxy ring is given in Fig. 1.1. Epoxy resins can chemically have one or more 1,2-epoxy groups and can convert to thermosetting materials. Since the 1930's when the preparation of epoxy resins was patented, many types of new epoxy resins have been developed from epoxides. Epoxy resins exist either as liquids with lower viscosity or as solids depending on their molecular weights. Tanaka [1.5] gave a complete list of epoxides and discussed their properties and preparation.

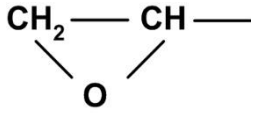

Fig. 1-1 Epoxide Group [1.6]

The resin that is the basis for most our epoxy formulations is the diglycidol ether of bisphenol A (DGEBA). Bisphenol A is the chemical product made from chemically combining two phenols with one acetone. Unreacted acetone and phenol are stripped from the bisphenol A which is then reacted with a material called epichlorohydrin. This reaction sticks the two (di) glycidyl groups on ends of the bisphenol A molecule. The resultant product is the diglycidyl ether of bisphenol A, or the basic epoxy resin. DGEBA accounts for more than 75% of the epoxy resin used in industrial applications, because it has excellent toughness, adhesiveness and chemical resistance. Epoxy resins such as DGEBA have the ability to react and cross-link by means of the epoxide group on each end to generate three-dimensional networks, which provide cured epoxy resins. The chemical formula of the DGEBA used in this research is shown in Fig. 1.2. Other types of epoxy resins are glycidyl ether of novolac resins, phenoxy epoxy resins, and (cyclo) aliphatic epoxy resins. Glycidyl ether of novolac resins, and phenoxy epoxy resins usually have high viscosity and better high temperatures properties while (cyclo) aliphatic epoxy resins have low viscosity and low glass transition temperatures.

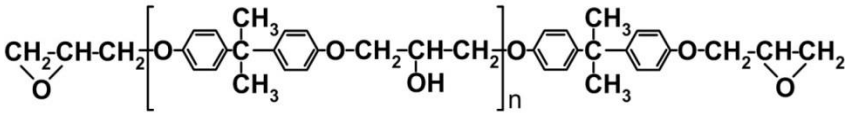

Fig. 1.2 Bisphenol A type (DGEBA) [1.6]

The epoxy resins will react with a large number of chemical species called curing agents or curatives or hardeners. During the ring opening reaction in epoxide groups, the active epoxide groups in the uncured epoxy can respond with many curing agents that contain hydroxyl, carboxyl, amine, and amino groups to obtain the different epoxy systems with a large range of chemical and physical properties. Selection of the curing agents determines characteristics of cured epoxy resins because they relate to the curing kinetics reaction rate, gel time, degree of cure, viscosity, curing cycle, and the final properties of the cured products. The most commonly used chemical classes of curing agents are amines, amine derivatives, and acid anhydrides. Among these, acid anhydride curing provides epoxy resins with a high glass transition temperature and excellent mechanical properties, especially at high temperature. In addition, the shrinkage caused by curing is small. Therefore, the chemical formula of the Methytetrahydrophthalic anhydride (MeTHPA) used in this research as the acid anhydride curing agent is shown in Fig. 1.3.

The anhydrides are sometimes used alone, but they are more frequently used in combination with such basic compounds such as tertiary amine catalysts to accelerate the curing. The chemical formula of the 2,4,6-Tris (dimethyl amino-methyl) phenol used in this research as the tertiary amine catalysts is shown in Fig. 1.4.

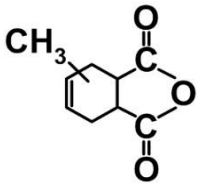

Fig. 1.3 Methytetrahydrophthalic anhydride (MeTHPA) [1.6]

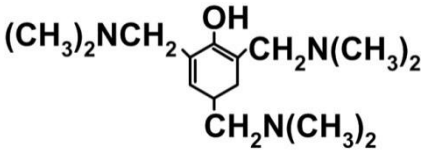

Fig. 1.4 2,4,6-Tris (dimethyl amino-methyl) phenol [1.6]

The curing reaction of epoxide is the process by which one or more kinds of reactants, i.e., an epoxide and one or more curing agents with or without the catalysts are transformed from low-molecular-weight to a highly crosslinked structure. As mentioned earlier, the epoxy resin contains one or more 1, 2-epoxide groups. Because an oxygen atom has a high electronegativity, the chemical bonds between oxygen and carbon atoms in the 1, 2-epoxide groups are the polar bonds, in which the oxygen atom becomes partially negative, whereas the carbon atoms become partially positive. Because the epoxide ring is strained (unstable), and polar groups (nucleophiles) can attack it, the epoxy group is easily broken. It can react with both nucleophilic curing reagents and electrophilic curing agents. The curing reaction is the repeated process of the ringopening reaction of epoxides, adding molecules and producing a higher molecular weight and finally resulting in a three-dimensional structure. The chemical structures of the epoxides have an important effect on the curing reactions.

Theoretically, a crosslinked thermoset polymer structure is obtained when equimolar quantities of resin and curing agent are combined. However, in practical applications, epoxy formulations are optimized for performance rather than to complete stoichiometric cures. The stoichiometric relationship between curing agents and resins has a great effect on the physical and the mechanical properties of the epoxy resin [1.7]. The different types of curing agents required addressing stoichiometric balance between the reacting species. A key parameter that determines resin suitability for use is the epoxy equivalent weight (EEW) which can be defined as the weight of the resin per epoxide group. The equivalent weight of a polymer is used to calculate the stoichiometric ratio between the epoxy resin and curing agent in order to optimize the cured properties.

Figure 1.5 shows a schematic diagram of a polyaddition reaction of an acid anhydride curing agent and a bisphenol A type epoxy resin according stoichiometric ratio. Figure 1.5(a) shows the epoxy groups of the epoxide resin monomer and the acid anhydride groups of the curing agent monomer. The epoxide resin monomer reacts with curing agent monomer to result a liner molecular chain shown in Fig. 1.5(b). After a liner molecular chain grows to form a branch structure when the new monomer of epoxide resin and curing agent join shown in Fig. 1.5(c), two branches merge to result cross-linked structure shown in Fig. 1.5(d). Finally, all polymer chains connect in cross-linked structure to produce complete network structures.

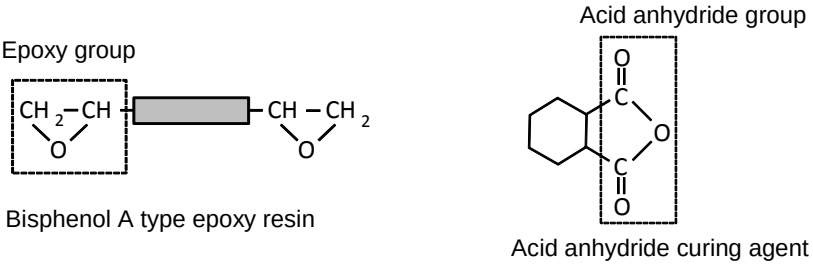

(a) Monomer

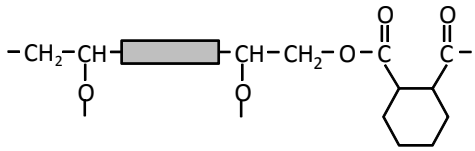

(b) Linear growth stage

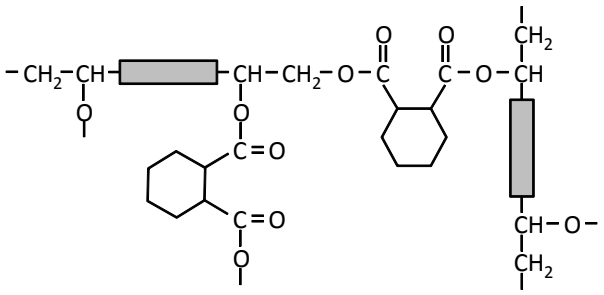

(c) Branch growth stage

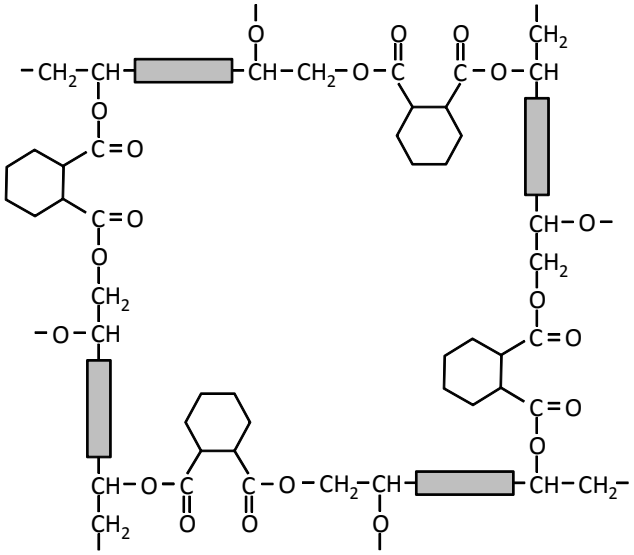

(d) Cross-linked structure formation stage

Fig. 1.5 A schematic diagram of a polyaddition reaction of an acid anhydride curing agent and a bisphenol A type epoxy resin [1.8, 1.9].

1.2. Particulate Reinforced Epoxy Composites

1.2.1. Inorganic particulate reinforced epoxy composites

Particulate reinforced polymer composites are defined as materials made up of two components and consisting of two phases such as a continuous polymer matrix phase and a discontinuous organic-inorganic reinforcement phase.

Polymer materials are in the broadest sense referring to that they are relatively brittle and have lower resistance to crack propagation even after curing process. For this reason most of the studies has been investigated to modify the polymer structure in order to improve its fracture toughness, flexibility, impact strength and other mechanical properties by reinforcing with highly stiffer inorganic particles, which have a wide dimensions from the macro-scale to nano-scale ranges [1.10].

The various types of reinforcing particles are classified by several ways, such as based on the origin: natural or synthetic, chemical composition: organic or inorganic, mean dimension: macro- to nano-size, and based on the shape: spherical or irregular, aspect ratio.

Generally, many of the reinforcements used for polymer composites are inorganic spherical particles of low aspect ratio [1.11]. The typical commercially available particles used as the reinforcement are as follows [1.12]:

1. *Calcium carbonate*: lowest cost particle and mostly used in polyvinylchloride (PVC), polypropylene (PP) and polyamides (PA). Because of reducing polymer's shrinkage during molding and curing, it is a usual particle in low shrink reinforced polyester sheet molding components. Even with a low aspect ratio and a fatty acids coating, resulting in a limited modulus increase in the composite and improvements in particle dispersion.
2. *Kaolin* (*Clay*): when used as a common particle in thermoplastics, clay is referred mainly to kaolinite. The particle is non-abrasive, chemical resisting and has relatively high surface area which results in high viscosities in liquid polymers. With various surface treatments, it is available to provide outstanding water resistance and electrical properties in a variety of polymers.
3. *Silica:* over 20 distinct phases of silica and produced in several synthetic ways. Low aspect ratio and usually spherical particle. Very high surface area and so fine in particle size provide a thixotropic effect and enhance properties and hardness in cured polymers.

Recently, several scientific and technical researches concerning particulate reinforced polymer composites have been conducted, because of that the possibilities with a wide range of applicative properties are numerous. There are many reasons for using the particulate reinforced polymer composites rather than the pure polymer materials. The initial reason for the use of various particles to reinforcing polymer materials is to reduce the cost, but mainly it is driven by the enhancements in mechanical and other properties of the composite. Some of these primary reasons are as follows [1.13–1.17]:

1. Increasing stiffness and/or strength.
2. Increasing heat distortion temperature (HDT).
3. Increasing toughness and/or impact strength.
4. Increasing dimensional stability due to the reduced coefficient of thermal expansion.
5. Increasing mechanical damping, and modifying electrical properties.
6. Reduced flammability, and permeability to gases and liquids because of the increased barrier property.

However, some disadvantages which should be reduced are also found.

1. Increased viscosity before curing, resulting in more difficult to manufacture processing.
2. Usually lost in transparency properties.
3. Sometimes reduced toughness at high volume of the reinforcement, compared to a tough polymers

From the perspective of described advantages, the particulate reinforced polymer composites are currently used in numerous electric and electronic applications as packaging or encapsulating materials, and have a wide range of applications in sensors, nanoelectronic devices, mobile phone, portable computers and batteries as structure materials [1.18–1.21].

1.2.2. Silica particles reinforced epoxy composites

The main drawback of the epoxies is brittleness, which gives limitation to extend engineering applications. Thus, numerous studies have been suggested the addition of silica particles in order to improve toughness properties of the epoxy without associated decrease of thermal and other important mechanical properties such as the strength and modulus [1.22]. Because the silica particle has the diversity of shape and size, and competitive cost compared to other reinforcements, as well as outstanding chemical, mechanical and thermal properties.

Silica particles reinforced epoxy composites described mainly in this study are extensively used as a molding compound in electronic device packages, which role to ensure the electrical insulation of the silicon chip and of circuit bonding wires upon handling in any circumstances [1.23]. Figure 1.6 shows the schematic illustration of packaging system of electronic device, and the general component ratio of packaging material is given in Fig. 1.7. The principal reason for using this composites for such applications is because of the addition of silica particle can consist in the improvement of the electrical properties, thermal dimensional stability and adhesion, etc. but it also can be an enhancement of their mechanical properties. Furthermore, shrinkage in size and other complexities of design for electronic device recently lead these package materials to have a high reliability performance which can be remarkably developed by increased toughness and thermal resistance of the silica particles reinforced epoxy composites [1.24, 1.25].

The properties of silica particulate reinforced epoxy composites are mainly governed by the intrinsic properties of the silica and epoxy, geometry of the reinforcing silica particles, morphology of the epoxy matrix, and also the interface properties between silica particles and epoxy matrix. Therefore, the desired properties of the composites could be obtained by varying some of these factors. In opposition, a variety of improved properties could be determined through modification of these factors [1.26].

Several researches have been focused on the particle effects to improve the properties of the composites. Previous researches concerning properties of silica particles reinforced epoxy composites are surveyed below.

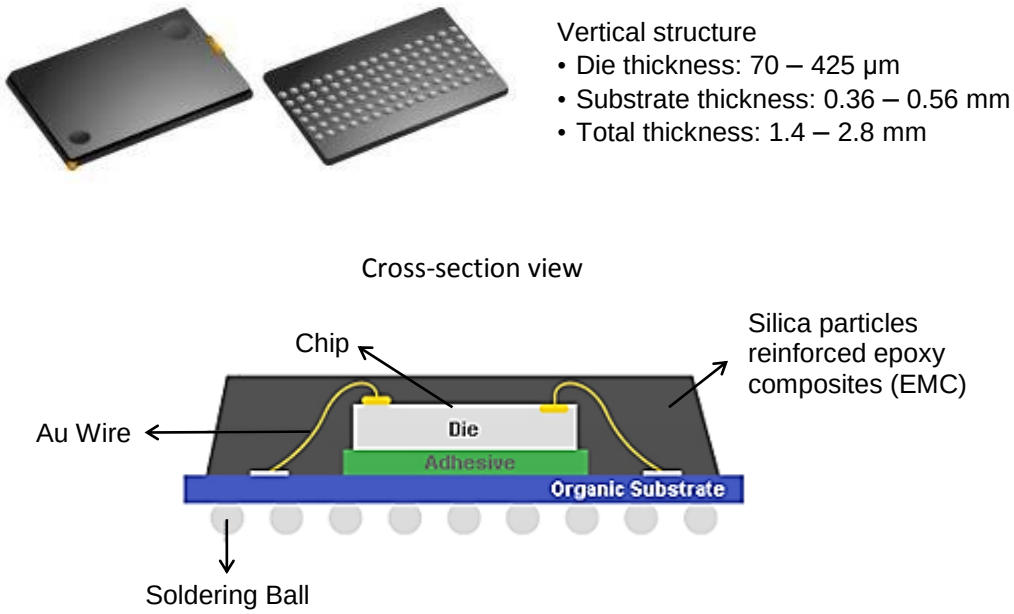

Fig. 1.6 Schematic diagram of semiconductor packaging system [1.27]

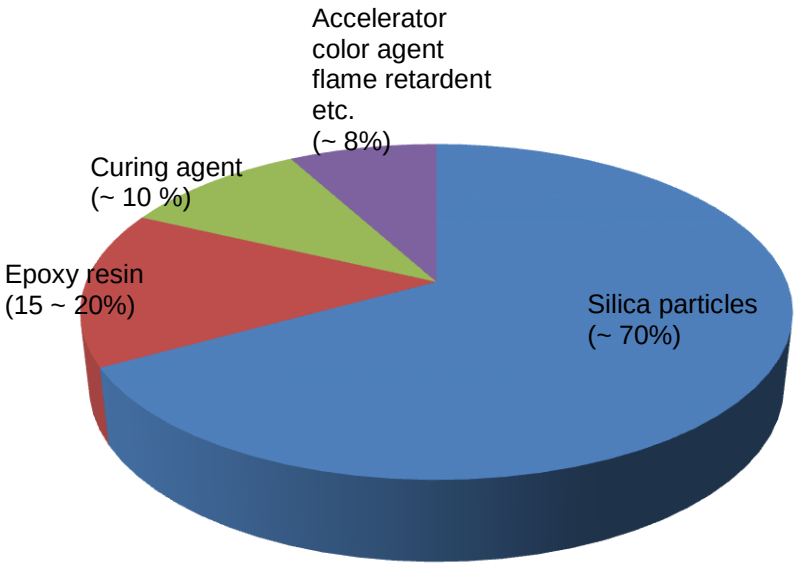

Fig. 1.7 General component ratio of packaging material [1.28]

(a) Mechanical properties

Several researcher reported mechanical properties of epoxy composites reinforced with silica particles having different shape, size and volume fraction.

Kausch et al. [1.29] reported deformation and fracture mechanisms in filled polymers, and proposed three types of fracture modes in highly particulate reinforced epoxy composites: rapid brittle fracture due to single particle debonding, crack propagation between debonded particle zones, crack propagation through coalescence of voids. Kishimoto et al. [1.30] and Adachi et al. [1.31] studied the Mode I and mixed-mode fracture behavior of silica particles reinforced epoxide resin (varied by volume fraction of silica particles) at room and high temperatures. The result showed the fracture behavior was relatively dependent on temperature and particle volume, and the fracture toughness was predicted for a wide range of temperatures by the thermo-viscoelastic characteristics.

Spanoudakis and Young [1.32, 1.33] reported the effect of spherical shaped silica particles from 4.5 to 62 μm filled epoxy composites on modulus and fracture toughness. For lower volume fractions (10 – 18 vol.%), the modulus was almost independent of particle size but for higher volume fractions (30 – 46 vol.%), there was a slight decrease in modulus with increasing particle size. The fracture properties strongly depended on particle size and volume contributing to the differences in crack propagation and interaction of particles with matrixes. Nakamura et al. [1.34–1.38] discussed the effect of spherical and irregular shaped silica particles from 2 to 30 μm on modulus, flexural strength and fracture toughness. It was found that fracture toughness was slightly higher for irregular shaped particles but other properties mostly depended on the volume fraction for a given particle size. Yaguchi et al. [1.39] observed that the fracture toughness increased with increasing volume fraction and with irregularly-shaped particles for highly silica particulate-filled epoxy resins. Yamamoto et al. [1.40] and Niinomi et al. [1.41] also found the remarkable increases in tensile properties and impact fatigue properties for the irregular crystalline silica particulate-filled epoxy composites.

McMurray et al. [1.42] showed that the flexural creep strength and fatigue properties of crystalline silica particulate-filled epoxy resins were dependent on the time and temperature. Koh et al. [1.43] investigated the fracture toughness and failure mechanisms of epoxy composites filled with silica particles (2 – 47 μm), and found a significant effects of temperature and loading rate on the impact fracture toughness. Zheng et al. [1.44] reported that the impact strength of epoxy composites increased

with the silica content up to about 2 vol.%, and then decreased. The decrease of the impact strength at high silica content was attributed to the increasing particle agglomeration.

Monette et al. [1.45] concluded that the reinforcement efficiency in epoxy composites significantly increased when decreasing the particle size. The Young's modulus not only depends on the volume fraction but also on the particle size. Wang et al. [1.46] observed that the increase in Young's modulus was directly proportional to silica particles content at room temperature, but the modulus and yield stress were not varied with the silica volume fraction at high temperature. Fiedler et al. [1.47] showed the Young's modulus for any silica content (up to 1 vol.%) and surface modification decreased compared to the neat epoxy, but the toughness and the strain to failure increased as the silica content increased up to about 0.5 vol.%.

Anderson et al. [1.48] reported that remarkable increase of fracture toughness showed at the silica content as low as 0.5 vol.%. Imanaka et al. [1.49] studied the effect of silica particle size (mean sizes in the range of 6 – 30 μm) and particle/matrix adhesion on the fracture toughness, and concluded that fracture toughness and interfacial strength depended on the particle size and content, respectively. Young et al. [1.50] and Kobayashi et al. [1.51] showed that the mechanical properties of silica particulate-filled epoxy composites resulted from the complex interfacial interactions between the particles and the matrix. Furthermore, Swanson et al. [1.52] observed the strong effects of shape and size of silica particles on the fracture strength of the epoxy resin.

Kawamura et al. [1.53] found the fracture toughness of silica particulate-filled epoxide resins (containing 70 wt.% of silica particles) slightly increased with moisture absorption while the bonding strength tended to decrease, and concluded that the discrepancy in strength and fracture toughness could be attributable to differences in the three-dimensional stress sate of the materials. Yoshida et al. [1.54] studied the mechanical properties of tensile and bending deformations of silica particulate-filled epoxy composites, and found that the adhesive effects between the particles and the matrix could be expressed as the square root of boiling time in water but the mechanical properties decreased with the water absorption time. Boonyapookana et al. [1.55] discussed fatigue crack growth behavior of silica particulate reinforced epoxy resin composite where the average particle size was 20 – 30 μm. They found that the present silica particle reinforcement significantly contributed to enhance the fatigue crack growth resistance.

Currently, the particle size is being decreased to below the micrometer level to form the nanocomposites with superior mechanical properties. The effect of the size and volume fraction of the particle, namely, the interaction effect between the particles and the epoxy matrix, has been study to determine how the properties of the nanocomposites can be improved. Adachi et al. [1.56–1.58] discussed the effect of particles diameter and volume fraction on fracture toughness of spherical-silica-particle-filled epoxy composites. The particle diameters ranged from 240 nm to 1.56 μm and the volume fraction ranged from 0 to 0.35. They found that the fracture toughness increased drastically as the volume fraction increased and the particles diameters decreased as shown in Fig. 1.8.

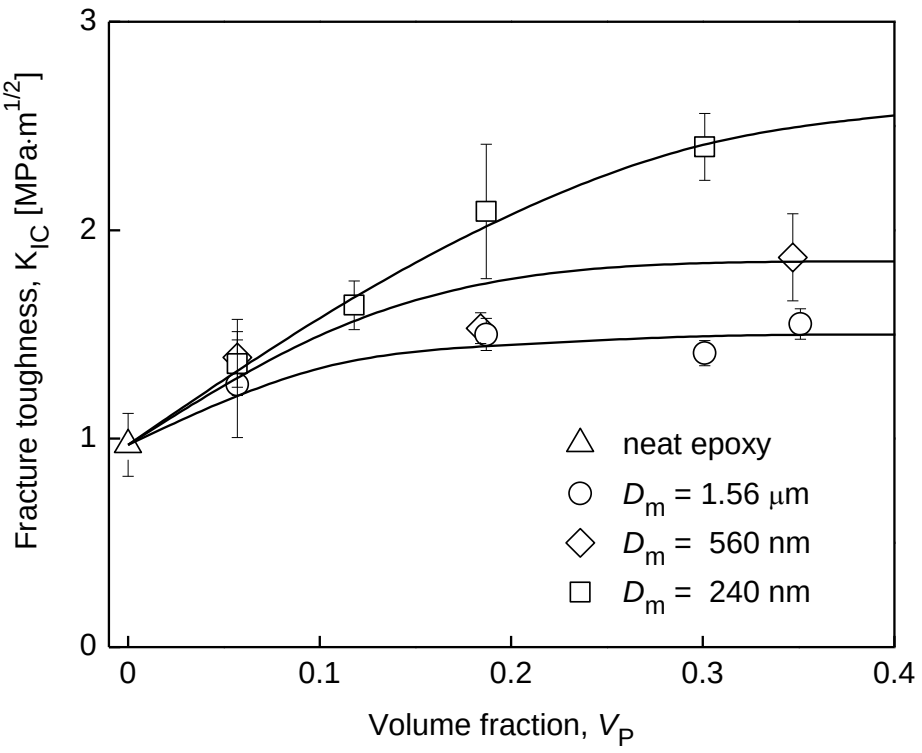

Fig. 1.8 Relation between fracture toughness and volume fraction of particle [1.56]

Kwon et al. [1.59–1.63] discussed the dispersion effects of nano (240 nm)- and micro (1.56 μm)-scale silica particles on mechanical properties of the composites. They reported that the bidispersion of nano- and micro-particles enabled tailoring composites strength and toughness due to more interactions between particles and the matrix that are governed by interparticle distance and particle packing. They also found that two-particle composition enabled significant increase in mechanical properties of the composite for a given constant volume fraction (V_P = 0.30) while maintaining a lower viscosity compared to single particle composites.

Olhero et al. [1.64] shown that the rheological behavior strongly depended on the particle size distribution. Preghenella et al. [1.65, 1.66] observed the thermo-mechanical properties of nanocomposites, and found that the huge viscosity increased in epoxy resins induced by the addition of nano-scale silica particles. By using atomic acoustic microscopy, they also confirmed that the mechanical properties strongly governed by the distribution of nano-particles.

Jumahat et al. [1.67] showed the addition of 25 wt.% nanosilica enhanced the tensile modulus and strength of about 38% and 24%, respectively, compared to the neat polymer. Veena et al. [1.68] found that the ultimate tensile strength, hardness, and electrical resistivity increased with 10 wt.% of nanoparticle with distribution range of 14 – 21 nm and after that deceased. Zheng et al. [1.69] discussed the influences of nano-silica particles (20 nm) in epoxy resin on the mechanical properties in terms of non-notched charpy impact strength and flexural strength. The results indicated that nano-silica particles could effectively increase both the toughness and strength of epoxy resin at low loadings (no more than 3 wt.%) when nano-silica particles could be well dispersed in epoxy matrix without any great aggregations.

Devaprakasam et al. [1.70] evaluated energy dissipation and failure mechanics of silica nano- and micro-particle-filled polymer composite, and explained that nanocomposite showed better tribo-mechanical performance compared with that of the micro-particle-filled composite. Jajam et al. [1.71] discussed nano (20 nm)- vs. micro (35 μm)-size filler and loading-rate effects on mode-I crack initiation and crack growth behaviors of silica filled epoxy. The fracture tests showed fracture toughness enhancement in case of nanocomposites relative to micro-particle filled ones, and the dynamic crack-initiation toughness was consistently higher for micro-particle filled composites relative to the nano-filler counterparts.

Chen et al. [1.72] found that increases of 25% in tensile modulus and 30% in fracture toughness were obtained for epoxy–nanocomposite resins filled with 12 nm spherical silica particles on loadings less than 10 wt%. Battistella et al. [1.73] discussed fracture, fatigue and tensile strength of silica/epoxy nanocomposites for the average particle diameter of 7 nm. The fracture toughness increased of 54% at 0.5 vol.% of silica particles and also fatigue crack growth resistance, but not so significant. On the other hand, the ultimate tensile strength was not significantly affected by the silica particles. Yao et al. [1.74] found that the nanocomposite with 3 wt.% nano-silica (average diameter 90 nm) had higher fracture toughness and larger deformation resisting capability than other nanocomposites weight contents. Ragosta et al. [1.75] showed that the addition of silica nanoparticles (10 – 15 nm) up to 10 wt.% carried about a considerable enhancement in fracture toughness and an increase in the critical crack length for the onset of crack propagation. Zhang et al [1.76] confirmed that the homogeneously distributed of silica nanoparticles with an average diameter of 25 nm were able to improve the static/dynamic modulus, microhardness, and fracture toughness of the nanocomposites with increasing silica content up to 14 vol.% (23 wt.%)

Zhang et al. [1.77] discussed fracture behaviours of silica nanoparticle-filled epoxy at different temperatures (296 K and 353 K) where the average diameter of silica nanoparticles was about 25 nm. The stiffness, strength and toughness were improved simultaneously and a strong particle–matrix adhesion was found by fractography analysis. Deng S. et al. [1.78] discussed fracture behaviours of nano-silica modified epoxies at low and elevated temperatures. Fracture toughness of the nano-silica (20 nm) modified epoxies was clearly increased at 296 K and 323 K, but the role of nano-silica particles in enhancing the fracture toughness became less pronounced at 273 K and 223 K and disappeared at 343 K.

Several researchers clarified two different diameters in nanometers. Chen et al. [1.79] discussed mechanical and fracture behavior of epoxy resin with 12 nm and 100 nm silica particles. They found that the tensile strength of all composites was independent of particle size and weight fraction, which was attributed to strong particle bonding and failure initiation in the matrix. They also reported that compared with neat epoxy, the fracture toughness of epoxy composites increased by 35% for 15 wt.% silica loading. Liang et al. [1.80] discussed toughening mechanisms in epoxy–silica nanocomposites with different average particle sizes (20 nm and 80 nm in diameter).

They observed that the fracture toughness of epoxy–silica nanocomposites increased as the nanosilica volume fraction increased up to 17.4 vol.%.

Moreover, several researchers clarified three different diameters in nano scale. Dittanet P. et al [1.81] and Bray et al [1.82] discussed the effect of volume fraction and particle size of the toughening of epoxy polymers reinforced three different diameters (23, 74 and 170 nm) of silica nanoparticles. They found that the fracture toughness increased significantly with the addition of silica nanoparticles and with increasing the concentration of silica nanoparticles, but no significant effects of particle size were found on the measured value of toughness. Zamanian et al. [1.83] discussed an epoxy resin was modified by the addition of different nanosilica particles where the diameters of silica particles were 12, 20, and 40 nm. They clarified that Young's modulus increased and the glass transition temperature was unchanged. The fracture energy increased to about 620 J/m^2 for the epoxy with 3.17 vol.% of 12 nm diameter nanoparticles.

The other researcher modified the structure/property of epoxy polymers and clarified the properties of composites. Hsieh et al. [1.84] clarified the mechanical and fracture properties of four different epoxy polymers containing 0, 10 and 20 wt.% of well-dispersed silica nanoparticles. They found that for any given epoxy polymer, their Young's modulus steadily increased as the volume fraction of the silica nanoparticles was increased. The presence of silica nanoparticles always led to an increase in the toughness of the epoxy polymer. However, to what extent a given epoxy polymer could be so toughened was related to structure/property relationships which were governed by the values of glass transition temperature and molecular weight between cross-links of the epoxy polymer, and the adhesion acting at the silica nanoparticle/epoxy-polymer interface.

Based on the available literatures, it can be concluded that mechanical properties of silica particles reinforced epoxy composites in general appeared to exhibit the advantages of increasing either the stiffness or the fracture toughness as silica particles reinforced. The mechanical properties also shown enhancement in case of nanocomposites relative to micro-particle filled. Consequently, these properties were well improved by a suitable volume and size reduction of silica particles, and it resulted that an optimal microstructure of silica particles should be proposed for the reinforcement of epoxy composites.

(b) Thermo-viscoelastic properties

Several papers are published to research the thermo-viscoelastic properties of epoxy composites reinforced with silica particles having different shape, size and volume fraction.

Li et al. [1.85], Unsworth et al. [1.86,1.87] and Kim et al. [1.88] found that the peak of dynamic loss factor (tan δ) and dynamic storage and loss modulus changed considerably during the glass transition, and the dynamic mechanical properties were very sensitive to the structural changes in the silica particulate-filled epoxy composites due to the thermal degradation. Goyanes et al. [1.89] studied the dynamic mechanical properties of silica particulate-filled epoxy composites, and found that the storage modulus increased strongly with increasing the silica content but this increase was more important at the rubbery state than at the glassy state. Kwon et al [1.90] discussed the effect of compositions of two sizes of spherical silica particles, 0.24 and 1.56 μm, at a fixed volume fraction (V_P = 0.30) on the thermo-viscoelastic properties of epoxy composites. The thermo-viscoelastic properties of the two-particle reinforced composites are dependent on temperature, and the composition ratio of the particles, and they are also governed by the maximum packing fraction of particles which is strongly related to the particle size distribution.

Kang et al. [1.91] investigated the surface modification effect of the silica particles (mean diameter of 400 nm) on the viscoelastic properties of the epoxy resin, and found an increase of glass transition temperature and a decrease of coefficient of thermal expansion as the silica content increased, but observed a decrease in glass transition temperature when the absence of reaction at the interfaces due to the surface modification. Sun et al. [1.92] studied that the nano- and micro-particles effect on the relaxation behavior of an epoxy resin, and found that the nano-silica particles increased slightly the glass transition temperature of the epoxy, but the particle content became higher than 5 – 10 wt.% and then the glass transition temperature decreased. Sangermano et al. [1.93] found a slight increase of glass transition temperature with an increase of silica particles content, and concluded it resulted from the restriction of the segmental motion of the epoxy by increasing silica particles. Barabanova et al. [1.94] clarified the glass transition temperatures of nanocomposites where the silica particle dimensions were 10 – 15 nm. They found that the glass transition temperatures of nanocomposites were 303 – 313 K higher than those of the neat epoxy resin.

An reinforcing silica particles played important role in order to improve the properties of epoxy composites, that are also an optimal microstructure of silica particles existed, and indeed interaction between silica particles and epoxy matrix in the thermo-viscoelastic and thermal properties reported by the researches especially for nanocomposites.

(c) Other properties

The following limited literature studies are published to broadly review the adhesive, tribological, and electrical properties of epoxy composites reinforced having different shape, size and volume fraction of silica particles.

Tishin et al. [1.95] investigated the particles effect on the adhesive properties of the epoxy as a function of the specific surface area and surface treatment of adding silica particles, and found the remarkable increased in adhesive and cohesive strength as the silica content was between 4 – 6 wt.%. Kinloch et al. [1.96] investigated the effect of silica particles (mean diameter of 20 nm) on the structural adhesive properties of the epoxy resin, and found the significant toughening of the epoxy with an increase in the adhesive fracture energy at silica content was 8 wt.%.

Xing et al. [1.97] discussed the wear behavior of epoxy matrix composites filled with uniform sized spherical silica particles in diameter of 120 and 510 nm. The wear test results showed that the spherical silica particles could improve the wear resistance of the epoxy matrix even though the content of the fillers was at a relatively low level (0.5 – 4.0 wt.%). Zhang et al. [1.98] studied the tribological properties of the epoxy composites filled with silica particles, and found that the wear rate and the fractional coefficient markedly increased with the surface treated nano-silica particles while no effect for the surface treated micro-particles. Wang et al [1.99] discussed the effect of nanoparticle content on the wear behavior of silica nanoparticle-reinforced composites correlated where it improved the wear resistance of nanocomposites. Veena et al. [1.100] clarified the tribological and electrical properties of epoxy composites filled with nano-sized silica particles with distribution range of 14 – 21 nm. They observed that 10 wt% loading of silica was very effective in reducing the wear loss and the dielectric strength, arc and track resistance increased with increase in filler loading (up to 15 wt%). With further increase of silica filler loading, the nanoparticles agglomerated and resulted in increase of the specific wear rate.

Akelah et al. [1.101], Friedrich et al. [1.102] and Yao et al. [1.103] reported a synergistic effect on the abrasion resistance, the impermeability to gas and moisture, and the structural characterization resulted from the addition of nano- and micro-silica particles.

The above literature surveys shown that reinforcing silica particles acted an important role in order to improve the adhesive, tribological, and electrical properties of epoxy nanocomposites, that are also an optimal microstructure of silica particles existed, and indeed interaction between silica particles and epoxy matrix was evidenced as a primary parameter for characterizing the properties.

1.3. Non-Stoichiometric Curing

1.3.1. Crosslinking network structure of thermoset

Based on the literature studies in Section 1.2.3, 1.2.4, and 1.2.5, the properties of silica particles reinforced epoxy composites in general appeared to exhibit the advantages of increasing the properties such as the stiffness or the fracture toughness as silica particles reinforced. In the case of nanocomposite, the interactions between silica particle and network structure of matrix resin increased highly because the nano-particles produced extremely large boundary surface created by decreasing of the interparticle distance, and also obtained unique internal structure in the composites. The interfacial interaction of the particles with the surrounding the matrix has a close relationship with the network morphology in the polymer matrix [1.104–1.106]. Therefore, the properties of nano-particle reinforced epoxy composites are considerably dependent not only on the particle geometry effect (size, shape, and specific surface or distribution) but also on the intrinsic properties of the epoxy matrix. Consequently, the optimal network morphology of matrix resin should be clarified to obtain excellent properties of composites.

In general, the network morphologies are characterized by the degree of cross-linking reaction, which are estimated from a variation of physical properties related to chemical reaction. Crosslinking density is one of the most important parameters for identifying the network morphology of matrix resins. Crosslinking density can be defined as the number of effective cross-link per unit volume of the thermoset material, in inverse relation to molecular weight between cross-link. Crosslinking density determines the properties of the cured resin, particularly the mechanical properties. Usually, a thermoset resin with high crosslinking density is harder but more brittle, while low density leads to increase flexibility, better impact strength, and higher elongation. Table 1.1 shows relationship of crosslinking density to polymers properties [1.107].

Tabel 1.1. Relationship of crosslinking density to polymers properties [1.107]

Increasing crosslinking density will cause decreasing	Increasing crosslinking density will cause increasing
Impact strength	Modulus
Elongation	Tensile strength
Fatigue properties	Hardness
Peel strength	Chemical resistance
Thermal shock resistance	Heat resistance
Coefficient of thermal expansion	Glass transition temperature
	Internal stress
	Brittleness

Several methods are obtained to modify the crosslinking densities of matrix network morphology, among others: modification of the resin or curing agent combination, modification of the cure process and modification of the resin or curing agent ratio in the reaction mixture. This last one is called non-stoichiometric curing method. The non-stoichiometric curing method can result the different crosslinking densities of epoxy network structures to optimize the properties of epoxy resins and composites. It provides different way of the modifying the network without modification of the chemical nature of polymer chains.

Three crosslinking network structures are formed by variation of epoxy/anhydride ratios of the epoxide resin monomer and acid anhydride based on non-stoichiometric curing method. The network structures are illustrated in Fig. 1.9. Figure I.9(a) expresses crosslinking network structures of stoichiometric curing between epoxy resin and acid anhydride. In this composition, the complete network structures can be resulted with maximum crosslinking density. Figure 1.9(b) shows crosslinking network structures of non-stoichiometric curing in case of epoxy resin excess. In this composition, incomplete network structures can be resulted with decreasing of crosslinking densities because the epoxide resin composition is surplus to produce unreacted parts of epoxy resin groups in cured epoxy resin. Figure 1.9(c) shows crosslinking network structures of non-stoichiometric curing in case of acid anhydride excess. In this composition, incomplete network structures can be resulted with decreasing of crosslinking densities because the curing agent composition is surplus to produce unreacted parts of acid anhydride groups in cured epoxy resin.

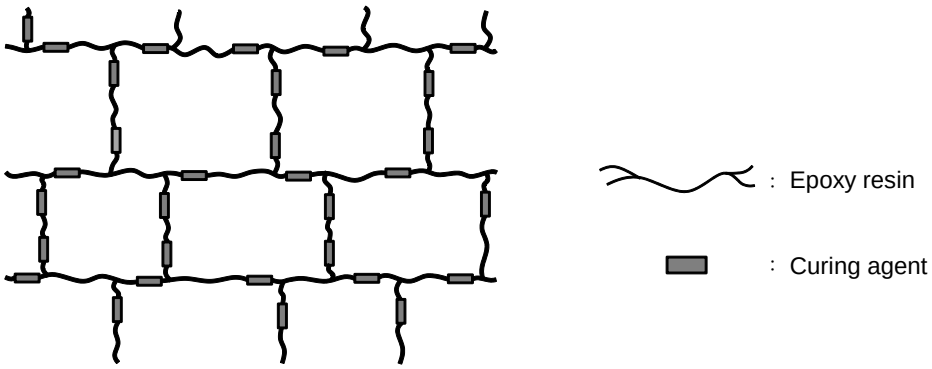

(a) Crosslinking network structures of stoichiometric curing between epoxy resin and acid anhydride.

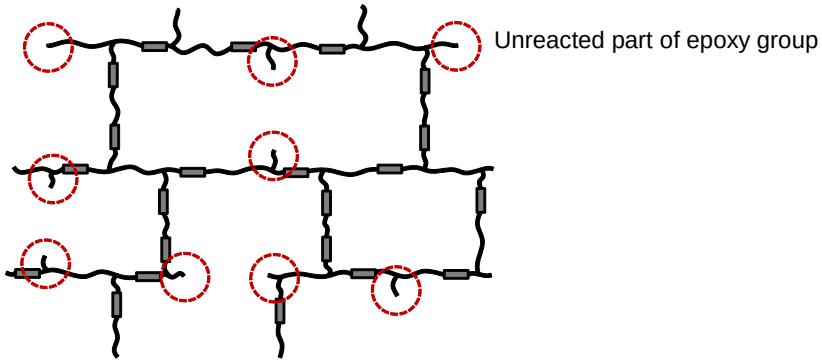

(b) Crosslinking network structures of non-stoichiometric curing in case of epoxy resin excess.

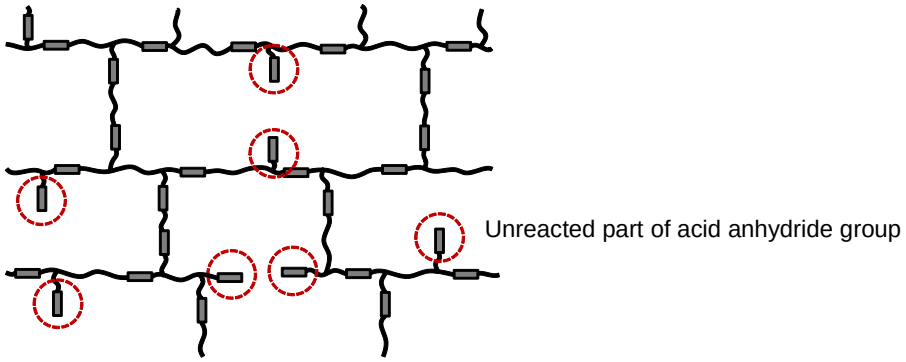

(c) Crosslinking network structures of non-stoichiometric curing in case of acid anhydride excess.

Fig. 1.9 Three types of crosslinking network structures formed by variation of epoxy/anhydride ratios

1.3.2. Methods of measuring crosslinking density of thermoset

There are a number of methods for measuring the crosslinking density of a thermoset resin: chemical analysis, infra-red/near-infrared, swelling, differential scanning calorimetry, and parallel plate rheometry. These methods measure the extent to which the active resin sites are consumed. Other methods can measure the properties that relate directly to the crosslinking density: heat distortion temperature, glass transition temperature, hardness, electrical resistivity, dynamic and mechanical properties, thermal expansion, and refractive index [1.107].

The most common method is to measure the elastic modulus of the thermoset in its rubbery regime using a thermal mechanical testing instrument and then to apply theory to calculate the crosslink density. In applying the theory to epoxy materials, the primary assumption is that at temperatures much higher than the glass transition temperature, the epoxy thermosets exhibit rubbery behavior [1.108, 1.109].

The use of swelling experiments is used to obtain quantitative crosslinking density value of epoxy thermoset because they are generally easier and lower cost to perform. The degree of swelling is an inverse dependency on the crosslinking density of thermoset network. The greater the crosslinking density is the lower the degree of swelling [1.107, 1.110, 1.111].

Differential scanning calorimetry is used to predict the change of crosslinking density by following the change of temperature that accompanies the chemical reaction of the curing process. The sample is heated at a programed rate so that the enough energy is provided to the potential reactive groups for reaction. The peak glass transition temperature, most often exothermic, correlates with the amount of molecule that reacted. When no peak is observed, it is accepted that all reactants (monomers) are fully cured [1.107].

The parallel plate test has great shearing ability, therefore it can be used to analyze hard thermoset resin. Like the differential scanning calorimetry test, the parallel plate test can identify additional chemical reaction by differences in the measured viscosity [1.112].

1.3.3. Mechanical properties of non-stoichiometrically cured epoxy resins

Generally in practical applications, non-stoichiometric curing is often used to clarify the network morphology effects in the epoxy matrix to determine the performance of epoxy composites. The mechanical properties of the non-stoichioterically cured epoxy resins with and without fillers have been reported in several papers.

Selby and Miller [1.113] investigated the variation of fracture and mechanical properties of epoxy resin cured with diaminodiphenyl-methane by variation of the resin/amine ratio. Observations of the crack tip have shown that fracture toughness variations can be attributed to the different blunting characteristics of the various resin/amine compositions. Wingard and Beatty [1.114] reported that glass transition temperature and secondary glass transition temperature of the epoxy resins identified from thermo-viscoelastic properties varied depending on the non-stoichiometrically cured epoxy resins used. Palmese and McCullough [1.115] found that the elastic modulus and glass transition temperature of the epoxy resin were significantly affected by relatively small variations in stoichiometry.

d'Almeida and Monteiro [1.116] showed that composites consisting of glass microspheres in the epoxy resins fabricated with a curing agent-rich formulation had the best deformation capacity. Vanlandingham et al. [1.117] denoted the relation between microstructure and properties in epoxy resins as a function of epoxy-amine stoichiometry. Calventus et al. [1.118] found that the glass transition temperatures of the cured epoxy resins became highest during stoichiometric curing.

d'Almeida et. al. [1.119] investigated the room temperature ageing of non-stoichiometric epoxy formulations. The results obtained show that the epoxy rich mixtures have their inherent brittleness increased by the ageing treatment. The initial reaction steps dominated by the amine addition reactions control the macromolecular structure and the mechanical performance of the stoichiometric and near stoichiometric formulation with excess of epoxy monomer. The amine rich mixtures have the more stable structures. Monteiro et. al. [1.120] investigated through mechanical tests and scanning electron microscopy observation epoxy matrix composites, with different parts of hardener per hundred of resin, reinforced with 10, 20 and 30 wt.% diamond particles. The results have shown that the non-stoichiometric epoxy formulation had the highest tensile strength more than the stoichiometric formulation. Moreover, the strength of the composite is decreased with the amount of incorporated diamond.

Fang et al. [1.121] improved the fracture toughness and flexural strength of graphene sheet/epoxy nanocomposite by amine-rich formulation to construct hierarchical interphase structures between the sheet and the matrix epoxy. Bignotti et

al. [1.122] reported that epoxy-clay nano-composites and the neat epoxy with the same stoichiometric ratio had basically the same crosslinking density. García et al. [1.123] clarified the influence of stoichiometry on curing the epoxy-clay nanocomposites and their viscoelastic properties.

As a result in the case of the particles reinforced epoxy composites, the interaction between particles and epoxy network structures will strongly affect to mechanical properties of the epoxy composites. This means that the mechanical properties of epoxy composites are considerably dependent not only on the particle size effect but also on the interaction between particles and network structures of matrix resin. To consider the interaction effects in nanocomposites, the different network structure must be proposed by non-stoichiometric curing to produce incomplete network structures in matrix resins. Investigations related interaction effects between network structures in epoxy matrix and nano-particles on mechanical properties using non-stoichiometric curing effects in matrix resin are highly limited. Moreover, the literatures of non-stoichiometric curing effects on mechanical properties of nano-silica particulate-reinforced epoxy composites to clarify the interaction effects between the particles and epoxy matrix resins are not available.

1.4. Objective of the Thesis

Nano-silica particulate-reinforced epoxy composites are important for industrial application to packaging materials in electronic devices, among other things. The properties of particles-reinforced epoxy composites are considerably dependent not only on the particle size effect but also on the interaction of particles and matrix resins.

The rapid decrease in the interparticle distance resulting from their small size to produce nanocomposites has in turn resulted in more interaction particles and the matrix resins. To consider the interaction effects in nanocomposites, the different network structure must be proposed to improve the performances of nanocomposites. The non-stoichiometric curing is developed to provide an alternative and different way of the modifying crosslinking network structure of epoxy matrix without modification of the chemical nature of epoxy chains. Therefore, developing relationships of nano-silica particles with different crosslinking network structures in epoxy matrix and interactions of them are necessary to understand the mechanical behavior of nano-silica particulate-reinforced epoxy composites.

In this dissertation, the interaction effects between different network structures in epoxy matrix and nano-silica particles are clarified and then discussed experimentally to improve the properties of epoxy nanocomposites by non-stoichiometric curing effects in matrix resin. The matrixes were prepared by curing with an excessive mixture of diglycidyl ether of bisphenol A type epoxy resin to the curing agent (methyl-tetrahydro-phthalic anhydride) for the stoichiometric condition. The matrix resin was a blend of the diglycidyl ether of bisphenol A type epoxy resin, with methyl-tetrahydro-phthalic anhydride as the curing agent and 2,4,6-tris (dimethyl aminomethyl) phenol as the accelerator. The mixture ratio of the epoxide resin and the curing agent was changed to consider the interaction between the silica particles and the network structures in the matrix resin. Silica particles with a median diameter of 240 nm were used as the filler of the composite. The volume fraction of the silica particles was 0.2 for every composite. The surfaces of the particles were not chemically coated.

The specific objectives of this study are denoted in Fig. 1.10. First is the modification network morphology by non-stoichiometric curing method of composites and neat epoxy resins to obtain different crosslinking density in matrix resins. Second is to clarify interaction effects between nano-silica particles and epoxy network structures on mechanical properties based on crosslinking density. Therefore, crosslinking density will be useful as a parameter for estimating the mechanical properties of materials. Furthermore, it can be a valuable guideline to the design of composites with appreciated properties.

1.5. Synopsis of the Thesis

This dissertation consists of five chapters. As sketched in Fig. 1.10, the outline of this dissertation is described as follows:

In chapter 2, "*Thermo-viscoelastic and bending behaviors*", the interaction effects between nano-silica particles and epoxy network structures on thermo-viscoelastic and bending properties of epoxy composites were investigated by non-stoichiometric curing in matrix resin. The non-stoichiometric curing effects were expressed by the crosslinking densities in matrix resins. The crosslinking densities can be determined from the dynamic storage moduli, *E'*, in the rubbery state according the rubber elasticity theory. The crosslinking densities in the composites are same with their cured resins because the crosslinking densities are concerned with the chemical reactions of the resin monomer and the curing agent [1.122]. The glass transition temperatures and the dynamic storage moduli of the neat epoxy resins and composites were identified from thermo-viscoelastic properties measured by dynamic mechanical analysis. Therefore, the relations between crosslinking densities and the mechanical properties were evaluated. The mechanical properties: thermo-viscoelastic and bending strength were obtained from dynamic mechanical thermal analysis and three-point bending test, respectively.

In chapter 3, "*Compression behavior*", the interaction effects between nano-silica particles and epoxy network structures on static and dynamic compression behaviors were discussed by non-stoichiometric curing in matrix resin using a material testing machine and a split Hopkinson pressure bar (SHPB) machine. The network structures of each neat epoxy resin and composite were appreciated by crosslinking densities of matrix resins obtained in chapter 2. Finally, the compressive yield stresses of composites and neat epoxy resins were discussed in order the interactive effects between nano-particles and different network structures in epoxy matrix resin.

In chapter 4, "*Fracture behavior"*, the interaction effects between nano-silica particles and epoxy network structures on Mode I fracture toughness was investigated and discussed by non-stoichiometric curing effects in matrix resin. The non-stoichiometric curing effects were expressed by the crosslinking densities in matrix resins identified from the thermo-viscoelastic properties of neat epoxy resins obtained in Chapter 2. The fracture toughness of the composites and the neat epoxy resins were clarified and were compared with the bending strength in Chapter 2.

In chapters 5, "*Conclusions"*, the main conclusion of this research was summarized from each chapter and an outlook is given regarding possible future researches on this research.

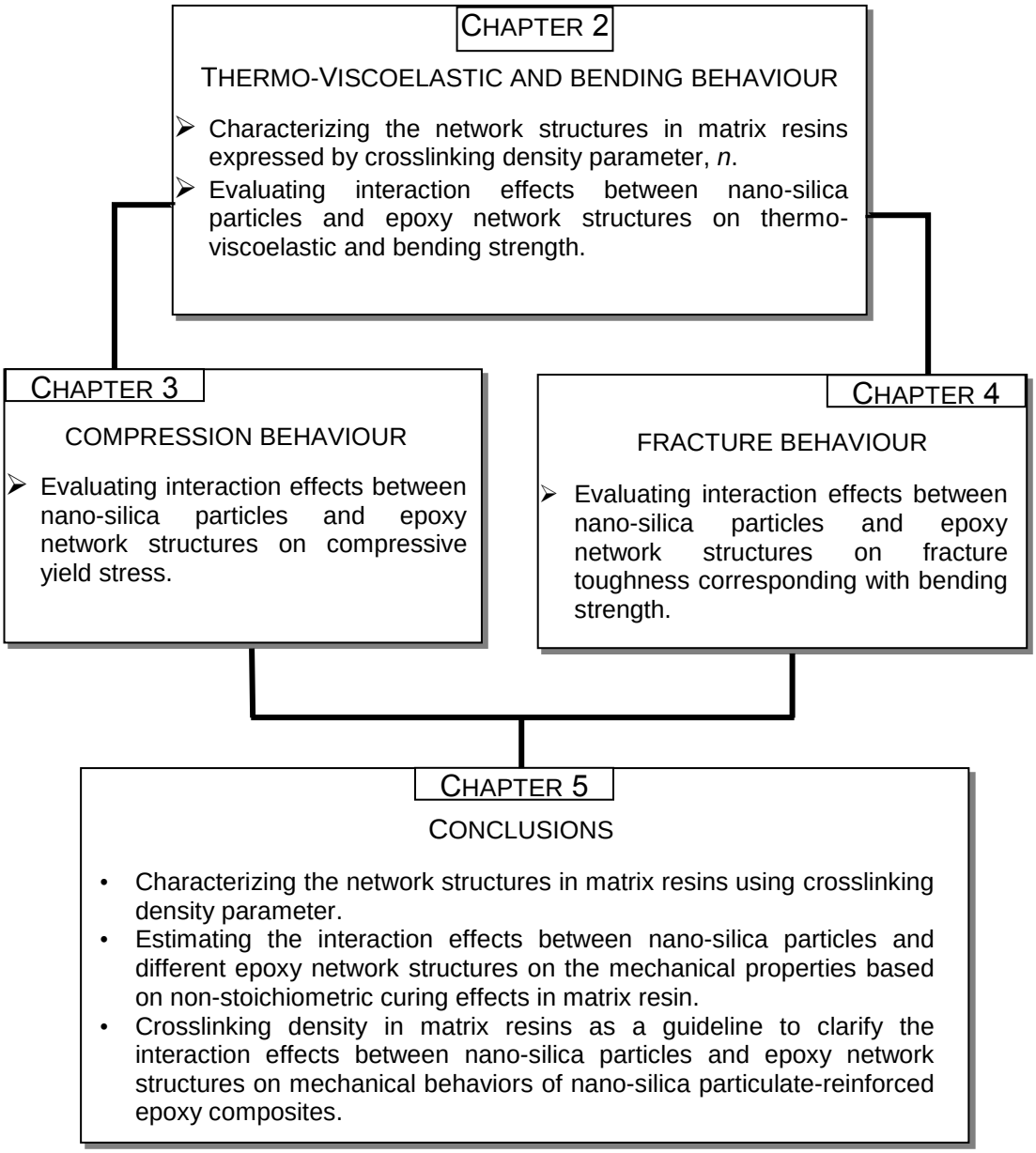

Fig. 1.10 Objectives of dissertation.

1.6 References

[1.1] May, C.A., Introduction to epoxy resins. in *Epoxy Resins Chemistry and Technology*, May, C. A., 2nd ed., Marcel Dekker, Inc., New York, 1988.

[1.2] Bradley, J.S., Hastings, G.W., Johnson, N.C., Carbon fibre reinforced epoxy as a high strength, low modulus material for internal fixation plates, *Biomaterials*, Vol. 1, p.38, 1980.

[1.3] Christel, P., Meunier, A., Abols, Y., Sedel, L., Morel, E., Vuichard, R., and Leray, J., Callus characteristics following intramedullary nailing with stainless steel or epoxy-carbon nails, *Archives of Orthopaedic and Trauma Surgery*, Vol. 103, p.131, 1984.

[1.4] Howard, C.B., Tayton, K.J.J., and Gibbs, A., The response of human tissues to carbon fibre reinforced epoxy resin, *Journal of Bone and Joint Surgery*, Vol. 67, p. 656, 1985.

[1.5] Tanaka Y., Synthesis and characteristics of epoxides, In *Epoxy Resins Chemistry and Technology*, May, C. A., 2nd ed., Marcel Dekker, Inc., New York, 1988.

[1.6] Araki W., *Thermo-viscoelastic effect on fracture toughness of epoxy resin*, Doctorial Thesis, Tokyo Institute of Technology, 2005.

[1.7] Goodman S.H., *Epoxy Resins*, *Handbook of Thermoset Plastics*, Chap.6, pp. 193–264, 1996.

[1.8] Muroi S., Shuichi I., *Introduction to epoxy resin*, Polymer Society publication, 1988.

[1.9] Kamon T., Furukawa H., Curing Mechanisms and Mechanical Properties of Cured Epoxy Resins, *Advances in Polymer Science*, Vol. 80, pp 173–202, 1986.

[1.10] Kwon S.Ch., *Mechanical behaviors of nano- and micro-silica particles reinforced epoxy composites*, Doctorial Thesis, Tokyo Institute of Technology, 2006.

[1.11] Rothon R. N., *Particulate-filled polymer composites*, Rapra Technology Limited, Shrewsbury, 2003.

[1.12] Peters S. T., *Handbook of composites*, Chapman & Hall, New York, 1998.

[1.13] Tolle T. B., Anderson D. P., The role of preconditioning on morphology development in layered silicate thermoset nanocomposites, *Journal of Applied Polymer Science*, Vol. 91, pp. 89-100, 2004.

[1.14] Theodore M., Dean D., Obore A., Nyairo E., Effect of nanoparticles on cure behavior and properties of epoxy/layered silicate nanocomposites, *Polymer Preprints*. Vol. 45, No. 1, p. 863, 2004.

[1.15] Hussain F., Hojjati M., Okamoto M., Gorga R. E., Review article: polymer-matrix nanocomposites, processing, manufacturing, and application: an overview, *Journal of Composite Materials*, Vol. 40, No. 17, pp. 1511-1565, 2006.

[1.16] Hamerton I., *Recent developments in epoxy resins*, Rapra Technology Limited, Shrewsbury, 1996.

[1.17] Ellis B., *Chemistry and technology of epoxy resins*, Chapman & Hall, New York, 1993.

[1.18] Koo J. H., Pilato L. A., Polymer nanostructured materials for high temperature applications, *Society for the Advancement of Material and Process Engineering Journal*, Vol. 42, No. 2, pp. 7-19, 2005.

[1.19] Koo J. H., *Polymer nanocomposites processing, characterization, and applications*, McGraw-Hill, New York, 2006.

[1. 20] Bose A., *Advances in particulate materials*, Butterworth-Heinemann College, Boston, 1995.

[1.21] Feda J., *Mechanics of particulate materials*, Elsevier Science, New York, 1982.

[1.22] Pascault J. P., Sautereau H., Verdu J., Williams R. J. J., *Thermosetting polymers*, Marcel Dekker, New York, 2002.

[1.23] Gonon P., Sylvestre A., Teysseyre J., Prior C., Dielectric properties of epoxy/silica composites used for microelectronic packaging, and their dependence on post-curing, *Journal of Materials Science: Materials in Electronics*, Vol. 12, pp. 81-86, 2001.

[1.24] Mahajan R., Nair R., Wakharkar V., Swan J., Tang J, Vandentop G., Emerging directions for packaging technologies, *Intel Technology Journal*, Vol. 9, No. 4, pp. 62-75, 2005.

[1.25] Mencinger N.P., A mechanism-based methodology for processor package reliability assessments, *Intel Technology Journal*, Vol. 4, No. 3, pp. 1-8, 2000.

[1.26] Nielsen L. E., Landel R. F., *Mechanical properties of polymers and composites*, Marcel Dekker, New York, 1994.

[1.27] Packaging Technology for Application Processors, *Plastic Ball Grid Array (PBGA)*, Samsung, 2014.

[1.28] Fillers Study Group, *Filler applications enclyclopedia comprehensive list*, Taiseisha Ltd, 1994.

[1.29] Kausch H.H., Beguelin P., Deformation and fracture mechanisms in filled polymers, *Macromolecular Symposia*, Vol. 169, pp. 79-87, 2001.

[1.30] Kishimoto K., Notomi M., Kadota S., Shibuya T., Kawamura N., Kawakami T., Mixed-mode fracture behavior of silica particulate filled epoxide resin, *The American Society for Testing and Materials Special Technical Publication*, No. 1359, pp. 129-142, 1999.

[1.31] Adachi T., Araki W., Nakahara T., Yamaji A., Gamou M., Fracture toughness of silica particulate-filled epoxy composite, *Journal of Applied Polymers Science* Vol. 86, pp. 2261-2265, 2002.

[1.32] Spanoudakis J., Young R.J., Crack propagation in a glass particle-filled epoxy resin. Part 1: Effect of particle volume fraction and size, *Journal of Materials Science*, Vol. 19, pp. 473-486, 1984.

[1.33] Spanoudakis J., Young R.J., Crack propagation in a glass particle-filled epoxy resin. Part 2: Effect of particle-matrix adhesion, *Journal of Materials Science*, Vol. 19, pp. 487-496, 1984.

[1.34] Nakamura Y., Yamaguchi M., Kitayama A., Okubo M., Matsumoto T., Effect of particle size on fracture toughness of epoxy resin filled with angular-shaped silica, *Polymer*, Vol. 32, No. 12, pp. 2221-2229, 1991.

[1.35] Nakamura Y., Yamaguchi M., Okubo M., Matsumoto T., Effect of particle size on impact properties of epoxy resin filled with angular shaped silica particles, *Polymer*, Vol. 32, No. 16, pp. 2976-2979, 1991.

[1.36] Nakamura Y., Yamaguchi M., Okubo M., Matsumoto T., Effects of particle size on mechanical properties of epoxy resin filled with angular-shaped silica, *Journal of Applied Polymer Science*, Vol. 44, pp. 151-158, 1992.

[1.37] Nakamura Y., Yamaguchi M., Okubo M., Matsumoto T., Effects of particle size on mechanical and impact properties of epoxy resin filled with spherical silica, *Journal of Applied Polymer Science*, Vol. 45, pp. 1281-1289, 1992.

[1.38] Nakamura Y., Okabe S., Iida T., Effects of particle shape, size and interfacial adhesion on the fracture strength of silica-filled epoxy resin, *Polymers and Polymer Composites*, Vol. 7, No. 3, pp. 177-186, 1999.

[1.39] Yaguchi A., Nishimura A., Kawai S., Fracture toughness measurement method and fracture properties of highly silica particulate filled epoxy epoxide resins, *Journal of the Japan Society of Materials Science*, Vol. 40, No. 452, pp. 554-560, 1991.

[1.40] Yamatomo I., Higashihara T., Kobayashi T., Effect of silica-particle characteristics on impact/usual fatigue properties and evaluation of mechanical characteristics of silica-particle epoxy resins, *the Japan Society of Mechanical Engineering International Journal*, Vol. 46, No. 2, pp. 145-153, 2003.

[1.41] Niinomi M., Kobayashi T., Uwai K., Ohishi T., Higashihara T., Impact fatigue and characteristics of SiO_2 fillers in epoxy resin, *Proceeding of International Conference on the Mechanical Behavior of Materials*, Vol. 2, pp. 549-555, 1992.

[1.42] Mcmurray M.K., Amagi S., The effect of time and temperature on flexural creep and fatigue strength of a silica particles filled epoxy resin, *Journal of Materials Science*, Vol. 34, pp. 5927-5936, 1999.

[1.43] Koh S.W., Kim J.K., Mai Y.M., Fracture toughness and failure mechanisms in silica-filled epoxy resin composites: effects of temperature and loading rate, *Polymer*, Vol. 34, No. 16, pp. 3446-3455, 1993.

[1.44] Zhang Y-P., Zhang Y., Ning R. H., Effects of nanoparticles SiO2 on the performance of nanocomposites, *Materials Letters*, Vol. 57, No. 19, pp. 2940-2944, 2003.

[1.45] Monette L., Anderson M.P., Wagner H.D., Mueller R.R., The young's modulus of silica beads/epoxy composites: experiments and simulation, *Journal of Applied Physics*, Vol. 75, No. 3, pp. 1442-1455, 1994.

[1.46] Wang H., Bai Y., Liu S., Wu J., Wong C.P., Combined effects of silica filler and its interface in epoxy resin, *Acta Materialia*, Vol. 50, 4369-4377, 2002.

[1.47] Fiedler B., Hojo M., Ochiai S., Schulte K., Ando M., Failure behavior of an epoxy matrix under different kinds of static loading, *Composites Science and Technology*, Vol. 61, pp. 1615-1624, 2001.

[1.48] Anderson D.P., Tolle T.B., Composite property enhance with nanoscale inorganic fillers, *Polymer Materials Science and Engineering*, Vol. 20, pp. 220-221, 2000.

[1.49] Imanaka M., Takeuchi Y., Nakamura Y., Nishimura A., Iida T., Fracture toughness of spherical silica-filled epoxy adhesives, *International Journal of Adhesion & Adhesives*, Vol. 21, pp. 389-396, 2001.

[1.50] Young R.J., Beaumont P.W.R., Failure of brittle polymers by slow crack growth: Part 3. Effect of composition upon the fracture of silica particulate-filled epoxy resin composites, *Journal of Material Science*, Vol. 12, No. 4, pp. 684-692, 1977.

[1.51] Kobayashi T., Higashihara T., Yamaya H., Hosoi K., Toda H., Effect of CTBN addition on mechanical properties of epoxy resins filled with SiO_2 particles, *Journal of the Japan Society of Material Science*, Vol. 48, No. 12, pp. 1386-1392, 1999.

[1.52] Swanson F., Gregornik N., Bulk effect of particulate fillers in epoxy resin compositions, *Modern Plastics*, Vol. 49, No. 11, pp. 4-6, 1972.

[1.53] Kawamura N., Kawakami T., Matsumoto K., Kishimoto K., Notomi M., Koizumi T., Method of test for fracture toughness of silica-particulate-filled epoxide resins and effects of moisture absorption on fracture properties, *Journal of the Japan Society of Mechanical Engineering*, Vol. 62, No. 596, pp. 902-907, 1996.

[1.54] Yoshida Y., Higashihara T., Nomura Y., Usui E., Hibi S., The effect of silane agent on tensile and bending properties of silica-filled epoxy after water absorption by boiling, *Electrical Engineering in Japan*, Vol. 129, No. 2, pp. 1-11, 1999.

[1.55] Boonyapookana A., Nagata K., Mutoh Y., Fatigue crack growth behavior of silica particulate reinforced epoxy resin composite, *Composites Science and Technology*, Vol. 7, pp. 1124-1131, 2011.

[1.56] Adachi T., Osaki M., Araki W., Kwon S.Ch., Fracture toughness of nano- and micro-spherical silica-particle-filled epoxy composite, *Acta Materialia*, Vol. 56, pp. 2101-2109, 2008.

[1.57] Adachi T., Araki W., Higuchi M., Mixture law including particle-size effect on fracture toughness of nano- and micro-spherical particle-filled composites, *Acta Mechanic,* Vol. 214, pp. 61-69, 2010.

[1.58] Adachi T., Imai Y., Higuchi M., Fracture Energy of Nano- and micro-silica particle-filled epoxy Composites, *International Journal of Theoretical and Applied Multiscale Mechanics*, Vol.2, No.1, pp.82-94, 2011.

[1.59] Kwon S.Ch., Adachi T., Araki W., Yamaji A., Effect of particle size on fracture toughness of spherical silica particles filled epoxy composite, *Key Engineering Materials*, Vol. 297-300, pp. 207-212, 2005.

[1.60] Kwon S.Ch., Adachi T., Strength and fracture toughness of nano and micron-silica particles bidispersed epoxy composites: evaluated by fragility parameter, *Journal of Materials Science*, Vol. 42, pp. 5516-5523, 2007.

[1.61] Kwon S.Ch., Adachi T., Araki W., Yamaji A., Mechanical properties of nano/micro-silica particles bidispersed epoxy composites. *Key Engineering Materials*. Vol. 345-346, pp. 1507-1510, 2007.

[1.62] Kwon, S.Ch., Adachi, T., Araki, W., Temperature dependence of fracture toughness of silica/epoxy composites: related to microstructure of nano- and micro-particles packing, *Composites Part B*, Vol. 39, pp. 773-781, 2008.

[1.63] Kwon S.Ch., Adachi T., Araki W., Yamaji A., Effect of composing particles of two sizes on mechanical properties of spherical silica-particulate-reinforced epoxy composites, *Composite Part B*, Vol. 39, pp. 740-746, 2008.

[1.64] Olhero S.M., Ferreira J.M.F., Influence of particle size distribution on rheology and particle packing of silica-based suspensions, *Powder Technology*, Vol. 139, pp. 69-75, 2004.

[1.65] Preghenella M., Pegoretti A., Migliaresi C., Thermo-mechanical characterization of fumed silica-epoxy nanocomposites, *Polymer*, Vol. 46, pp. 12065-12072, 2005.

[1.66] Preghenella M., Pegoretti A., Migliaresi C., Atomic force acoustic microscopy analysis of epoxy-silica nanocomposites, *Polymer Testing*, Vol. 25, pp. 443–451, 2006.

[1.67] Jumahat A., Soutis C., Abdullah S. A., Kasolang S., Tensile properties of nanosilica/epoxy nanocomposites, *Procedia Engineering*, Vol. 41, pp. 1634-1640, 2012.

[1.68] Veena M.G., Renukappa N.M., Raj J.M., Ranganathaiah C., Shivakumar K.N., Characterization of nanosilica-filled epoxy composites for electrical and insulation applications, *Journal of Applied Polymer Science,* Vol. 121, pp. 2752-2760, 2011.

[1.69] Zheng Y., Chonung K., Wang G., Wei P., Jiang P., Epoxy/Nano-Silica Composites: Curing Kinetics, Glass Transition Temperatures, Dielectric, and Thermal–Mechanical Performances, *Journal of Applied Polymer Science*, Vol. 111, pp. 917-927, 2009.

[1.70] Devaprakasam D., Hatton P.V., Mobus G., Inkson B.J., Nanoscale Tribology, Energy Dissipation and Failure Mechanisms of Nano- and Micro-silica Particle-filled Polymer Composites, *Tribology Letters*, Vol. 34, pp. 11-19, 2009.

[1.71] Jajam K.C., Tippur H.V., Quasi-static and dynamic fracture behavior of particulate polymer composites: A study of nano- vs. micro-size filler and loading-rate effects, *Composites Part B*, Vol. 43, pp. 3467-348, 2012.

[1.72] Chen C., Justice R.S., Schaefer D.W., Baur J.W., Highly dispersed nanosilica–epoxy resins with enhanced mechanical properties, *Polymer*, Vol. 49, pp. 3805-3815, 2008.

[1.73] Battistella M., Cascione M., Fiedler B., Wichmann M.H.G., Quaresimin M., Schulte K., Fracture behaviour of fumed silica/epoxy nanocomposites, *Composites Part A*, Vol. 39, pp. 1851-1858, 2008.

[1.74] Yao X.F., Zhou D., Yeh H.Y., Macro/microscopic fracture characterizations of SiO2/epoxy nanocomposites, *Aerospace Science and Technology*, Vol. 12, pp. 223-230, 2008.

[1.75] Ragosta G., Abbate M., Musto P., Scarinzi G., Mascia L., Epoxy-silica particulate nanocomposites: Chemical interactions, reinforcement and fracture toughness, *Polymer*, Vol. 46, pp. 10506-10516, 2005.

[1.76] Zhang H., Zhang Z., Friedrich K., Eger C., Property improvements of in situ epoxy nanocomposites with reduced interparticle distance at high nanosilica content, *Acta Materialia*, Vol.54, pp.1833-1842, 2006.

[1.77] Zhang H., Tang L.C., Zhang Z., Friedrich K., Sprenger S., Fracture behaviours of in situ silica nanoparticle-filled epoxy at different temperatures, *Polymer*, Vol. 49, pp. 3816-3825, 2008.

[1.78] Deng S., Ye L., Friedrich K., Fracture behaviours of epoxy nanocomposites with nano-silica at low and elevated temperatures, *Journal of Material Science*, Vol. 42, pp. 2766-2774, 2007.

[1.79] Chen Q., Chasiotis I., Chen C., Roy A., Nanoscale and effective mechanical behavior and fracture of silica nanocomposites, *Composites Science and Technology*, Vol. 68, pp. 3137-3144, 2008.

[1.80] Liang Y.L., Pearson R.A., Toughening mechanisms in epoxy–silica nanocomposites (ESNs), *Polymer*, Vol. 50, pp. 4895-4905, 2009.

[1.81] Dittanet P., Pearson R. A., Effect of silica nanoparticle size on toughening mechanisms of filled epoxy, *Polymer*, Vol. 53, pp. 1890-1905, 2012.

[1.82] Bray D.J., Dittanet P., Guild F.J., Kinloch A.J., Masania K., Pearson R.A., Taylor A.C., The modelling of the toughening of epoxy polymers via silica nanoparticles: The effects of volume fraction and particle size, *Polymer*, Vol. 54, pp. 7022-7032, 2013.

[1.83] Zamanian M., Mortezaei M., Salehnia B., Jam J.E., Fracture toughness of epoxy polymer modified with nanosilica particles: Particle size effect, *Engineering Fracture Mechanics*,Vol. 97, pp. 193-206, 2013.

[1.84] Hsieh T.H., Kinloch A.J., Masania K., Taylor A.C., Sprenger S., The mechanisms and mechanics of the toughening of epoxy polymers modified with silica nanoparticles, *Polymer*, Vol. 51, pp. 6284-6294, 2010.

[1.85] Li Y., Unsworth J., Effect of physical aging on dielectric, thermal and mechanical properties of cast-epoxy insulators, *IEEE Transactions on Dielectrics and Electrical Insulations*, Vol. 1, No. 1, pp. 9-17, 1994.

[1.86] Unsworth J., Li Y., Gao B., Dynamic mechanical thermal analysis and dielectric studies of physical aging in an epoxy composite, *Materials Forum*, Vol. 16, No. 2, pp. 163-166, 1992.

[1.87] Unsworth J., Li Y., Thermal degradation of epoxy/silica composites monitored via dynamic mechanical thermal analysis, *Journal of Applied Polymer Science*, Vol. 46, No. 8, pp. 1375-1379, 1992.

[1.88] Kim K.H., Son I.H., Lee D.J., Kim M.H., Jang K.U., Kim J.H., The dielectric and mechanical characteristics of SiO_2 filled epoxy composites, *International Conference on Properties and Applications of Dielectric Materials*, Vol. 11P21, pp. 896-899, 1997.

[1.89] Goyanes S.N., Konig P.G., Marconi J. D., Dynamic mechanical analysis of particulate-filled epoxy resin, *Journal of Applied Polymer Science*, Vol. 88, pp. 883-892, 2003.

[1.90] Kwon S.Ch., Adachi T., Araki W., Yamaji A., Thermo-viscoelastic properties of silica particulate reinforced epoxy composites: considered in terms of particle packing model*, Acta Materialia*, Vol. 54, pp. 3369-3374, 2006.

[1.91] Kang S., Hong S.I., Choe C.R., Park M., Rim S., Kim J., Preparation and characterization of epoxy composites filled with functionalized nanosilica particles obtained via sol-gel process, *Polymer*, Vol. 42, pp. 879-887, 2001.

[1.92] Sun Y., Zhang Z., Moon K.S., Wong C.P., Glass transition and relaxation behavior of epoxy nanocomposites, *Journal of Polymer Science*, Vol. 42, pp. 3849-3558, 2004.

[1.93] Sangermano M., Malucelli G., Amerio E., Priola A., Billi E., Rizza G., Photopolymerization of epoxy coatings containing silica nanoparticles, *Progress in Organic Coatings*, Vol. 54, pp. 134-138, 2005.

[1.94] Barabanova A.I., Philippova O.E., Askadskii A.A., Khokhlov A.R., Transparent Epoxy/Silica Nanocomposites with Increased Glass Transition Temperatures, *Procedia Chemistry*, Vol. 4, pp. 352-359, 2012.

[1.95] Tishin S.A., Tishin V.A., Bakaev E.S., Shipilevskiy B.A., Kestelman V.N., Epoxy polymer adhesive properties in the presence of fine powder silicas with modified surfaces, *Journal of Materials Science*, Vol. 28, pp. 325-328, 1998.

[1.96] Kinloch A. J., Lee J. H., Taylor A., Sprenger S., Eger C., Egan D., Toughening structural adhesives via nano- and micro-phase inclusions, *Journal of Adhesion*, Vol. 79, pp. 867-873, 2003.

[1.97] Xing X.S., Li R.K.Y., Wear behavior of epoxy matrix composites filled with uniform sized sub-micron spherical silica particles, *Wear*, Vol. 256, pp. 21-26, 2004.

[1.98] Zhang Q., Archer L.A., Poly (ethylene oxide)/silica nanocomposites: structure and rheology, *Langmuir*, Vol. 18, pp. 10435-10442, 2002.

[1.99] Wang Z.Z, Gu P., Wu X.P., Zhang H., Zhang Z., Chiang M.Y.M., Micro/nano-wear studies on epoxy/silica nanocomposites, *Composites Science and Technology*, Vol. 79, 49-57, 2013.

[1.100] Veena M.G., Renukappa N.M., Suresha B., Shivakumar K.N., Tribological and Electrical Properties of Silica-Filled Epoxy Nanocomposites, *Polymer Composites*, Vol. 32, pp. 2038-2050, 2011.

[1.101] Akelah A., Moet A., *Functionalized polymers and their applications*, Chapman & Hall, London, 1990.

[1.102] Friedrich K., Fakirov S., Zhang Z., *Polymer composites: from nano- to micro-scale*, Springer, New York, 2005.

[1.103] Yao X.F., Yeh H.Y., Zhou D., Zhang Y.H., The structural characterization and properties of SiO_2-epoxy nanocomposites, *Journal of Composite Materials*, Vol. 40, No. 4, pp. 371-381, 2006.

[1.104] Rong M.Z., Zhang M.Q., Pan S.L., Lehmann B., Friedrich K., Analysis of the interfacial interactions in polyprotlene/silica nanocomposites, *Polymer International,* Vol. 53, pp.176-183, 2004.

[1.105] Brechet Y., Cavaille J.Y.Y., Chabert E., Chazeau L., Dendievel R., Flandin L., Gauthier C., Polymer based nanocomposites: effect of filler-filler and filler-matrix interactions*, Advanced Engineering Materials,* Vol. 3, pp. 571-577, 2001.

[1.106] Kovacevic V., Lucic S., Leskovac M., Morphology and failure in nanocomposites Part I: structural and mechanical properties*, Journal of Adhesion Science and Technology,* Vol. 16, pp. 1343-1365, 2002.

[1.107] Dodiuk H., Goodman S.H., *Handbook of thermoset plastic*, 3th ed., Elsevier, Burlinton, 2013.

[1.108] Lemay J.D., Swetlin B.J., Kelley F.N., Characterization of Highly Cross-linked Polymers, *ACS Symposium Series*, Vol.243, pp.165-183, 1984.

[1.109] Chen J.S., Ober C.K., Poliks M.D., Zhang Y., Wiesner U., Cohen C., Controlled degradation of epoxy networks: analysis of crosslink density and glass transition temperature changes in thermally reworkable thermosets, *Polymer*, Vol. 45, pp. 1939-1950, 2004.

[1.110] Bell J.P., Structure of a typical amine-cured epoxy resin, *Journal of Polymer Science*, Part a-2-Polym Phys, Vol. 8, pp. 417-436, 1970.

[1.111] Murayama T., Bell J.P., Relation between the network structure and dynamic mechanical properties of a typical amine-cured epoxy polymer, *Journal of Polymer Science*, Part a-2-Polym Phys, Vol.8, pp.437-445, 1970.

[1.112] Sperling L.H., *Introduction to physical polymer science*, 4th ed., Jhon wiley & Sons, 2006.

[1.113] Selby K., Miller L.E., Fracture toughness and mechanical behavior of an epoxy resin, *Journal of Materials Science*, Vol. 1, no. 10, pp. 12-24, 1975.

[1.114] Wingard C.D., Beatty C.L., Crosslinking of an epoxy with a mixed amine as a function of stoichiometry. II. Final properties via dymanic mechanical spectroscopy, *Journal of Applied Polymer Science*, Vol. 41. pp.2539-2554, 1990.

[1.115] Palmese G.R., McCullough R.L., Effect of epoxy-amine stoichiometry on cured resin material properties, *Journal of Applied Polymer Science*, Vol. 46, pp. 1863-1873, 1992.

[1.116] d'Almeida J.R.M., Monteiro S.N., The resin/hardner ratio as a processing parameter for modifying the mechanical behaviour of epoxy-matrix/glass microsphere composites, *Composites Science and Technology*, Vol. 58, pp.1593-1598, 1998.

[1.117] Van landingham M.R., Eduljee R.F., Gillespie Jr.J.W., Relationships Between Stoichioetry, Microstructure, and Properties for Amine-Cured Epoxies, *Journal of Applied Polymer Science*, Vol. 71, pp. 699-712, 1992.

[1.118] Calventus Y., Montserrat S., Hutchinson J.M., Entalpy relaxation of non-stoichiometric epoxy-amine resins, *Polymer*, Vol. 42, pp. 7081-7093, 2001.

[1.119] d'Almeida J.R.M., de Menezesb G.W., Monteirob S.N., Ageing of the DGEBA/TETA epoxy system with off-stoichiometric compositions, *Materials Research*, Vol. 6, no. 3, pp. 415-420, 2003.

[1.120] Monteiro S.N., de Menezes G.W., Rodriguez R.J.S., Bobrovnitchii G.S., Skury A.L.D., Technical characteristics of diamond reinforced epoxy composites, *Revista Matéria*, Vol. 10, n. 4, pp. 564-570, 2005.

[1.121] Fang M., Zhang Z., Li J., Zhang H., Lu H., Yang Y., Constructing hierarchically structured interphases for strong and tough epoxy nanocomposites by amine-rich graphene surfaces, *Journal of Materials Chemistry*, Vol. 20, pp. 9635-9643, 2010.

[1.122] Bignotti F., Pandini S., Baldi F., De Santis R., Effect of the resin/hardener ratio on curing, structure and glass transition temperature of nanofilled epoxies, *Polymer Composites*, Vol. 32, pp. 1034-1048, 2011.

[1.123] García del Cid M.A., Prolongo M.G, Salom C., Arribas C., Sánchez-Cabezudo M., Masegosa R.M., The effect of stoichiometry on curing and properties of epoxy-clay nanocomposites, *Journal of Thermal Analysis and Calorimetry*, Vol.108, pp. 741-750, 2012.

CHAPTER 2

THERMO-VISCOELASTIC AND BENDING BEHAVIORS

2.1. Introduction

Currently, epoxy resins are widely applied to various engineering fields due to their excellent mechanical and insulation properties. These resins are reinforced with various particles or fibers to improve the properties further. The particle size is currently being decreased to below the micrometer level to form nanocomposites with superior mechanical properties.

The mechanical properties of nancomposites have been investigated in several previous studies. The effects of the size and volume fraction of the particles, namely, the interaction effect between the particles and the epoxy matrix, has been studied to determine how the properties of the nanocomposites can be improved. The mechanical properties of composites are strongly dependent on the network structure and shape of the silica particles, as found by Yamamoto et al. [2.1], Moloney et al. [2.2–2.4], and Adachi et al. [2.5–2.7], and for the size, shape, and specific surface of the silica particles, clarified by Nakamura et al. [2.8–2.10]. In order to further clarify the effect of particle size on the mechanical properties, properties of the composites filled with particles having different distributions of particle size have been investigated. The mechanical properties of these composites were found to be governed by the distributions [2.11–2.15]. The rapid decrease in the interparticle distance resulting from their small size has in turn resulted in more interactions between particles and the epoxy matrix. The interfacial interaction of particles with the surrounding matrix has a close relationship with the crosslinking network morphology in the polymer matrix [2.16–2.18]. As a result, the mechanical properties of nano or micron-particle-reinforced epoxy composites are considerably dependent not only on the particle size effect but also on the intrinsic properties of the epoxy matrix.

Nano-silica particulate-reinforced epoxy composites are important for industrial application to packaging materials in electronic devices, among other things. The mechanical properties of the composites need to be improved to increase the reliability of the devices. Therefore, the interaction effects between network structures in the epoxy resins and the silica particles on the mechanical properties must be clarified.

The objective of the present chapter was to investigate the interaction between nano-particles and network structures on thermo-viscoelastic and bending properties of nano-silica particulate-reinforced epoxy composites by non-stoichiometric curing effects in matrix resin. The non-stoichiometric curing effects were expressed by crosslinking densities in matrix resins. The matrixes were prepared by curing with an

excessive mixture of diglycidyl ether of bisphenol A type epoxy resin to the curing agent (methyl-tetrahydro-phthalic anhydride) for the stoichiometric condition. The crosslinking densities in the matrix resins were characterized from the dynamic storage moduli of neat epoxy resins in a rubbery state, and the glass transition temperatures of the neat epoxy resins and the composites were determined from the temperature dependence of the loss tangents. The thermo-viscoelastic was measured by dynamic mechanical analysis. Elastic moduli and strengths of the composites and the neat epoxy resins were measured by three-point bending tests.

2.2. Specimens

The materials used for specimens in this study were bisphenol A type epoxy composites filled with spherical silica particles.

The matrix resin was a blend of the diglycidyl ether of bisphenol A type epoxy resin (Asahi Kasei E-Materials, AER 2603), with methyl-tetrahydro-phthalic anhydride (New Japan Chemical, RIKACID MH-700) as the curing agent and 2,4,6-tris (dimethyl aminomethyl) phenol (Mitsubishi Chemical, jER BMI12) as the accelerator. The equivalent weight of the epoxide resin was 188 grams/equivalent and the acid anhydride equivalent weight of the curing agent was 162 grams/equivalent. The stoichiometric-mixture-weight ratio of the epoxide resin, the curing agent, and the accelerator was 100: 86: 0.5.

The mixture ratio of the epoxide resin and the curing agent was changed to consider the interaction between the silica particles and the network structures in the matrix resin. In this research, the changed mixture ratio is hereafter expressed as the epoxy-equivalent-weight ratio (EEWR) defined by the epoxide resin weight over the stoichiometric epoxide resin weight in the mixture. In the experiment, the EEWR ranged from 1.0 to 3.2 and the accelerator was kept constant at 0.5, as listed in Table 2.1. The neat epoxy resins manufactured for the EEWR over 3.2 were too weak to measure the viscoelastic properties mentioned below. We did not use any epoxy-equivalent-weight ratios below 1.0 to manufacture the resin or the composites because unreacted curing agents might leak out of the cured resins.

Silica particles with a median diameter of 240 nm (Tatsumori, SO-C1) were used as the filler of the composite. The volume fraction of the silica particles was 0.2 for every composite. The surfaces of the particles were not chemically coated.

The silica particles were added to the epoxy resin containing the curing agent and accelerator. After stirring sufficiently to disperse the particles without agglomeration, the mixture was stored in a vacuum vessel to remove voids and then poured into an aluminum mold coated with a Teflon sheet. The mold was 260 mm long, 5 mm wide, and 120 mm deep. The mixture in the mold was heated for curing in an oven. The curing procedure was performed in two steps: first, the mixture was kept at 373 K for 2 h to gel the matrix resin (pre-curing), and second, the post-curing, which greatly affects the crosslinking reaction of the resin, was performed at 403 K for 15 h. The heating rate from pre-curing to post-curing was kept constant at 72 K h^{-1}. A schematic of preparation process, mold geometry, and curing process are illustrated in Figs. 2.1, 2.2, and 2.3, respectively. Cured epoxy resins without silica particles were also prepared in the same process as that for the composites. Hereafter, the cured epoxy resins without the silica particles are referred to as neat epoxy resins. Both the neat epoxy resins and the composites were used in the experiment listed in Table 2.1.

Densities of the cured materials were measured in accordance with ASTM standard 792-08. The results are listed in Table 2.1. The densities of both the neat epoxy resins and the composites were confirmed to be independent of the EEWR.

Table 2.1 Neat epoxy resins and composites.

Materials	Matrix (weight ratio)			Epoxy-equivalent-weight ratio	Volume fraction of silica particles	Density (kg/m^3)
	Epoxide resin	Curing agent	Accelerator			
Neat epoxy resin	100	86	0.5	1.0	-	1200
	160	86	0.5	1.6	-	1200
	200	86	0.5	2.0	-	1200
	240	86	0.5	2.4	-	1200
	280	86	0.5	2.8	-	1200
	320	86	0.5	3.2	-	1200
Composite	100	86	0.5	1.0	0.2	1400
	160	86	0.5	1.6	0.2	1400
	200	86	0.5	2.0	0.2	1400
	240	86	0.5	2.4	0.2	1400
	280	86	0.5	2.8	0.2	1400
	320	86	0.5	3.2	0.2	1410

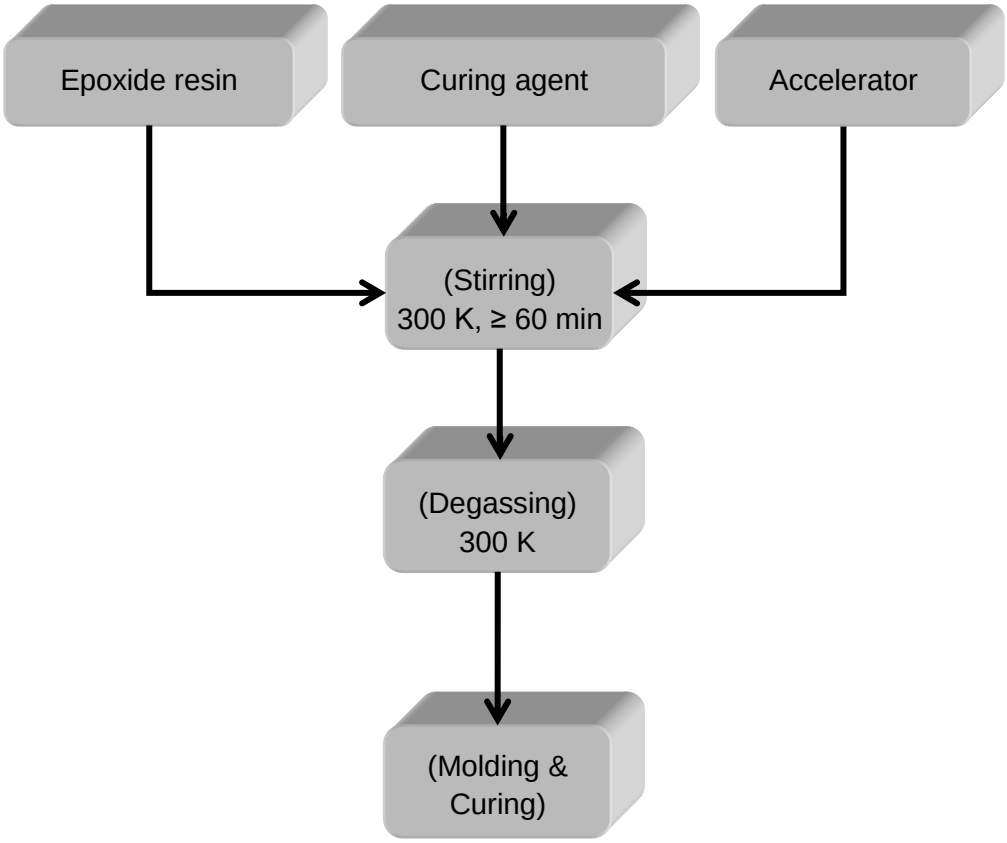

Fig. 2.1 Schematic of preparation process.

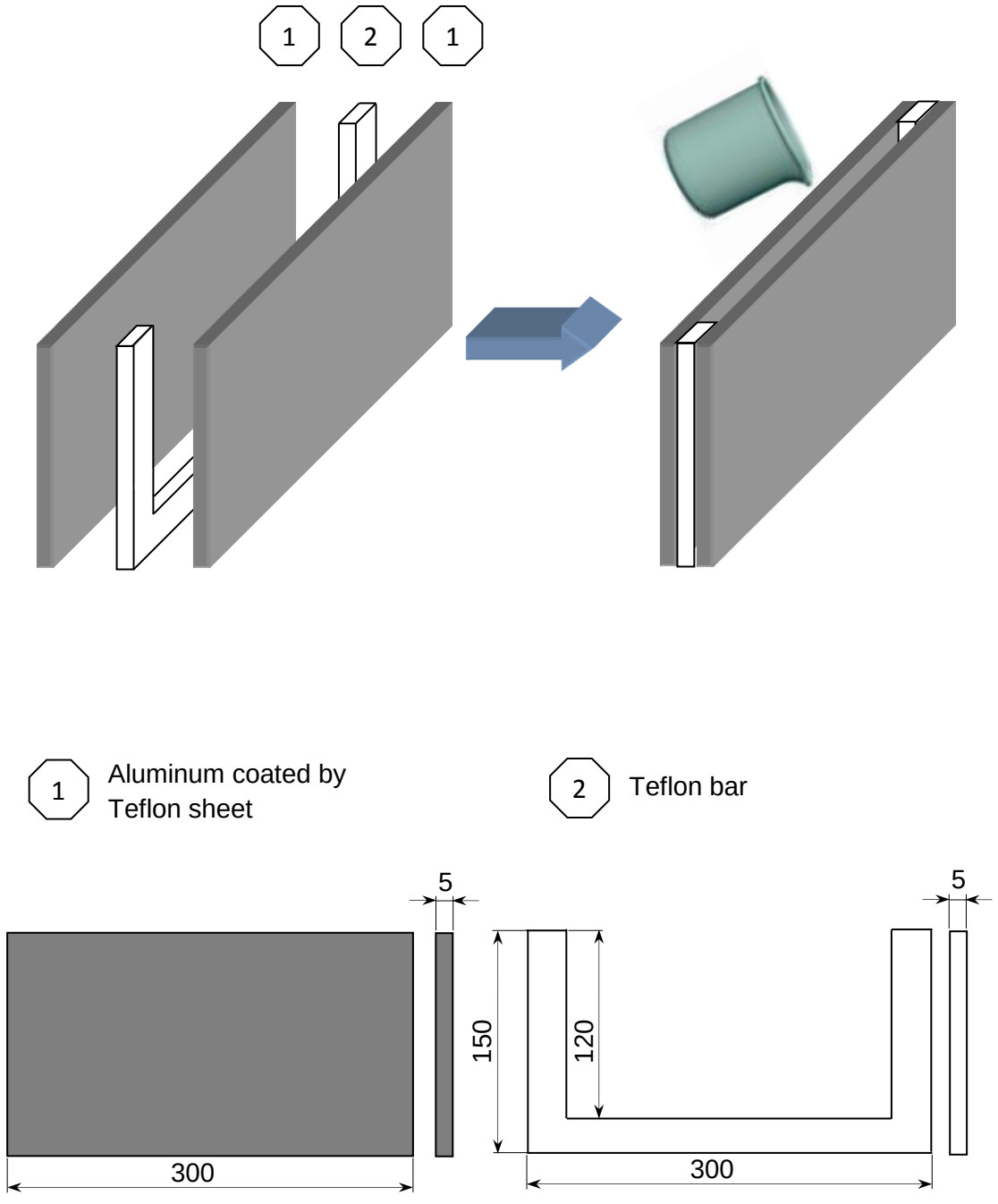

Fig. 2.2 Mold geometry (not to scale). Units in mm.

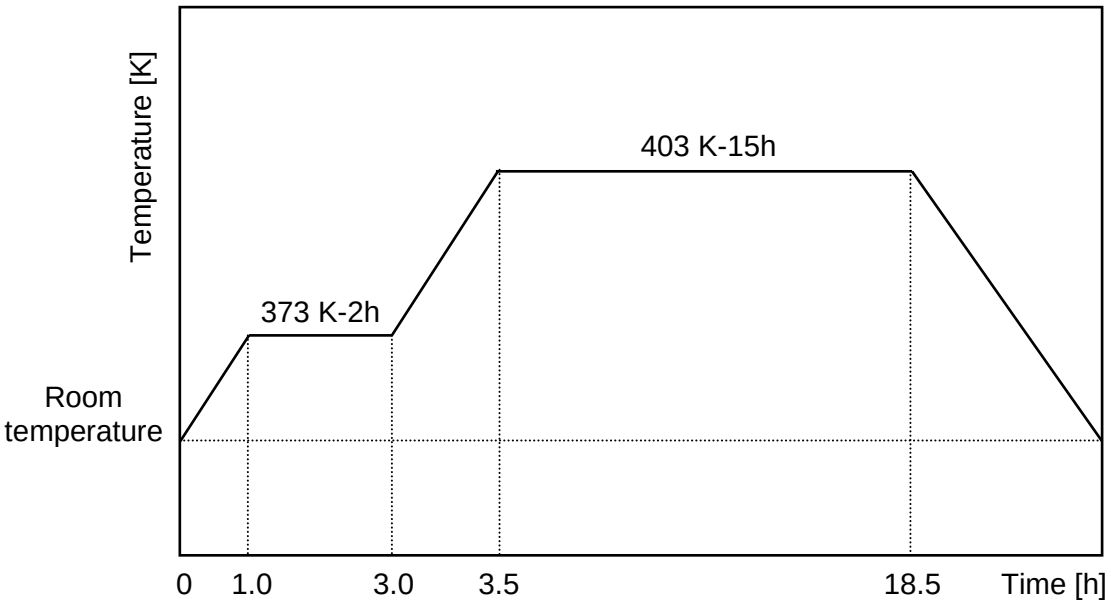

Fig. 2.3 Curing process.

2.3. Experiments

2.3.1. Dynamic mechanical test

The dynamic mechanical properties of the neat epoxy resins and composites were measured by using a non-resonance tensile method with a dynamic viscoelastometer (Rheogel-E4000, UBM), as shown in Fig. 2.4. The specimen was 40 mm long, 5 mm wide, and 2 mm thick.

The dynamic complex moduli of the specimens for the tensile oscillation with a frequency of 10 Hz were measured at each 1 K ranging from 223 K to 493 K. The heating rate was 1 K min^{-1}. The glass transition temperature, T_g, was determined at peaks of the maximum tan δ.

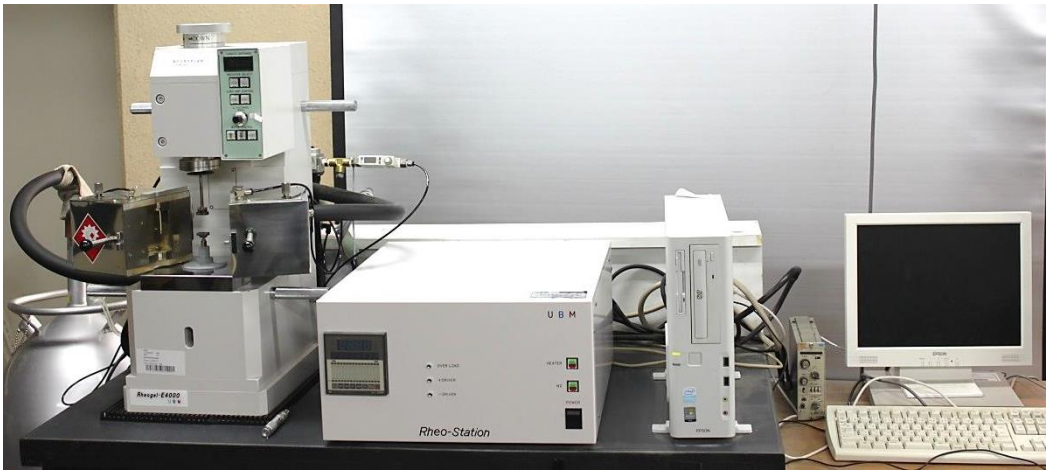

(a) Experimental apparatus

Fig. 2.4 Dynamic viscoelastometer.

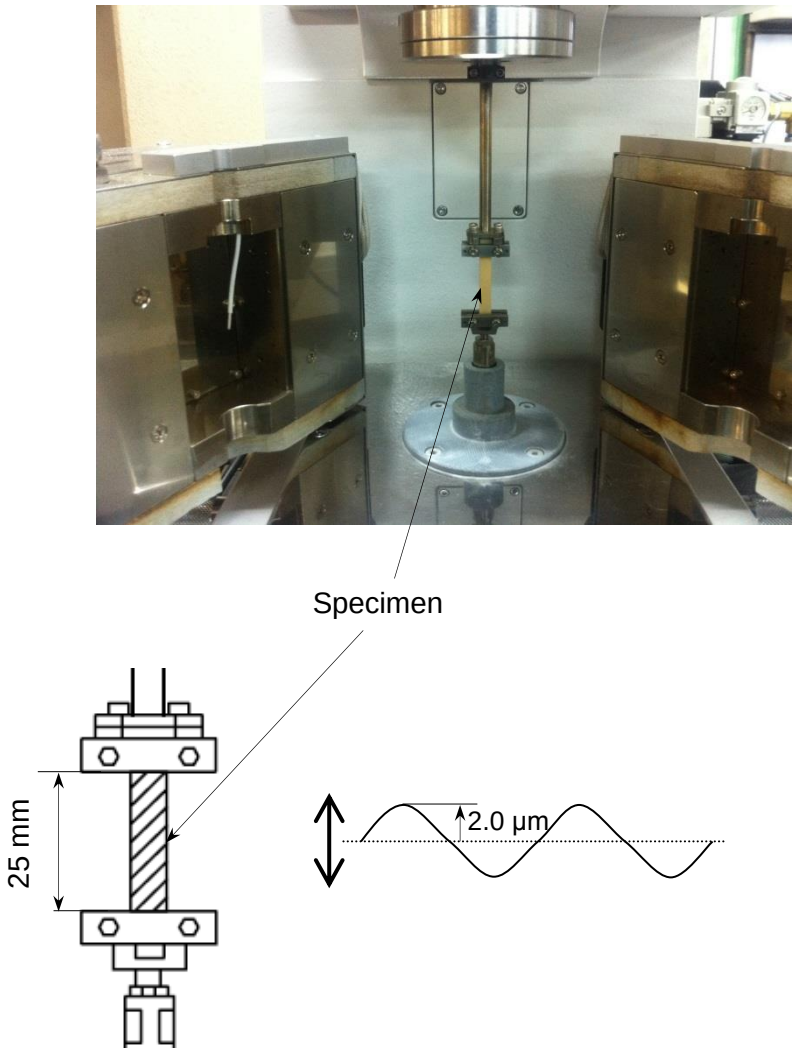

(b) Clamped tension

Fig. 2.4 Dynamic viscoelastometer. (*Continued*).

2.3.2. Bending test

Three-point bending tests were performed on the specimens at room temperature in accordance with ASTM standard D790-07 to measure the bending elastic moduli and the bending strengths. The geometry of the three-point bending test is shown in Fig. 2.5. The specimens cut from the cured materials were 100 mm long, 15 mm wide, and 5 mm thick. The span length between the supports was 60 mm. The constant deflection rate (50 μm s^{-1}) at the loading point was applied and the load was recorded by using a universal materials testing machine (Shimadzu, AGS-J).

The bending elastic modulus, E_B, and bending strength, σ_B, was calculated by

$$E_B = \frac{L^3 m}{4WB^3} \tag{2.1}$$

$$\sigma_B = \frac{3P_{max}L}{2WB^2}, \tag{2.2}$$

where m, P_{max}, W, B, and L are the slope of the initial linear portion of the load-deflection curve, maximum load, width, thickness, and span length of the specimens, respectively.

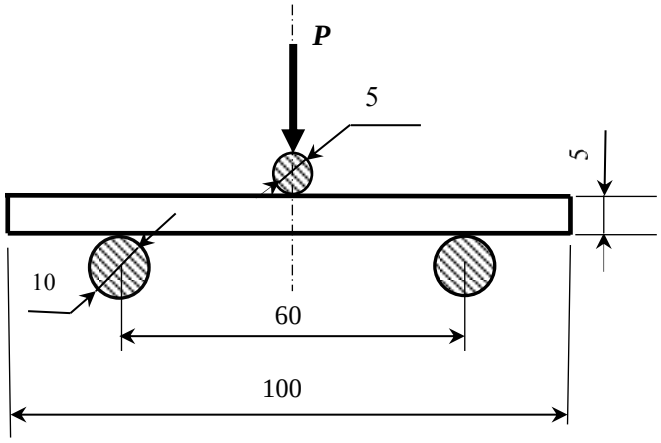

Fig. 2.5 Three-point bending test. Shaded areas represent stainless steel. Specimen unit is mm.

2.4. Experimental Results

2.4.1. Dynamic mechanical result

Figure 2.6 shows the temperature dependences of the dynamic storage moduli, *E',* of the neat epoxy resins and the composites with different EEWRs. The dynamic storage moduli of the neat epoxy resins and the composites decreased gradually as the temperature increased in the glassy states and decreased rapidly in a narrow temperature range near the glass transition temperatures. After that, the moduli increased gradually in the rubbery states. The dynamic storage moduli in the glassy and rubbery states, as well as the glass transition temperature, were clarified to be strongly dependent on the EEWRs. For both the neat epoxy resins and the composites with a higher EEWR, the dynamic storage modulus was larger in the glassy state but smaller in the rubbery state. A comparison of the moduli of the composites and the neat epoxy resins with the same EEWR showed that the composites (Fig. 2.6(b)) had a consistently higher storage moduli than the neat epoxy resins (Fig. 2.6(a)) because the composites were reinforced by silica particles that had a high elastic modulus.

The results of tan δ for the neat epoxy resins and composites are shown in Fig. 2.7. The tan δ of both the composites and the neat epoxy resins had one sharp peak, similar to general epoxy resin. The temperatures at the peaks of the tan δ, namely, the glass transition temperatures, were found to decrease as the ratios of the EEWRs increased.

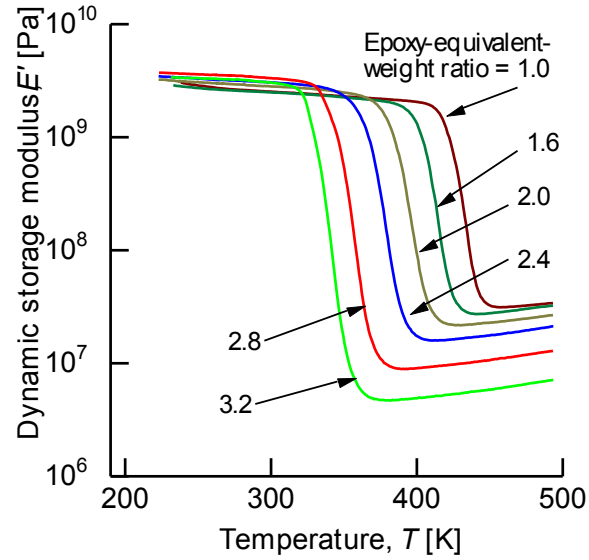

(a) Neat epoxy resins

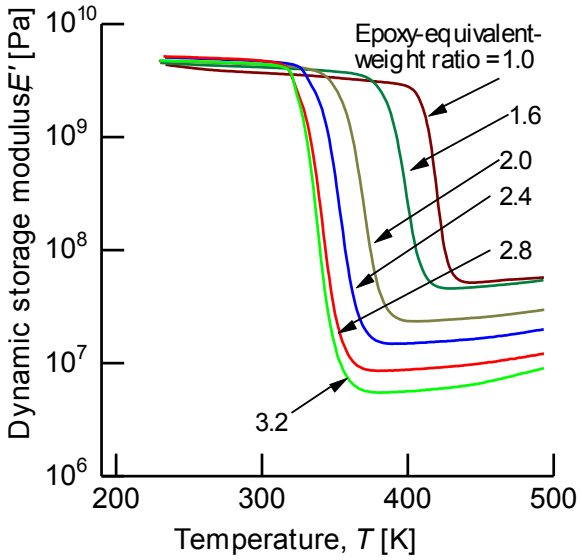

(b) Composites

Fig. 2.6 Temperature dependence of dynamic storage modulus.

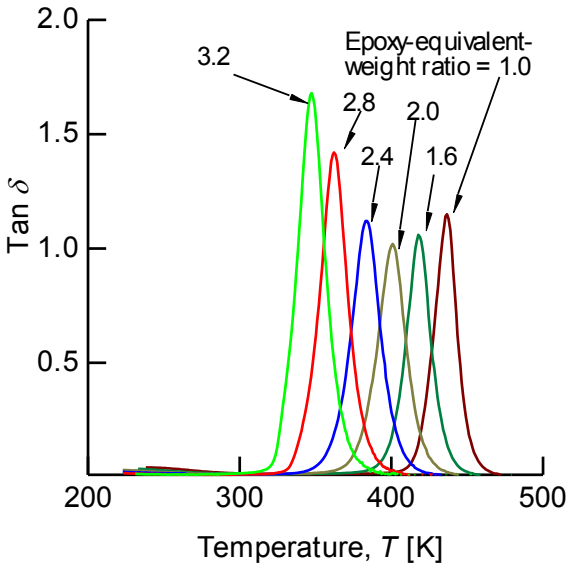

(a) Neat epoxy resins

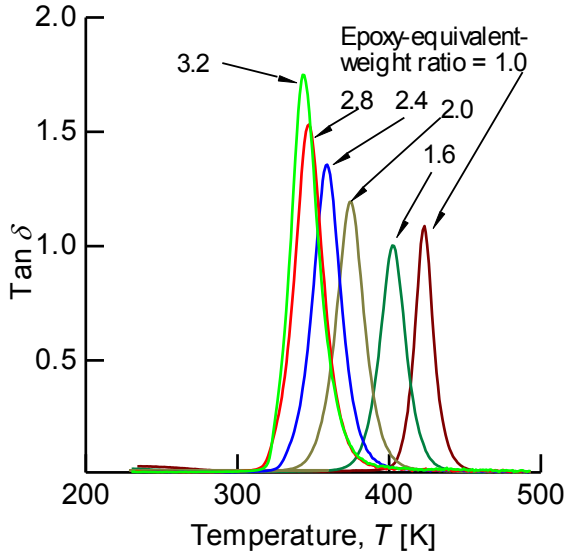

(b) Composites

Fig. 2.7 Temperature dependences of tan *δ*.

2.4.2. Bending test result

Figure 2.8 shows the typical load-deflection curves of the three-point bending tests for the neat epoxy resins and the composites. The load-deflection relations for the neat epoxy resins and the composites were linear and curved near the maximum load, indicating that they were either brittle or quasi-brittle. The slope of the curves for the composites was larger than that for the neat epoxy resins due to the addition of silica particles to the epoxy resin. The maximum load for the neat epoxy resins and the composites increased as the EEWRs decreased. The bending deformations of the neat epoxy resins and the composites were found to strongly depend on the EEWR.

After the bending tests, the fracture surfaces of the composites were observed by SEM as shown in Fig. 2.9. The unevenness of the fracture surfaces were approximately the same even if the composites had different EEWRs. No particles were found to be on every fracture surface. This means that the particles were surrounded by a polymer region, namely the interphase region [2.6, 2.19]. Therefore, the fracture surfaces were not dependent on the EEWRs in the matrix resins.

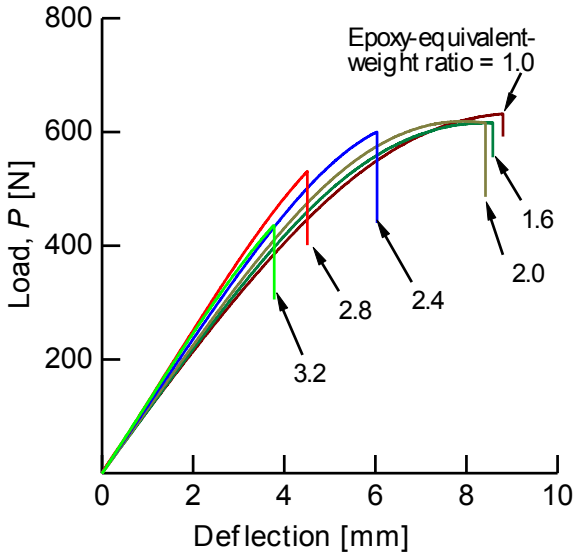

(a) Neat epoxy resins

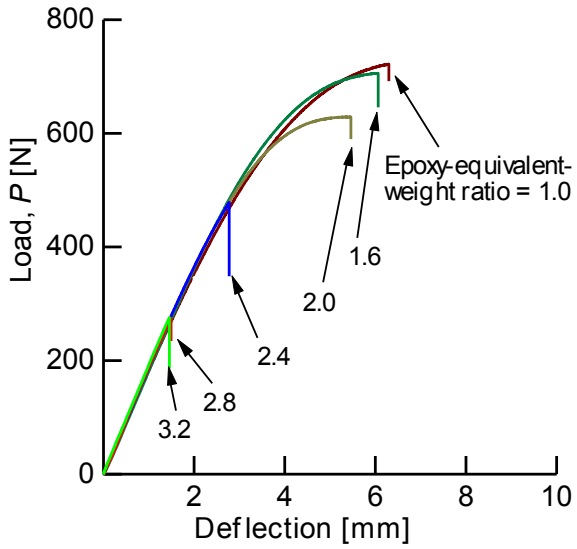

(b) Composites

Fig. 2.8 Load-deflection curves of bending tests.

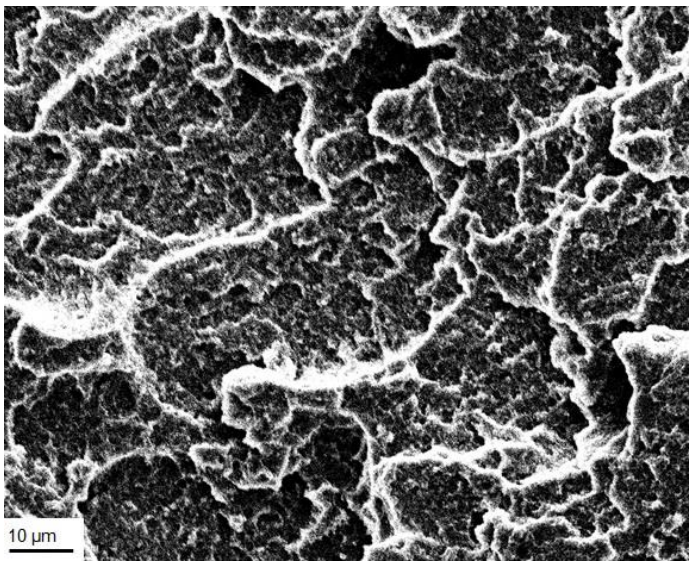

(a) Epoxy equivalent weight ratio = 1.0.

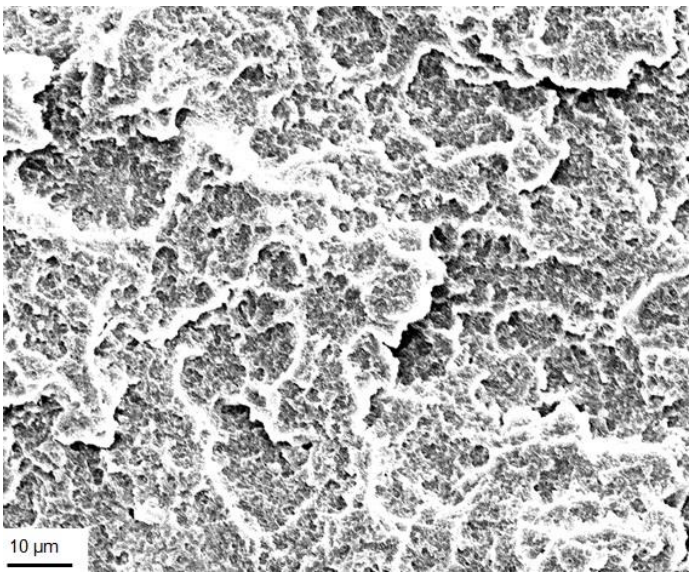

(b) Epoxy equivalent weight ratio = 1.6.

Fig. 2.9 Fracture surface.

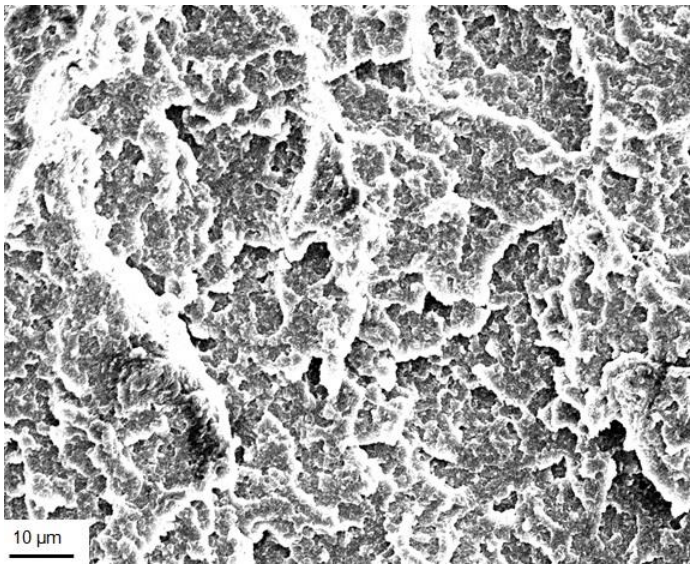

(c) Epoxy equivalent weight ratio = 2.4.

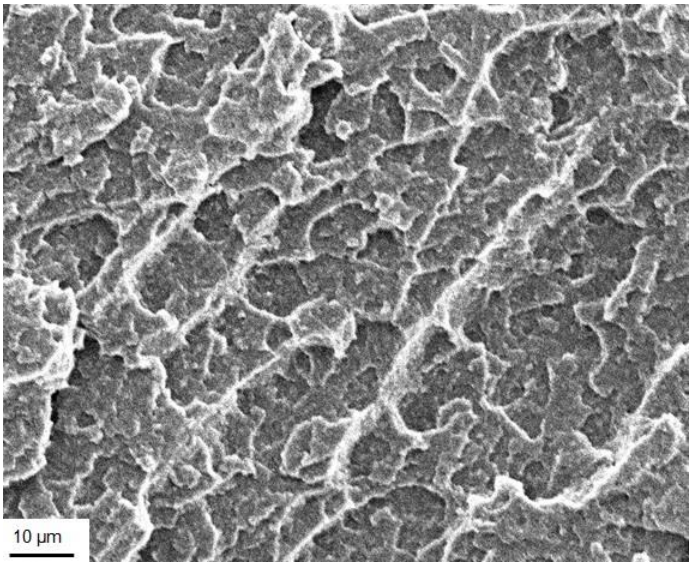

(d) Epoxy equivalent weight ratio = 3.2.

Fig. 2.9 Fracture surface. *(Continued)*

2.5. Discussion

2.5.1. Crosslinking density and glass transition temperature

Network structure is expressed by the degree of cross-linking reaction. Regarding the rubber elasticity theory for incompressible material, the crosslinking density, n, can be determined from the dynamic storage moduli, E', in the rubbery state according to [2.20, 2.21]

$$E' = 3nRT, \tag{2.3}$$

where R is the gas constant (= 8.3145 J mol^{-1} K^{-1}).

The curve slopes of dynamic storage moduli for the neat epoxy resins in Fig. 2.2(b) were calculated from the temperature range of T_g + 30 K to T_g + 50 K. The crosslinking densities in neat epoxy resins with different EEWRs were calculated using Eq. (2.3). The results (Fig. 2.10) indicate that the crosslinking densities were inversely correlative to the EEWRs. The crosslinking densities in the composites were assumed to be the same as the ones of the neat epoxy resins with the same EEWRs [2.20] because the EEWRs are concerned with the chemical reactions of the epoxide resin and the curing agent.

The glass transition temperatures of the neat epoxy resins and the composites were defined as the temperatures having maximum values of the tan δ. The relation between the glass transition temperature, T_g, and the crosslinking densities, n, are shown in Fig. 2.11. The T_g of the neat epoxy resins decreased linearly as the crosslinking densities decreased from the stoichiometric condition (n = 2740 mol m^{-3}). The T_g of the composites, which was lower than that of the neat epoxy resins, is known to be affected not only by the volume fractions of particles, the curing condition, and the system of dispersing particles [2.22, 2.23] but also by the mobility of polymer molecules caused by local adsorption on the silica particles [2.24] and by particles packing [2.15]. The matrix resins with EEWRs both near and far from the stoichiometric conditions were predicted to be very fine and very rough polymer network structures, respectively. Because the interaction between nano-particles and very fine or rough network structures would not be sufficiently strong, the relation between crosslinking densities and the glass transition temperatures for the composite was the same as the one of the neat epoxy resin for the crosslinking densities near 2700 mol m^{-3} and 500 mol m^{-3} in Fig. 2.11. Chain entanglement of the molecules in the matrix resins was considered to be encumbered by the particles in the composites. Therefore, the glass transition temperatures of the composites with crosslinking densities ranging approximately from 1000 mol m^{-3} to 2500 mol m^{-3} were lower than the ones of the neat epoxy resins in Fig. 2.11.

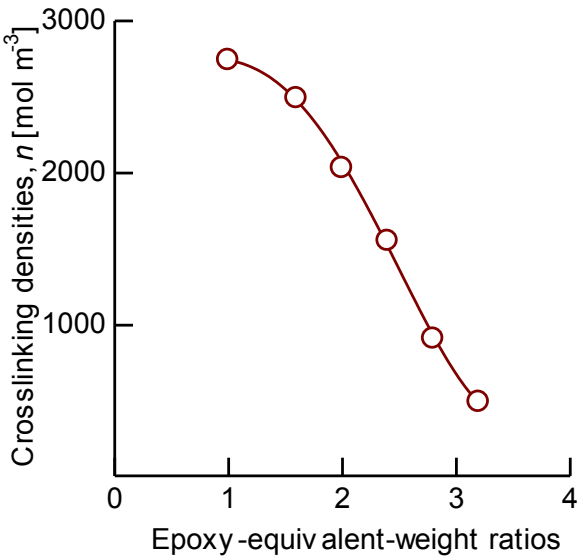

Fig. 2.10 Relation between crosslinking densities and epoxy-equivalent-weight ratios for neat epoxy resins.

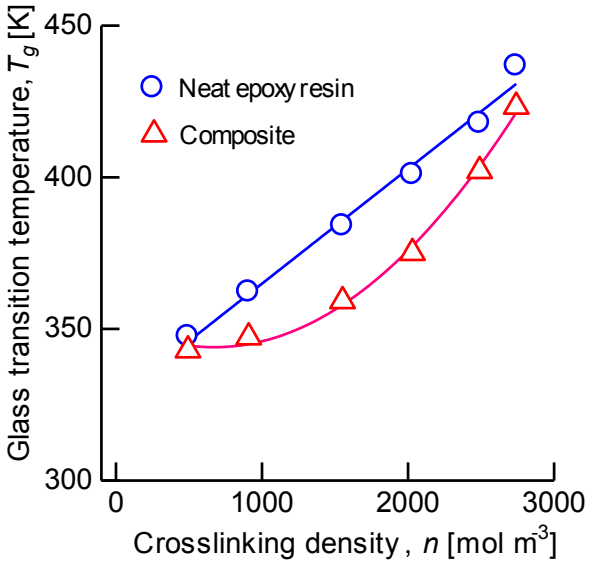

Fig. 2.11 Relation between glass transition temperature and crosslinking densities.

2.5.2. Elastic bending modulus

The bending elastic moduli of the neat epoxy resins and the composites were determined from the load-deflection curves by using Eq. (2.1) (as shown in Fig. 2.12). The circles and triangles in Fig. 2.12 denote the average over seven experiments, and the error bars denote their standard deviations. It is difficult to see the error bars because the standard deviations were less than 6 %. The elastic moduli of composites, E_c, were calculated by using Lewis and Nielsen's equation with the elastic moduli of the neat epoxy resins. The equation is expressed mathematically as [2.5, 2.15, 2.25–2.27]

$$E_C = E_m \frac{1 + ABV_P}{1 - B\psi V_P}, \tag{2.5}$$

where

$$A = \frac{7 - 5\nu_m}{8 - 10\nu_m}, \quad B = \frac{E_P / E_m - 1}{E_P / E_m + A}, \quad \psi = 1 + \left(\frac{1 - \varphi_{\max}}{\varphi_{\max}^2} \right) V_P .$$

Here, V_P, E_P, E_m, and ν are the volume fraction of the silica particles, Young's modulus of particles, Young's modulus of matrix, and Poisson's ratio of matrix, respectively. The subscripts m and p donate the matrix and the particles. The Young's modulus of the particles and Poisson's ratio of the epoxy resins are 72.1 GPa and 0.38, respectively. The maximum packing fraction, φ_{max}, is 0.74 for spheres in closed packing [2.5–2.7, 2.25, 2.27]. The solid line in Fig. 2.8 denotes the result of Lewis and Nielsen's equation with the measured Young's modulus of the epoxy resins.

The bending moduli of the composites were larger than the ones of the neat epoxy resins due to the addition of the silica particles. The moduli of the composites increased slightly as the crosslinking densities decreased from the stoichiometric condition (n = 2740 mol m^{-3}). The measured bending modulus of the composites agreed well with the results calculated from the experimental results of the neat epoxy resins with Lewis and Nielsen's equation. These results indicate that the interaction between the particles and the polymer network structure in the matrix resins did not affect the bending moduli of the composite, because Lewis and Nielsen's equation is derived with the assumption that a composite is a mixture of bulk materials without the interaction effect. This corresponds to the fact that an elastic modulus is generally insensitive to micro-structure in a material and tends to have average properties.

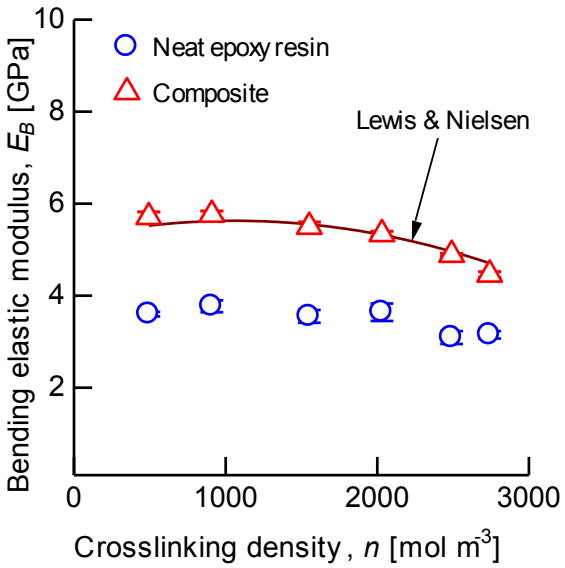

Fig. 2.12 Relation between crosslinking densities and bending elastic moduli.

2.5.3. Dynamic storage modulus

Figure 2.13 shows the dynamic storage modulus of the neat epoxy resins and the composites having different crosslinking densities in the glassy state, with a temperature of T_g – 50 K, and in the rubber state, with a temperature of T_g + 40 K. In the figures, the solid line denotes the moduli of the composites calculated from the result of the neat epoxy resins by using Eq. 2.3.

The dynamic storage modulus of the composites in the glassy state in Fig. 2.13(a) agreed with the results of Lewis and Nielsen's equation. This is the same result as the bending modulus in Fig. 2.12. The storage modulus of both the composites and the neat epoxy resins decreased when the crosslinking densities increased, so the storage modulus was lowest at the highest crosslinking density (stoichiometry ratio). This was caused by the β-relaxation of the epoxy, which occurred at about 185 K, and by the aftermath of low molecular packing [2.15, 2.26, 2.28, 2.29]. The elastic deformation in the glassy state was confirmed to be insensitive to the interaction between the particles and the polymer network structure in the matrix resins.

In contrast, the dynamic storage modulus in the rubbery state disagreed with the results of Lewis and Nielsen's equation (Fig. 2.13(b)). The dynamic storage moduli of the composites were lower than the ones of the neat epoxy resins and were nonlinear; however, those of the neat epoxy resins were linear to the crosslinking densities. Because the mobility of the network structures in the matrix resins became active above the glass transition temperature, the interaction between the particles and the network structures increased. Therefore, the dynamic storage modulus could not be predicted by the mixture law.

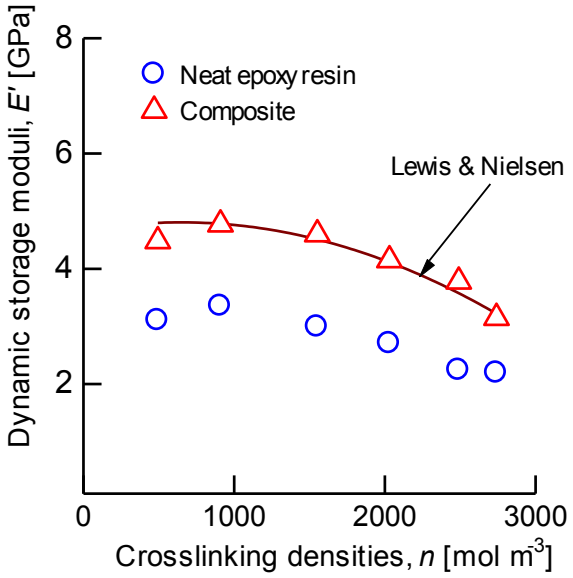

(a) Glassy state

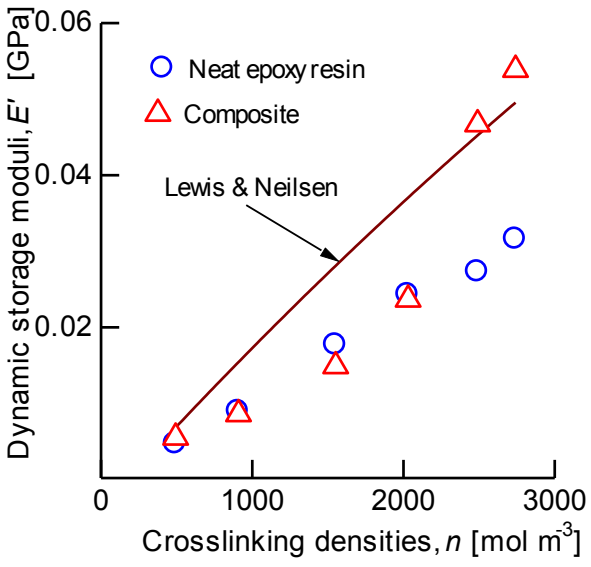

(b) Rubbery state

Fig. 2.13 Dynamic storage moduli for crosslinking densities as a function of temperature.

The bending strengths of the neat epoxy resins and the composites were evaluated from the load-deflection curves by using Eq. (2.2). The results are plotted in Fig. 2.14. The circles and the triangles are the averages of the neat epoxy resins and the composites calculated from more than five experimental results. The error bars indicate the standard deviations of the experiment data and the solid lines show the fitting curves.

The bending strengths of the neat epoxy resins were an approximately constant 150 MPa for the crosslinking densities more than 1500 mol m^{-3} and then decreased suddenly from 150 MPa to 100 MPa for the crosslinking densities less than 1500 mol m^{-3}. As the crosslinking densities of the neat epoxy resins decreased from the density of the stoichiometrically cured resins, weak entangling of the molecular chains in the matrix resins with rough network structures and low crosslinking density reduced the bending strength.

The bending strengths of the composites decreased gradually in the crosslinking density ranging approximately from 2740 mol m^{-3} to 2000 mol m^{-3} but decreased drastically below the crosslinking density of 2000 mol m^{-3}. The strengths of the composites were considerably smaller than the ones of the neat epoxy resins, in spite of the added silica particles. In the end, the decrease to the strengths became more moderate. The drastic reduction of the strengths was caused not only by reducing the crosslinking density in the matrix resins but also by the interaction effect between the silica particles and the network structures in the matrix resins. The existence of the nano-silica particles encumbered the entanglements of the molecular chains in the matrix resins with rough network structures and low crosslinking density. Therefore, adding the nano-silica particles was totally counterproductive in terms of strengthening the composites with matrix resins having low crosslinking densities.

The elastic moduli were confirmed to be governed by the volume fraction of the silica particles and the strengths were found to be strongly dependent on network structures, namely, the crosslinking densities. It should be noted that the strength of the composites is likely to be weakened by adding nano-particles to matrix resins with a low crosslinking density.

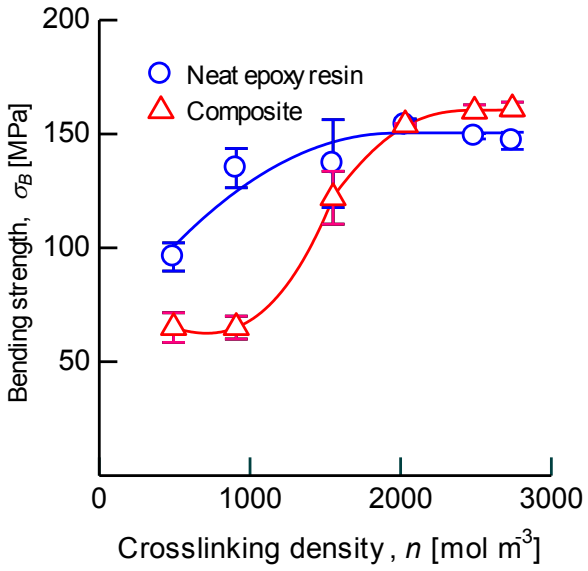

Fig. 2.14 Effect of crosslinking densities on bending strength.

2.6. Conclusion

This chapter provided thermo-viscoelastic and bending strength for nano-silica particulate-reinforced epoxy composites with different crosslinking densities in matrix resins. The composite materials were prepared by adding silica particles that had a median diameter of 240 nm to the diglycidyl ether of bisphenol A type epoxy resin that were then cured methyl-tetrahydro-phthalic anhydride as a curing agent in several non-stoichiometric mixed quantities. The volume fraction of the particles was kept at 0.2 for every composite.

The glass transition temperatures of the neat epoxy resins decreased linearly as the crosslinking densities decreased from the stoichiometric condition, and the glass transition temperatures of the composite were lower than those of the neat epoxy resins. The interaction effects between nano-particles and network structures in matrix resin reduced the glass transition temperatures of the composite because the chain entanglement of the molecules in the matrix resin was considered to be encumbered by the particles.

Both the bending moduli and the dynamic storage moduli in the glassy state of the composites were larger than those of the neat epoxy resins and increased slightly as the crosslinking densities decreased from the stoichiometric condition. The interaction effects between the silica particles and the polymer network structure in the matrix resins did not affect either the bending moduli or the dynamic storage moduli in the glassy state of the composite because an elastic modulus is typically insensitive to microstructures in a material. The mobility of the molecules in the matrix resins became active above the glass transition temperature, and the interaction increased, so the dynamic storage moduli could not be predicted by the mixture law.

The bending strengths were very sensitive to the microstructures, and the strengths for the composites were more sensitive than those of the neat epoxy resins. The interaction effects between nano-particles and network structures reduced the bending strengths because the existence of the nano-silica particles encumbered the entanglements of the molecular chains in the matrix resins having rough network structures with low crosslinking densities.

2.7. References

[2.1] Yamatomo I., Higashihara T., Kobayashi T., Effect of silica-particle characteristics on impact/usual fatigue properties and evaluation of mechanical characteristics of silica-particle epoxy resins, *the Japan Society of Mechanical Engineering International Journal*, Vol. 46, No. 2, pp. 145–153, 2003.

[2.2] Moloney A.C., Kausch H.H., Stieger H.R., The fracture of particulate-filled epoxide resins, *Journal of Materials Science*, Vol. 18, pp. 208-216, 1983.

[2.3] Moloney A.C., Kausch H.H., Kaiser T., Beer H.R., Review parameters determining the strength and toughness of particulate filled epoxide resins, *Journal of Materials Science*, Vol. 22, pp. 381-393, 1987.

[2.4] Moloney A.C., Cantwell W.J., Kausch H.H., Parameters determining the strength and toughness of particulate-filled epoxy resins, *Polymer Composites*, Vol. 8, pp. 314-323, 1987.

[2.5] Adachi T., Araki W., Nakahara T., Yamaji A., Gamou M., Fracture toughness of silica particulate-filled epoxy composite, *Journal of Applied Polymers Science,* Vol. 86, pp. 2261–2265, 2002.

[2.6] Adachi T., Osaki M., Araki W., Kwon S.Ch., Fracture toughness of nano- and micro-spherical silica-particle-filled epoxy composite, *Acta Materialia*, Vol. 56, pp. 2101–2109, 2008.

[2.7] Adachi T., Araki W., Higuchi M., Mixture law including particle-size effect on fracture toughness of nano- and micro-spherical particle-filled composites, *Acta Mechanic,* Vol. 214, pp. 61–69, 2010.

[2.8] Nakamura Y., Yamaguchi M., Kitayama A., Okubo M., Matsumoto T., Effect of particle size on fracture toughness of epoxy resin filled with angular-shaped silica, *Polymer*, Vol. 32, No. 12, pp. 2221–2229, 1991.

[2.9] Nakamura Y., Yamaguchi M., Okubo M., Matsumoto T., Effect of particle size on impact properties of epoxy resin filled with angular shaped silica particles, *Polymer*, Vol. 32, No. 16, pp. 2976–2979, 1991.

[2.10] Nakamura Y., Yamaguchi M., Okubo M., Matsumoto T., Effects of particle size on mechanical properties of epoxy resin filled with angular-shaped silica, *Journal of Applied Polymer Science*, Vol. 44, pp. 151–158, 1992.

[2.11] Preghenella M., Pegoretti A., Migliaresi C., Atomic force acoustic microscopy analysis of epoxy-silica nanocomposites, *Polymer Testing*, Vol. 25, pp. 443–451, 2006.

[2.12] Kitey R., Tippur H. V., Dynamic crack growth in particulate bimaterials having discrete and diffuse interfaces: Role of microstructure, *Engineering Fracture Mechanics*, Vol. 72, pp. 2721-2743, 2005.

[2.13] Brechet Y., Cavaille J.Y.Y., Chabert E., Chazeau L., Dendievel R., Flandin L., Gauthier C., Polymer based nanocomposites: effect of filler-filler and filler-matrix interactions*, Advanced Engineering Materials,* Vol. 3, pp. 571–577, 2001.

[2.14] Kwon S.Ch., Adachi T., Araki W., Yamaji A., Effect of particle size on fracture toughness of spherical silica particles filled epoxy composite, *Key Engineering Materials*, Vol. 297-300, pp. 207–212, 2005.

[2.15] Kwon S.Ch., Adachi T., Araki W., Yamaji A., Thermo-viscoelastic properties of silica particulate reinforced epoxy composites: considered in terms of particle packing model*, Acta Materialia*, Vol. 54, pp. 3369–3374, 2006.

[2.16] Rong M.Z., Zhang M.Q., Pan S.L., Lehmann B., Friedrich K., Analysis of the interfacial interactions in polyprotlene/silica nanocomposites, *Polymer International,* Vol. 53, pp.176–183, 2004.

[2.17] Brechet Y., Cavaille J.Y.Y., Chabert E., Chazeau L., Dendievel R., Flandin L., Gauthier C., Polymer based nanocomposites: effect of filler-filler and filler-matrix interactions*, Advanced Engineering Materials,* Vol. 3, pp. 571–577, 2001.

[2.18] Kovacevic V., Lucic S., Leskovac M., Morphology and failure in nanocomposites Part I: structural and mechanical properties*, Journal of Adhesion Science and Technology,* Vol. 16, pp. 1343–1365, 2002.

[2.19] Zhang H., Zhang Z., Friedrich K., Eger C., Property improvements of in situ epoxy nanocomposites with reduced interparticle distance at high nanosilica content, *Acta Materialia*, Vol.54, pp.1833–1842, 2006.

[2.20] Bignotti F., Pandini S., Baldi F., De Santis R., Effect of the resin/hardener ratio on curing, structure and glass transition temperature of nanofilled epoxies, *Polymer Composites*, Vol. 32, pp. 1034–1048, 2011.

[2.21] Ward IM, *Mechanical properties of solid polymers*, 2nd edn., Wiley, New York, 1990.

[2.22] Yasmin A., Danial I. M., Mechanical and thermal properties of graphite platelet/epoxy composites, *Polymer*, Vol. 45, pp. 8211-8219, 2004.

[2.23] Lopez J., Ramirez C., Abad M. J., Barral L., Cano J., Diez F., Dynamic mechanical analysis of an epoxy/thermoplastic blend: polymerization-induced phase separation, *Polymer International*, Vol. 51, pp. 1100-1106, 2002.

[2.24] Nikkeshi S., Kudo M., Masuko T., Dynamic viscoelastic properties and thermal properties of Ni powder-epoxy resin composites, *Journal of Applied Polymer Science*, Vol. 69, pp. 2593-2598, 1998.

[2.25] Kwon S.Ch., Adachi T., Araki W., Yamaji A., Effect of composing particle of two sizes on mechanical properties of spherical-silica-particulate-reinforced epoxy composite, *Composites Part B*, Vol. 39, pp. 740-746, 2008.

[2.26] Kwon, S.Ch., Adachi, T., Araki, W., Temperature dependence of fracture toughness of silica/epoxy composites: related to microstructure of nano- and micro-particles packing, *Composites Part B*, Vol. 39, pp. 773–781, 2008.

[2.27] Nielsen L.E., Landel R.F., *Mechanical properties of polymers and composites*, 2nd edn. Marcel Deckker, New York, 1994.

[2.28] Munz M., Sturm H., Stark W., Mechanical gradient interphase by interdiffusion and antiplasticisation effect-study of an epoxy/thermoplastic system, *Polymer*, Vol. 46, pp. 9097-9112, 2005.

[2.29] García del Cid M.A., Prolongo M.G, Salom C., Arribas C., Sánchez-Cabezudo M., Masegosa R.M., The effect of stoichiometry on curing and properties of epoxy-clay nanocomposites, *Journal Thermal Analyze Calorim*, Vol.108, pp. 741–750, 2012.

CHAPTER 3
COMPRESSION BEHAVIOR

3.1. Introduction

Epoxy composite filled with silica particles is widely applied to various engineering fields, such as for industrial application to packaging materials in electronic devices, aircraft and automotive components, etc., because of their excellent mechanical and insulation properties. The size of silica particles is currently decreased below the micrometer level to manufacture nano-composites with superior mechanical properties [3.1–3.9]. The dynamic mechanical properties of the composites are required to improve the reliability of devices or components. Therefore, the interaction effects between network structures in epoxy resins and silica particles on the dynamic mechanical properties must be clarified.

Several researchers have investigated the dynamic compression behavior responses of nano-silica particle filled epoxy composites. Zheng et al. [3.10] considered the impact strengths of composites having different contents of silica particles. They denoted that inhomogeneous dispersion of the nano-particles caused variation in the impact strengths. Gou and Li [3.11] concluded that the performance of silica/epoxy nano-composites in quasi-static and dynamic responses was dependent on loading rates and nano-particle dispersion. Jajam and Tippur [3.12] reported that quasi-static fracture toughness of silica nano-composites was significantly higher than the micro-silica particle filled epoxies. The reduction of interparticle distance owing to their small particle size resulted in more interactions between particles and the epoxy matrix. The interfacial interaction of particles with a surrounding matrix has a close relationship with the crosslinking network morphology in a polymer matrix [3.13–3.16]. The dynamic behaviors of nano- or micron-silica particle-reinforced epoxy composites are considerably dependent not only on the particle size but also on the network structure of the epoxy resin matrix.

As previously reported in Chapter 2, the interactions between nano-particles and network structures increase the bending strengths for high crosslinking densities [3.17]. In this chapter, the interaction effects between nano-particles and network structures on the compression properties of nano-silica particulate-reinforced epoxy composites were clarified experimentally by using non-stoichiometric curing effects in matrix resin. Static and dynamic compression tests were performed by using a universal material testing machine and a split Hopkinson pressure bar testing machine [3.18, 3.19]. The crosslinking densities and glass transition temperatures of the neat epoxy resins and composites were identified from thermo-viscoelastic properties measured by dynamic

mechanical analysis. Finally, the compressive yield stresses of the composites were discussed in order to consider the interaction between the particles and the network structures in the matrix resins.

3.2. Specimens

3.2.1. Materials

Epoxy resin was filled with silica particles to make the composite materials for the specimens. The epoxide resin in the experiment was a diglycidyl ether of bisphenol A type epoxy resin (Asahi Kasei E-Materials, AER 2603), and the equivalent weight was 188 grams/equivalent. The curing agent was methyl-tetrahydro-phthalic anhydride (New Japan Chemical, Rikacid MH-700), and the acid anhydride equivalent weight was 162 grams/equivalent. The accelerator was 2,4,6-tris (dimethyl aminomethyl) phenol (Mitsubishi Chemical, jER BMI12). The mixture weight ratio of the epoxide resin, the curing agent, and the accelerator was 100 : 86 : 0.5 according to stoichiometry.

The filler of the composite was spherical silica particles with a median diameter of 240 nm (Tatsumori, SO-C1), and the volume fraction of the silica particles was 0.2 for every composite. The surfaces of the particles were not chemically coated.

3.2.2. Preparation

In this chapter, the mixture ratio was changed in order to consider the interaction between the silica particles and the matrix resins. The mixture ratio of the epoxy resin to the curing agent is hereafter denoted as the epoxy-equivalent-weight ratio (EEWR) obtained by changing the epoxide resin weight over the stoichiometric epoxide resin weight in the mixture. The EEWRs in this experiment were modified in a range from 1.0 to 3.2, and the accelerator was kept constant at 0.5, as shown in Table 3.1. The complete network structures in the matrix resin was produced at stoichiometric composition, corresponding to EEWR = 1.0, and the incomplete network structures in the matrix resin were produced for EEWRs > 1 caused by the exaggerated mixtures of epoxide resin. The EEWRs over 3.2 were not selected because the materials cured with EEWR > 3.2 were too weak to measure viscoelastic properties and unreacted curing agents in the materials with EEWR < 1.0 could be transferred out of the cured resins.

To produce composite materials as specimens, nano-spherical-silica particles were mixed with epoxide resin, a curing agent, and an accelerator until any

agglomerates of particles disappeared. The mixtures of epoxy/silica were stored in a vacuum vessel to remove voids, poured into an aluminum mold coated with a Teflon sheet, and then set in an oven. The mold was 260 mm long, 5 mm wide, and 120 mm deep. The curing procedure was performed in two steps. For the first step, pre-curing, the epoxy was kept at 373 K for 2 h to gel the matrix resin. The second step, post-curing, which greatly affects the crosslinking reaction of the resin, was performed at 403 K for 15 h. The heating rate from pre-curing to post-curing was constant at 72 K/h. For comparison, neat epoxy resins were also prepared and cured in the same process as that for the composites. Both the neat epoxy resins and the composites were used in the experiment listed in Table 3.1.

The densities of the cured materials were measured in accordance with ASTM standard 792-08. The results are listed in Table 3.1. The densities of both the neat epoxy resins and the composites were confirmed to be independent of the EEWR.

Table 3.1 Neat epoxy resins and composites used in experiment

Materials	Matrix (weight ratio)			EEWR	Volume fraction of silica particles	Density [kg/m^3]
	Epoxide resin	Curing agent	Accelerator			
Composite	100	86	0.5	1.0	0.2	1400
	160	86	0.5	1.6	0.2	1400
	200	86	0.5	2.0	0.2	1400
	240	86	0.5	2.4	0.2	1400
	280	86	0.5	2.8	0.2	1400
	320	86	0.5	3.2	0.2	1410
Neat epoxy resin	100	86	0.5	1.0	-	1200
	160	86	0.5	1.6	-	1200
	200	86	0.5	2.0	-	1200
	240	86	0.5	2.4	-	1200
	280	86	0.5	2.8	-	1200
	320	86	0.5	3.2	-	1200

3.2.3. Characterization

A dynamic viscoelastometer (Rheogel-E4000, UBM) using a non-resonance tensile method was conducted to measure the dynamic mechanical properties of the neat epoxy resins and composites. The specimen was 40 mm long, 5 mm wide, and 2 mm thick. The dynamic complex moduli of the specimens for the tensile oscillation with a frequency of 10 Hz were measured at each 1 K ranging from 223 K to 493 K. The heating rate was 1 K/min.

Figure 3.1 shows the dependency of the dynamic storage moduli, *E*', and loss tan δ, on the temperature of the neat epoxy resins and the composites with different EEWRs. The dynamic storage moduli of the neat epoxy resins and the composites decreased gradually as the temperature increased in the glassy states and decreased rapidly in a narrow temperature range near the glass transition temperatures, after which the moduli increased gradually in the rubbery states. The tan δ of both the composites and the neat epoxy resins had one sharp peak, similar to general epoxy resin. The dynamic storage moduli in the glassy and rubbery states, as well as the temperatures at the peaks of the tan δ, namely, the glass transition temperatures T_g, were clarified to be strongly dependent on the EEWRs.

Network structures in the epoxy resins were expressed by the degree of the cross-linking reaction. Regarding the rubber elasticity theory for incompressible material, the crosslinking density *n* can be determined from *E*' in the rubbery state, which can be expressed as follows [3.20, 3.21]:

$$E' = 3nRT, \tag{3.1}$$

where *T* and *R* are the absolute temperature and the gas constant (= 8.3145 J $mol^{-1}K^{-1}$). From the neat epoxy resin curve slopes of the dynamic storage moduli (Fig. 3.1 (a)) with the temperature range of T_g + 30 K to T_g + 50 K, the crosslinking densities in matrix resins with different EEWRs were calculated by using eq. (3.1). Because the EEWRs are concerned with the chemical reactions of the epoxide resin and the curing agent, the crosslinking densities in the composites were assumed to be the same as those of the neat epoxy resins with the same EEWRs [3.20]. The relation between the glass transition temperature T_g and the crosslinking densities *n* are shown in Fig. 3.2. The T_g of the neat epoxy resins decreased linearly as the crosslinking densities decreased from the stoichiometric condition. The T_g of the composites was lower than that of the neat epoxy resins.

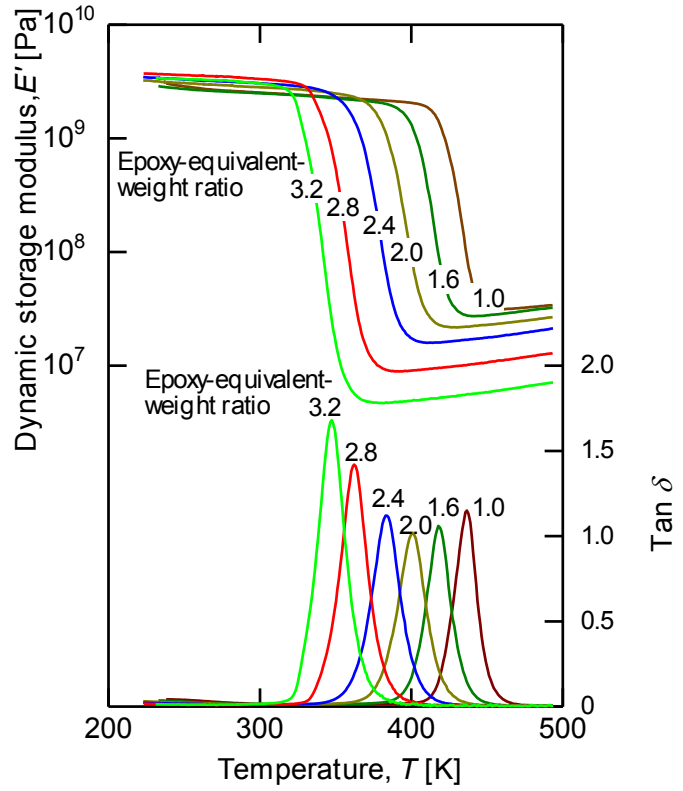

(a) Neat epoxy

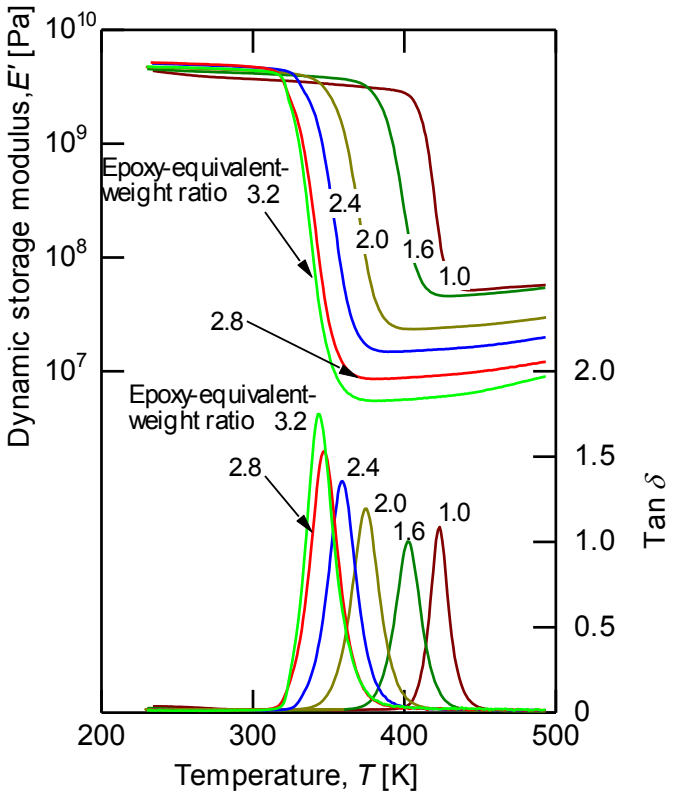

(b) Composites

Fig. 3.1 Temperature dependence of dynamic storage modulus and tan δ.

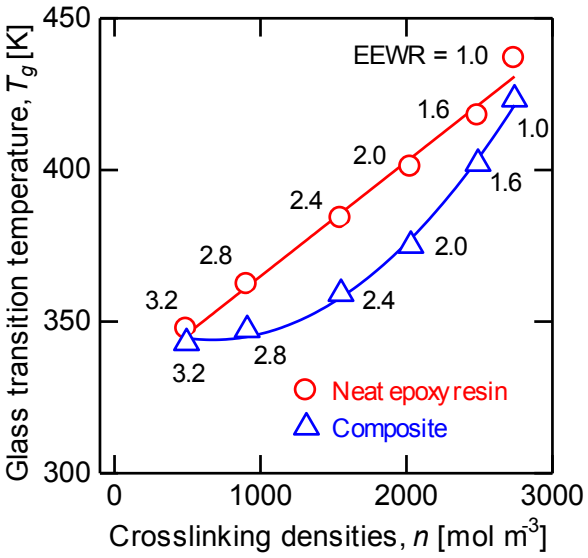

Fig. 3.2 Relation between glass transition temperature and crosslinking densities.

3.3. Compression Tests

Static compression tests were performed on a material testing machine (Autograph DCS-25 T, Shimadzu) with a constant displacement rate, 1 mm/min at room temperature, as shown in Fig. 3.3. The specimens were 5 mm high, 10 mm long, and 10 mm wide. The strain rate for the tests was approximately 3.3×10^{-3} 1/s.

Fig. 3.3 Material testing machine (Autograph DCS-25 T, Shimadzu).

Dynamic compression tests were conducted at a high strain rate ranging from 500 to 1500 1/s by using a split Hopkinson pressure bar (SHPB) machine [3.19] at room temperature, depicted in Fig. 3.4. The specimens cut from the cured materials were square plates that were 10 mm long, 10 mm wide, and 5 mm thick. In the preliminary, we confirmed that the measured stress-strain curves for the square-plate specimens were the same as those for specimens having smaller or larger shapes than the cross-section of the bars in the SHPB test. Strain gauges (KFG-5-120-C1, Kyowa) were attached on the input and output bars to measure the pulses incident, reflected and transmitted to the specimens. The strain gauge signals were measured by using DC strain amplifiers (AS2101, NEC) and a data logger (Hicoder 8835, Hioki). The material type of bars is high strength aluminum A7075-T6 (E = 73.2 GPa, and ρ= 2800 kg/m^3). The strain wave's incident, $\varepsilon_I(t)$, reflecting, $\varepsilon_R(t)$, and transmitting, $\varepsilon_T(t)$, to the specimens were evaluated from the strain histories, $\varepsilon_1(t)$ measured at the middle point of the input bar and $\varepsilon_2(t)$ measured at 500 mm from the tip of the output bar. On the basis of the hypotheses of equilibrium and uniform strain in the specimen, the histories of stress, $\sigma(t)$, strain, $\varepsilon(t)$, and strain rate, $\dot{\varepsilon}(t)$, of the test samples were calculate by using the following equations,

$$\sigma(t) = E\{\varepsilon_I(t) + \varepsilon_R(t)\} = E\varepsilon_T(t), \tag{3.2}$$

$$\varepsilon(t) = -2\frac{C}{L_S}\int_0^t \varepsilon_R(t)dt, \tag{3.3}$$

$$\dot{\varepsilon}(t) = -2\frac{C}{L_S}\varepsilon_R(t), \tag{3.4}$$

where C and E are the velocity of the longitudinal elastic wave and the Young's modulus of a bar. L_S refers to the thickness of the specimens. The stress-strain curves of the specimens were calculated from the histories of the stress and strain. The strain rate was evaluated by averaging the numerical results calculated from eq. (3.4).

Figure 3.5 plots the strain histories, $\varepsilon_1(t)$ and $\varepsilon_2(t)$, in the input and output bars for the composite specimen with EEWR = 1.0 as an example. The stress histories on the front and back faces of the specimens were evaluated by using the middle and right equations of eq. (3.2) substituted with the experimental results in Fig. 3.6. Both stress histories on the front and back sides of the specimens were confirmed to coincide mutually. Therefore, dynamic equilibrium during the SPBH test was found to be satisfied. The validities of the other SHPB tests were also confirmed.

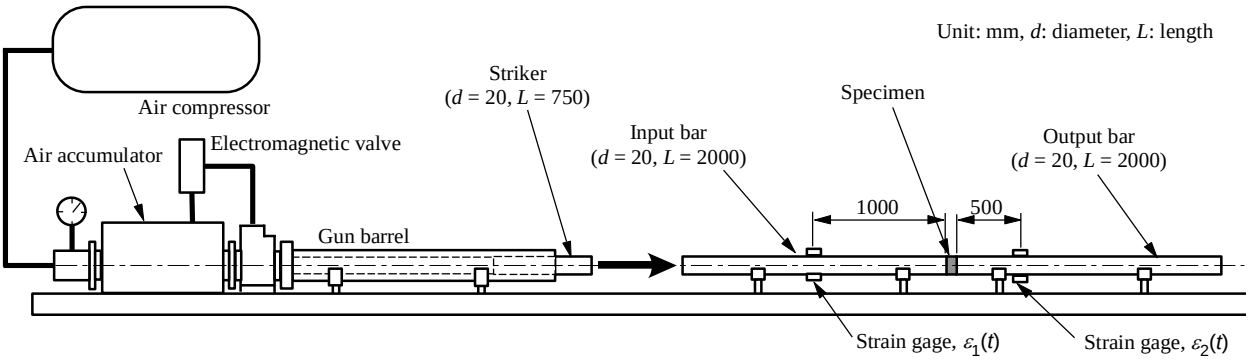

Fig. 3.4 Split Hopkinson pressure bar (SHPB) testing machine.

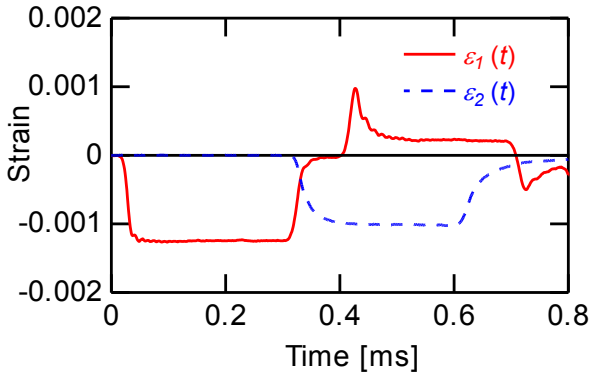

Fig. 3.5 Strain histories on input and output bars for composite with EEWR = 1.0 and strain rate 760 1/s.

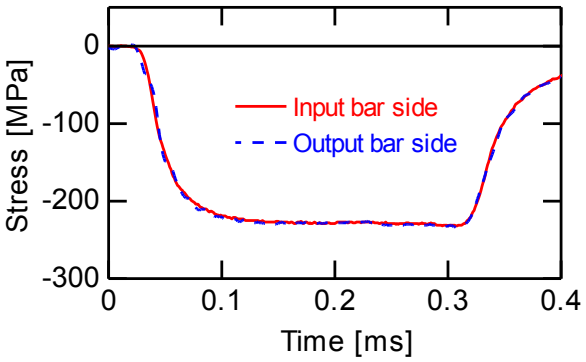

Fig. 3.6 Histories of stresses applied to sides of input and output bars for composite material with EEWR = 1.0 and strain rate of 760 1/s.

3.4. Experimental Results

Figure 3.7 shows compressive stress-strain curves of the composites and the neat epoxy resins that were measured under various strain rates in the dynamic and static compression tests. The neat epoxy resins and the composites were not broken within the stress-strain curves in Fig. 3.7. The interruptions of stress-strain curves mean that unloading processes began in the SHPB tests.

The compressive stress-strain curves for the stoichiometrically cured epoxy resins and composites (EEWR = 1.0) under various strain rates of the composites and the neat epoxy resins are shown in Fig. 3.7(a). The stress-strain relations for the composites and the neat epoxy resins were linearly elastic before yielding and were relatively constant after the yield stress. The compressive stresses varied rapidly after the region of constant stress. The yield stress of both the composites and the neat epoxy resins increased when the strain rate increased from the static compression test condition. The yield stresses and the Young's moduli of the composites were higher than the neat epoxy resins because the epoxy resins were reinforced by adding the silica particles.

As the strain rates increased, the Young's modulus of both the neat epoxy resins and composites increased similar to the viscoelastic properties (Figs. 3.1 and 3.2), and the yield stresses also increased. The stress-strain curves of the non-stoichiometrically cured epoxy resin having EEWR = 1.6 are shown in Fig. 3.7(b). The yield stresses of the composites were higher than the neat epoxy resins under the same strain rate. Moreover, the stresses after the yielding reduced for both the composite and the neat epoxy resin. The yield stresses of the material having the EEWRs = 2.0 (Fig. 3.7(c)) and 2.4 (Fig. 3.7(d)) were approximately the same for high strain rates, although the yield stresses of the composites were higher than those of the neat epoxy resins for low strain rates.

The stress-strain curves of the composites and neat epoxy resins having an EEWR larger than 2.8 are shown in Figs. 3.7(e) and (f). The Young's moduli could be explained by the viscoelastic properties. The yield stresses of the neat epoxy resins were higher than those of the composites with the same strain rate. In general, the stress-strain curves of the composites and the neat epoxy resins were strongly dependent on the strain rates. For both the neat epoxy resins and composites, softening after yielding was found remarkably in low crosslinking densities.

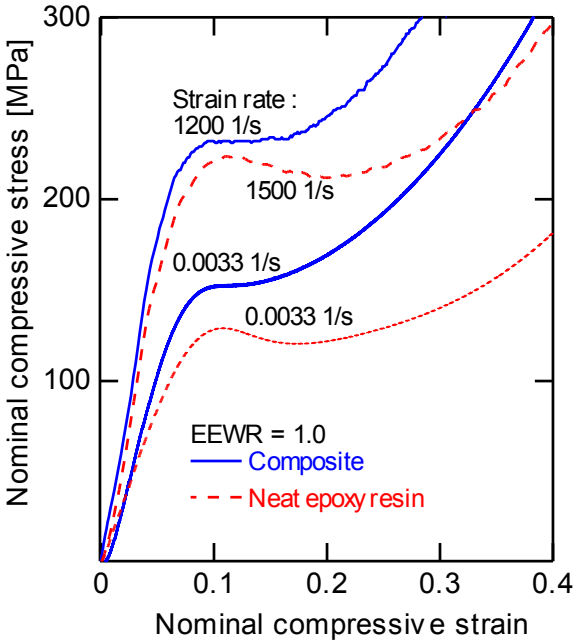

(a) EEWR 1.0

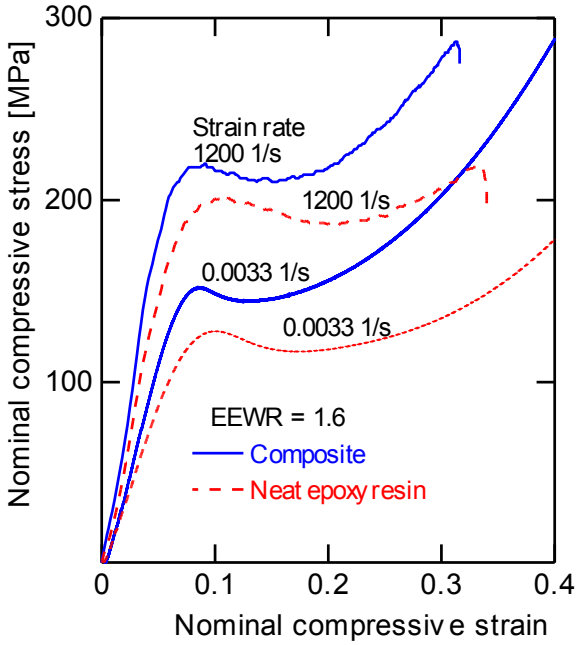

(b) EEWR 1.6

Fig. 3.7 Stress-strain curves of static and dynamic compression tests.

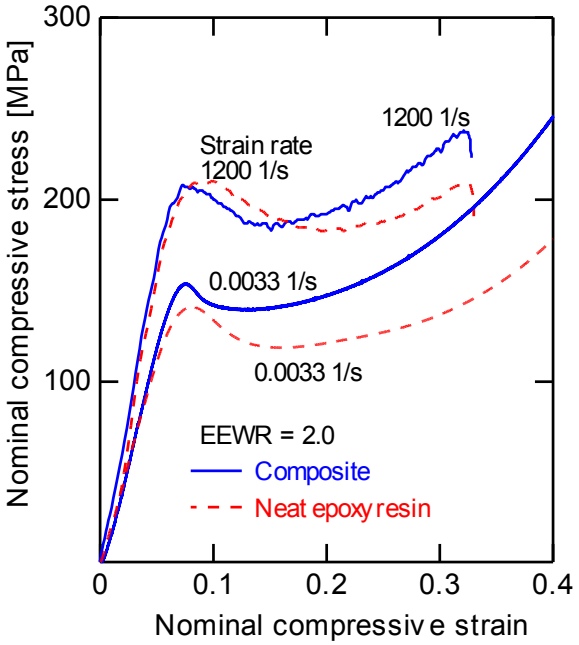

(c) EEWR 2.0

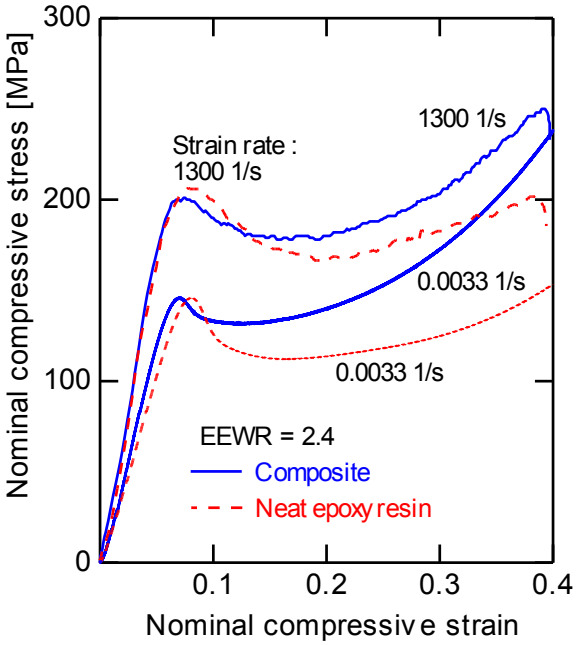

(d) EEWR 2.4

Fig. 3.7 Stress-strain curves of static and dynamic compression tests. *(Continued)*

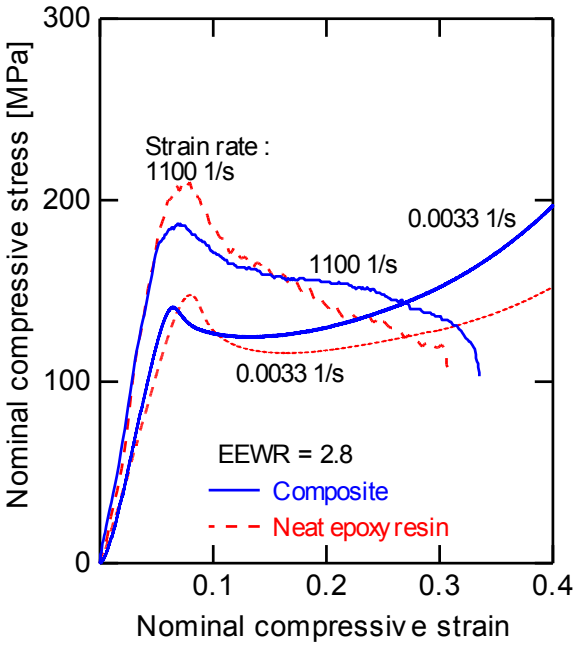

(e) EEWR 2.8

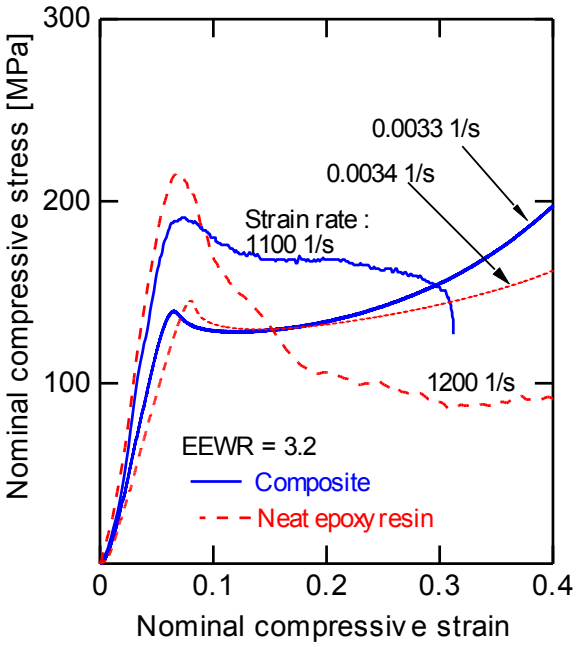

(f) EEWR 3.2

Fig. 3.7 Stress-strain curves of static and dynamic compression tests. *(Continued)*

3.5. Discussion

3.5.1. Yield stress

Figure 3.8 shows the strain rate dependence of the yield stresses of the neat epoxy resins and the composites. In the figure, the results of the composites for the strain rate that was approximately 600 1/s were removed because the compressive deformation at this strain rate was not enough to evaluate the stress-strain curves after yielding in the SHPB test. The yield stresses of the neat epoxy resins and the composites were largely reduced for higher strain rates.

The yield stresses of the neat epoxy resins (Fig. 3.8(a)) increased to 1.7 times as the strain rate increased. The yield stresses were independent of the crosslinking densities and could be approximated by one fitting line. Because the decreasing of the crosslinking densities was counterbalanced with the increasing entanglement of the chains in the resins, the crosslinking densities were not significant to the yield stresses.

The yield stresses of the composites (Fig. 3.8(b)) were found to be dependent on the crosslinking densities and the strain rates. The yield stresses of the composites with high crosslinking densities increased to approximately 1.5 times as the strain rate increased to 1500 1/s, although the increases in the yield stresses were smaller for lower crosslinking densities. As the crosslinking densities decreased from the non-stoichiometric condition, the yield stress of the composites decreased. This fact means that the existence of the nano-silica particles in the matrix resins prevented yielding due to the interaction of the particles and the network structures of the matrix resin.

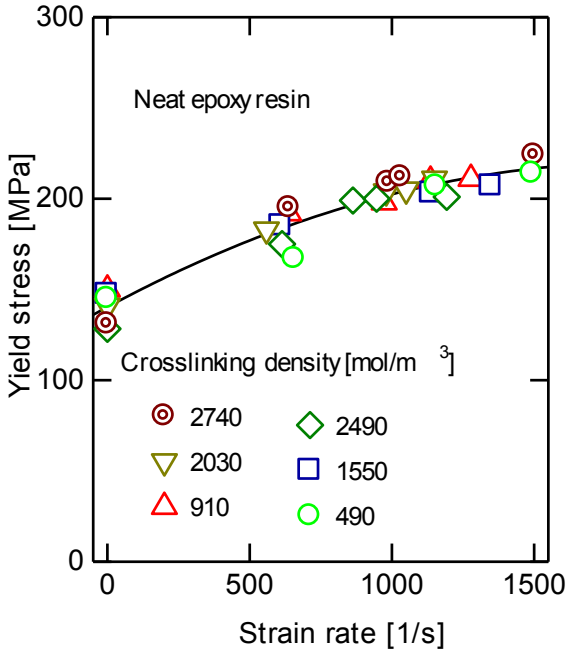

(a) Neat epoxy resin

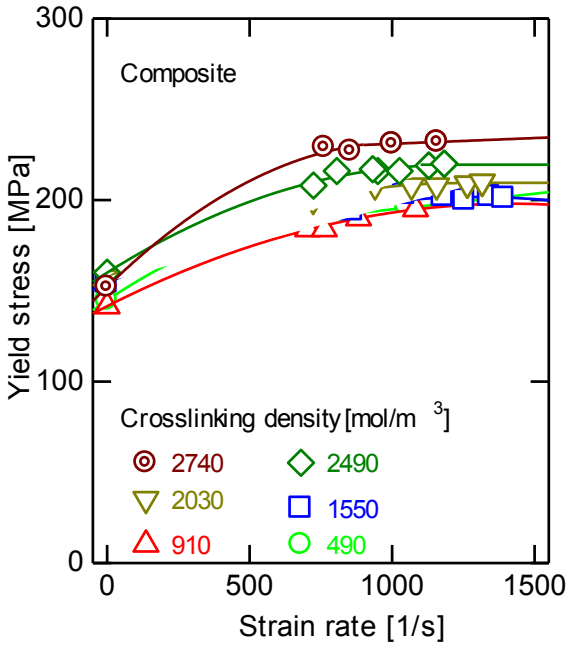

(b) Composite

Fig. 3.8 Relation between yield stress and strain rate.

3.5.2. Strain softening after yielding

The ratios of minimum stress after yielding to yield stresses for the neat epoxy resins and the composites are shown in Fig. 3.9 to clarify strain softening after yielding. In Fig. 3.9(a), the stress after the yielding of the neat epoxy resins reduced rapidly to 80% at a high strain rate especially for a lower crosslinking density (n = 490 mol/m^3), although the stress after yielding for the stoichiometrically cured epoxy resins kept constant regardless of the strain rates because the entanglement of the chain molecules in the epoxy resin was easily released after yielding due to the low crosslinking density and high strain rate deformation. However, the stresses after yielding of the composites (Fig. 3.9(b)) were clarified to reduce a little to approximately 20% because the existence of the nano-silica particles interfered with the release of entanglements.

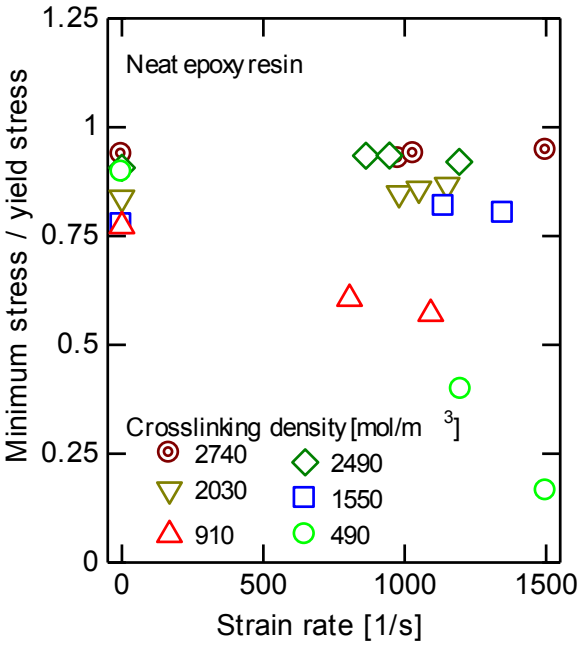

(a) Neat epoxy resin

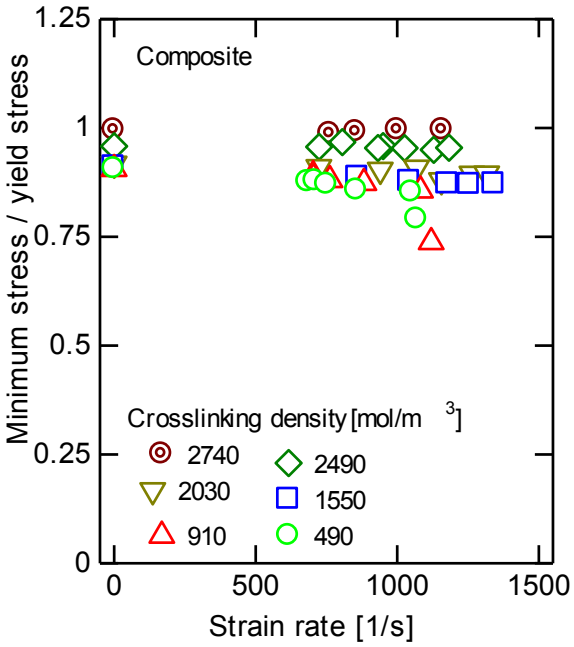

(b) Composite

Fig. 3.9 Dependence of ratio of minimum stress to yield stress on strain rate.

3.6. Conclusion

The compression properties of nano-silica particulate-reinforced epoxy composites with different crosslinking densities in matrix resins were investigated experimentally by using static and dynamic tests to clarify the interaction effects between the nano-particles and network structure in the matrix resin.

The composite materials were prepared by adding silica particles having a median diameter of 240 nm to the diglycidyl ether of bisphenol A type epoxy resin that was then cured with methyl-tetrahydro-phthalic anhydride as a curing agent in several non-stoichiometric mixed quantities. The volume fraction of the particles was kept at 0.2 for every composite. The range of the crosslinking densities of the cured epoxy resin was from 490 to 2740 mol/m^3. The compressive behavior was measured within a strain rate that ranged from 3.3×10^{-3} to 1500 1/s.

The compressive yield stresses of the neat epoxy resins increased to 1.7 times as the strain rate increased to 1500 1/s. Although the compressive yield stresses were independent of the crosslinking densities, the compressive yield stresses of the composites were found to be dependent on the crosslinking densities and the strain rates. The compressive yield stresses of the composites with high crosslinking densities increased to approximately 1.5 times as the strain rate increased to 1500 1/s. The increases in the yield stresses of the composites were smaller for lower crosslinking densities. The strain softening of the composite after the yielding was clarified to reduce a little to approximately 20% at most as the strain rate increased to 1500 1/s, while the strain softening of the neat epoxy for higher strain rates reduced rapidly to approximately 80%.

3.7. References

[3.1] Moloney A.C., Kausch H.H., Kaiser T., Beer H.R., Review parameters determining the strength and toughness of particulate filled epoxide resins, *Journal of Materials* Science, Vol. 22, pp. 381-393, 1987.

[3.2] Nakamura Y., Okabe S., Iida T. Effect of particle size on the fracture toughness of epoxy resin filled with spherical silica, *Polymer*, Vol. 33(16), pp. 3415-3426, 1992.

[3.3] Nakamura Y., Okabe S., Iida T., Effects of particle shape, size and interfacial adhesion on the fracture strength of silica-filled epoxy resin, *Polymers and Polymer Composites*, Vol. 7(3), pp. 177-186, 1997.

[3.4] Kwon S.C., Adachi T., Araki W., Yamaji A., Thermo-viscoelastic properties of silica particulate reinforced epoxy composites: considered in terms of particle packing model, *Acta Materialia*, Vol. 54, pp. 3369-3374, 2006.

[3.5] Kwon S.C., Adachi T., Strength and fracture toughness of nano and micron-silica particles bidispersed epoxy composites: evaluated by fragility parameter, *Journal of Materials Science*, Vol. 42, pp. 5516-5523, 2007.

[3.6] Kwon S.C., Adachi T., Araki W., Yamaji A., Effect of composing particle of two sizes on mechanical properties of spherical-silica-particulate-reinforced epoxy composite, *Composites Part B*, Vol. 39, pp. 740-746, 2008.

[3.7] Kwon S.C., Adachi T., Araki W., Temperature dependence of fracture toughness of silica/epoxy composites: related to microstructure of nano- and micro-particles packing, *Composites Part B*, Vol. 39, pp. 773-781, 2008.

[3.8] Adachi T., Osaki M., Kwon SC., Araki W., Fracture toughness of nano- and micro-spherical silica-particle-filled epoxy composite, *Acta Materialia*, Vol.56, pp. 2101-2109, 2008.

[3.9] Adachi T., Araki W., Higuchi M., Mixture law including particle-size effect on fracture toughness of nano- and micro-spherical particle-filled composites, *Acta Mechanic*, Vol. 214, pp. 61-69, 2010.

[3.10] Zheng Y., Zheng Y., Ning R., Effects of SiO_2 on the performance on nanocomposites, *Materials Letters,* Vol. 57, pp. 2940-2944, 2003.

[3.11] Guo Y., Li Y., Quasi-static/dynamic response of SiO_2-epoxy nanocomposites, *Materials Science and Engineering Part A,* Vol. 458, pp. 330-335, 2007.

[3.12] Jajam K.C., Tippur H.V., Quasi-static and dynamic fracture behavior of particulate polymer composites: A study of nano- vs. micro-size filler and loading-rate effects, *Composites Part B*, Vol. 43, pp. 3467–348, 2012.

[3.13] Rong M. Z., Zhang M. Q., Pan S. L., Lehmann B., Friedrich K., Analysis of the interfacial interactions in polyprotlene/silica nanocomposites, *Polymer International*, Vol. 53, pp. 176-183, 2004.

[3.14] Brechet Y., Cavaille J. YY., Chabert E., Chazeau L., Dendievel R., Flandin L., Gauthier C., Polymer based nanocomposites: effect of filler-filler and filler-matrix interactions, *Advanced Engineering Materials*, Vol. 3, pp. 571-577, 2001.

[3.15] Kovacevic V., Lucic S., Leskovac M., Morphology and failure in nanocomposites Part I: structural and mechanical properties, *Journal of Adhesion Science and Technology*, Vol. 16, pp. 1343-1365, 2002.

[3.16] Adachi T., Imai Y., Higuchi M., Fracture Energy of Nano- and Micro-Silica Particle-Filled Epoxy Composites, *International Journal of Theoretical and Applied Multiscale Mechanics*, Vol. 2, No.1, pp.82-94, 2011.

[3.17] Umboh M.K., Adachi T., Oishi K., Higuchi M., Major Z., Mechanical properties of nano-silica particulate-reinforced epoxy composites considered in terms of crosslinking effect in matrix resins, *Journal of Materials Science*, Vol. 48, pp. 5148-5156, 2013.

[3.18] Kuln H., Medlin D., *ASM Handbook Vol. 8, ASM International*, Materials Park, Ohio, 2000.

[3.19] Chen W.W., Song B., *Split Hopkinson (Kolsky) Bar Design Testing and Applications*, Springer, New York, 2011.

[3.20] Bignotti F., Pandini S., Baldi F., De Santis R., Effect of the resin/hardener ratio on curing, structure and glass transition temperature of nanofilled epoxies, *Polymer Composites*, Vol. 32, pp. 1034-1048, 2011.

[3.21] Ward I. M., *Mechanical Properties of Solid Polymers,* Second ed., Wiley, New York, 1990.

CHAPTER 4
FRACTURE BEHAVIOR

4.1. Introduction

Particulate-reinforced epoxy composites are widely used for applications in various engineering fields such as for packaging materials in electronic devices and components of aircraft and automotive, because of their excellent mechanical and insulation properties. Fracture toughness is one of most important mechanical properties of materials to improve the reliability of these devices and components. By diminishing of particle size from the micrometer to the nanometer level, nanocomposites are produced to further improve mechanical properties.

The fracture properties of silica particulate-reinforced epoxy composites have been investigated in several previous studies. Several researchers have conducted intensive studies regarding the effects of particles volume fraction and its size on the properties of micro- or nano-silica particulate-reinforced epoxy composites. Spanoudakis and Young [4.1, 4.2], Moloney et al. [4.3], Nakamura et al. [4.4, 4.5], and Adachi et al. [4.6] reported that fracture properties strongly depended on particle size, shape, and volume contributing to the differences in crack propagation and interaction of particles with matrixes. Preghenella et al. [4.7], Kitey et al. [4.8], Butcher et al. [4.9], Kwon et al. [4.10–4.15], and Adachi et al. [4.16–4.18] clarified that the fracture properties strongly related to the size distributions of silica particles due to enhanced interactions between the particles and the matrixes. Rapid interparticle distance with decreasing particle size resulted in more interactions between particles and epoxy matrixes. The interfacial interaction of particles with the surrounding matrix is closely related with the crosslinking network morphology in polymer matrixes [4.19–4.21]. Therefore, the fracture properties of nano- or micron-particle-reinforced epoxy composites are considerably dependent not only on the particle size effect but also on the internal network structures of the epoxy matrixes.

The previous study of Chapter 3 reported dynamic compression behavior of non-stoichiometrically cured epoxy resin [4.22] and nano-silica particulate-reinforced epoxy composites [4.23] to consider what effects the incomplete network structured the resins had on the dynamic properties. Moreover, the previous study of Chapter 2 investigated the interaction effects between nano-particles and epoxy network structures on bending strengths using incomplete network structures in epoxy composites and reported that the interactions increased the bending strengths for high crosslinking densities [4.24]. These mean that not only the size distribution and volume friction of

particles but also the incomplete network structures in epoxy composites are important take into consideration the mechanical properties of composites.

In this chapter, the interaction effects between nano-particles and epoxy network structures on the fracture toughness of nano-silica particulate-reinforced epoxy composites using incomplete network structures in epoxy composites were experimentally clarified by comparing them with bending strength [4.24] where the bending strength data referred to Chapter 2. The incomplete network structures in epoxy composites were resulted by non-stoichiometric curing effects and were expressed by the crosslinking densities in matrix resins identified from the thermo-viscoelastic properties of materials in Chapter 2. The fracture toughness of the composites and the neat epoxy resins were performed at room temperature (RT) to measure mode I fracture. Finally, the interactive effects between nano-particles and the network structures in matrix resin were considered on the basis of fracture toughness and the bending strengths of the specimens.

4.2. Specimens

4.2.1. Materials

Epoxy resin was filled with spherical silica particles to produce the composite materials for the specimens. The epoxy resin was a mixture of diglycidyl ether of bisphenol A type epoxy resin (Asahi Kasei E-Materials, AER 2603), with methyl-tetrahydro-phthalic anhydride (New Japan Chemical, Rikacid MH-700) as the curing agent and 2,4,6-tris (dimethyl aminomethyl) phenol (Mitsubishi Chemical, jER BMI12) as the accelerator. The equivalent weight of the epoxide resin was 188 g/equivalent and the acid anhydride equivalent weight of the curing agent was 162 g/equivalent. The weight ratio of the resin, the agent, and the accelerator was 100: 86: 0.5 according to stoichiometry.

The filler for the composites was made of silica particles with a median diameter of 240 nm (Tatsumori, SO-C1), and the surfaces of the particles were not chemically coated. The volume fraction of the silica particles was 0.2 for every composite.

The mixture ratio of the epoxide resin to the curing agent was varied in the study to take into consideration the interaction between the silica particles and the network structures in the matrix resin. The mixture ratio of the epoxy resin to the curing agent was defined in the experiment as the epoxy-equivalent-weight ratio (EEWR) expressed by the epoxide resin weight over the stoichiometric epoxide resin weight in the mixture.

The EEWRs were prepared in a range from 1.0 to 3.2 and the accelerator was kept constant at 0.5, as listed in Table 4.1. The chemical reaction in the matrix resins resulted in complete network structures under stoichiometric condition (EEWR = 1.0) and incomplete network structures were formed due to the excess mixtures of epoxide resins for EEWRs > 1. We did not manufacture EEWRs over 3.2 to produce resins or composites because the specimens were too weak to enable viscoelastic properties to be measured and unreacted curing agents could be transferred from the cured resins for EEWRs below 1.0.

To manufacture the composite materials, the nano-silica particles were blended with the epoxy resin containing the curing agent and accelerator until all particles dispersed without agglomeration. The complete mixture was degassed in a vacuum vessel and then poured into an aluminum mold coated with a Teflon sheet. The mold was 260 mm long, 5 mm wide and 120 mm deep. The mixture in the mold was heated to cure it in an oven. The curing procedure was done in two steps of pre-curing, where the mixture was kept at 373 K for 2 h to gel the matrix resin, and post-curing, which greatly affected the crosslinking reaction of the resin, and this was performed at 403 K for 15 h. The heating rate from pre-curing to post-curing was kept constant at 72 K h^{-1}. Cured epoxy resins without silica particles, expressed as neat epoxy resins, were also prepared in the same process as that for the composites. The composites and the neat epoxy resins produced in the study are listed in Table 4.1.

The results of the densities of the cured materials according to the American Society for Testing and Materials (ASTM) standard 792-08 are listed in Table 4.1. The densities of the neat epoxy resins and the composites were constant regardless with the EEWRs.

4.2.2. Characterization

The thermo-viscoelastic properties of the neat epoxy resins and composites were measured with a dynamic viscoelastometer (Rheogel-E4000, UBM) using a non-resonance tensile method. The dynamic complex moduli of the specimens for tensile oscillation with a frequency of 10 Hz were measured at 1 K intervals ranging from 223 K to 493 K. The heating rate was 1 K min^{-1}. The glass transition temperatures of the composites and the neat epoxy resins were determined at peaks of the maximum tan δ of their loss moduli. The crosslinking density of the composites and the neat epoxy

resins were calculated from the dynamic storage moduli in a rubbery state according to [4.25, 4.26]

$$E' = 3nRT, \quad (4.1)$$

where T and R are the absolute temperature and gas constant (= 8.3145 J mol^{-1} K^{-1}). The crosslinking densities in the composites were assumed to be the same as those of the neat epoxy resins with the same EEWRs [4.25] because the EEWRs are concerned with the chemical reactions of the epoxide resin and the curing agent. The results for the glass transition temperatures, T_g, and the crosslinking densities, n, are listed in Table 4.1 [4.22, 4.24]. The crosslinking densities of the neat epoxy resins and the matrix resins of the composites ranged from 2740 to 490 mol m^{-3}.

Table 4.1 Neat epoxy resins and composites

Materials	Matrixes (weight ratios)			Epoxy-equivalent-weight ratios	Volume fractions of silica particles	Densities [kg/m^3]	Glass transition temperatures, *Tg* [K]	Crosslinking densities [mol/m^3]
	Epoxide resins	Curing agents	Accelerators					
Neat epoxy resins	100	86	0.5	1.0	-	1200	437	2740
	160	86	0.5	1.6	-	1200	417	2490
	200	86	0.5	2.0	-	1200	401	2030
	240	86	0.5	2.4	-	1200	384	1550
	280	86	0.5	2.8	-	1200	362	910
	320	86	0.5	3.2	-	1200	347	490
Composites	100	86	0.5	1.0	0.2	1400	423	2740
	160	86	0.5	1.6	0.2	1400	402	2490
	200	86	0.5	2.0	0.2	1400	375	2030
	240	86	0.5	2.4	0.2	1400	359	1550
	280	86	0.5	2.8	0.2	1400	347	910
	320	86	0.5	3.2	0.2	1410	342	490

4.3. Experimental Procedure

Single edge notched bending test were performed at RT to measure the mode I fracture toughness of the neat epoxy resins and the composites in terms of the critical stress intensity factor, K_{IC}, according to ASTM standard D5045-99. Figure 4.1 outlines the geometrical conditions for the fracture test. The specimens had a length of 100 mm, a height of 20 mm, and a width of 5 mm. The lengths of pre-cracks at the middle point of the specimen and span length between the supports corresponded to 10 mm and 60 mm. The constant deflection rate of 50 μm s^{-1} was applied at the loading point and the load was recorded by using a universal materials testing machine (Shimadzu, AGS-J). The fracture toughness was calculated as

$$K_{IC} = \frac{3}{2}\frac{P_{max}L\sqrt{\alpha}}{WB^{3/2}}\left[\frac{1.99-\alpha(1-\alpha)\{2.15-3.93(\alpha+2.7\alpha^2)\}}{(1+2\alpha)(1-\alpha)^{3/2}}\right], \quad (4.2)$$

where $\alpha = a / W$. P_{max}, B, L, W, and a correspond to the maximum load, width, span length, height, and pre-crack length of the specimens.

The fracture surface of the neat epoxy resins and the composites were observed 2 mm from the pre-crack tip after the fracture test with a scanning electron microscope (SEM) (Keyence, VE-8800) as shown in Fig. 4.2.

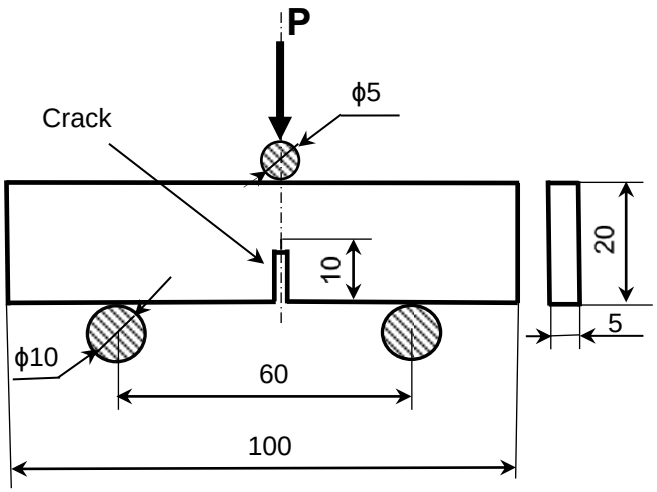

Fig. 4.1 Single edge notched bending tests. Units are in millimeters.

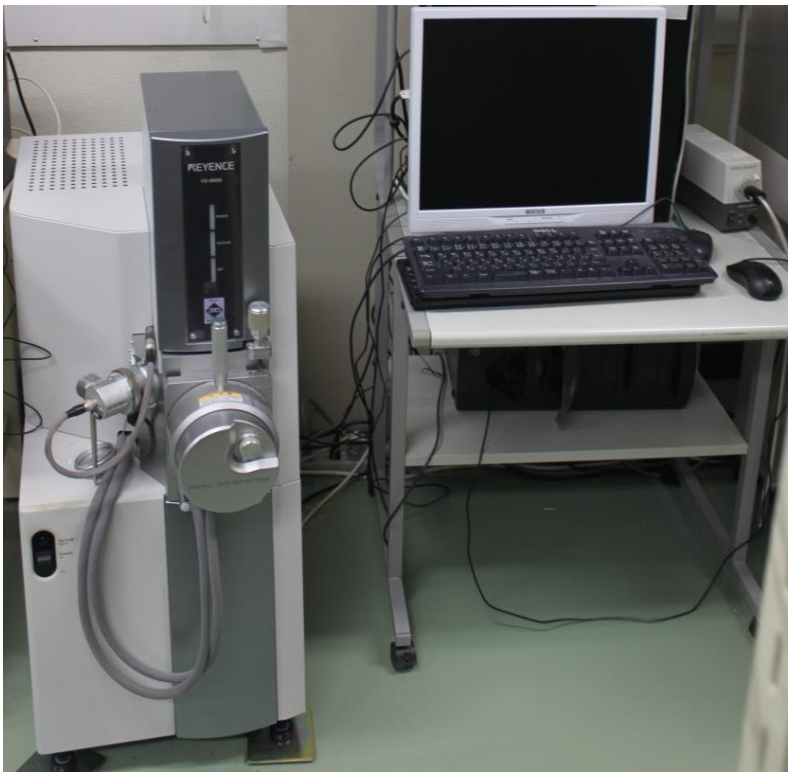

Fig. 4.2 Scanning electron microscope (SEM) (Keyence, VE-8800).

4.4. Experimental Results

4.4.1. Load-deflection curves

Figure 4.3 plots typical load-deflection curves for the neat epoxy resins and the composites measured with the single edge notched bending tests. Every specimen had a linear load-deflection relation until brittle fractures occurred regardless of the EEWRs. We therefore applied Eq. (4.1) on the basis of linear elastic fracture mechanics to determine the fracture toughness of the neat epoxy resins and composites. The average values for the fracture toughness were evaluated with their standard deviations from more than five experimental results. The results for both properties are listed in Table 4.2

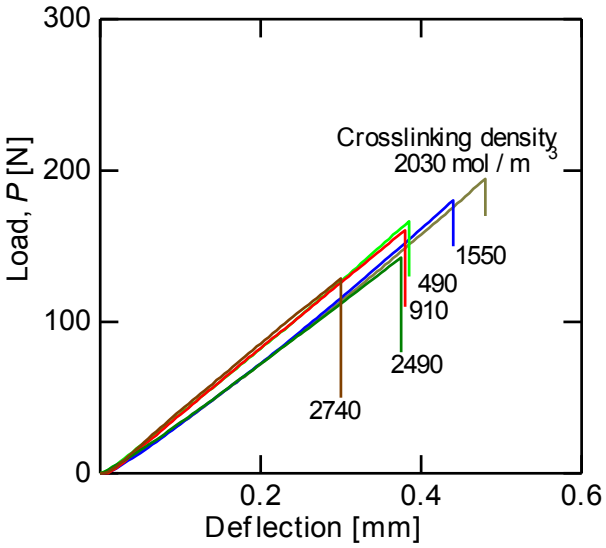

(a) Neat epoxy resins

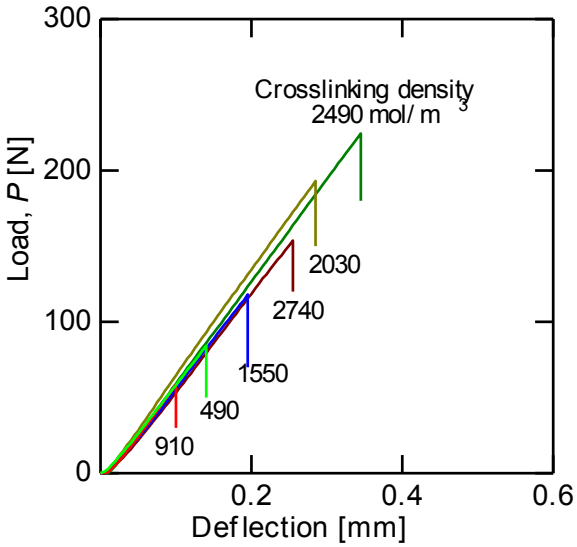

(b) Composites

Fig. 4.3 Typical load-deflection curves measured with single edge notched test.

Table 4.2 Fracture toughness and bending strength.

Materials	Crosslinking densities [mol/m^3]	Fracture toughness [MPa m$^{1/2}$]			Bending strengths [MPa]		
		Averages	Standard deviations	Normalized with Eq. (4.3)	Averages	Standard deviations	Normalized with Eq. (4.4)
Neat epoxy resins	2740	0.99	0.51	-	147	3.76	-
	2490	1.34	0.40	-	149	1.18	-
	2030	1.72	0.09	-	154	2.60	-
	1550	1.71	0.08	-	137	19.30	-
	910	1.36	0.16	-	135	8.60	-
	490	1.44	0.30	-	96	6.20	-
Composites	2740	1.73	0.17	0.75	161	2.99	0.10
	2490	2.27	0.06	0.69	160	2.82	0.07
	2030	1.88	0.06	0.09	154	0.62	0.00
	1550	1.19	0.11	-0.30	122	11.61	-0.11
	910	0.65	0.09	-0.52	65	5.02	-0.52
	490	0.75	0.16	-0.48	65	6.53	-0.32

4.4.2. Fracture surface

The fracture surfaces of specimens observed by SEM after the single edge notched bending tests are shown in Fig. 4.4. Because the particles on the fracture surfaces were found to be surrounded by the matrix resins, namely interphase regions [4.16, 4.18], it could be concluded that cracks propagated in the matrix resins regardless of crosslinking densities. The state was the same as the fracture surfaces in Adachi et al. [4.16, 4.18] and those after bending tests in Chapter 2 [4.24]. Therefore, the properties of the matrixes near particles, which would be dependent on the interaction between the particles and matrixes, were important to take into consideration fractures in the specimens.

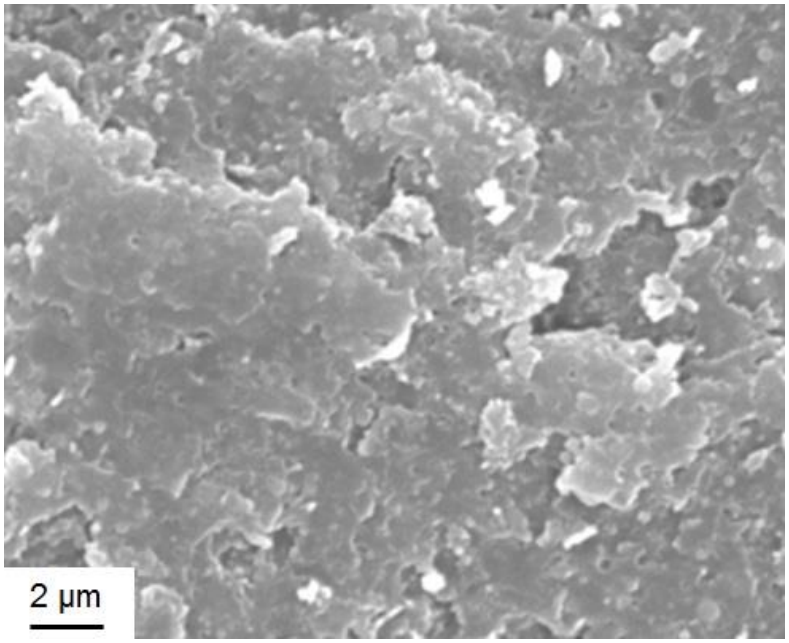

(a) Crosslinking density: 2740 mol/m^3

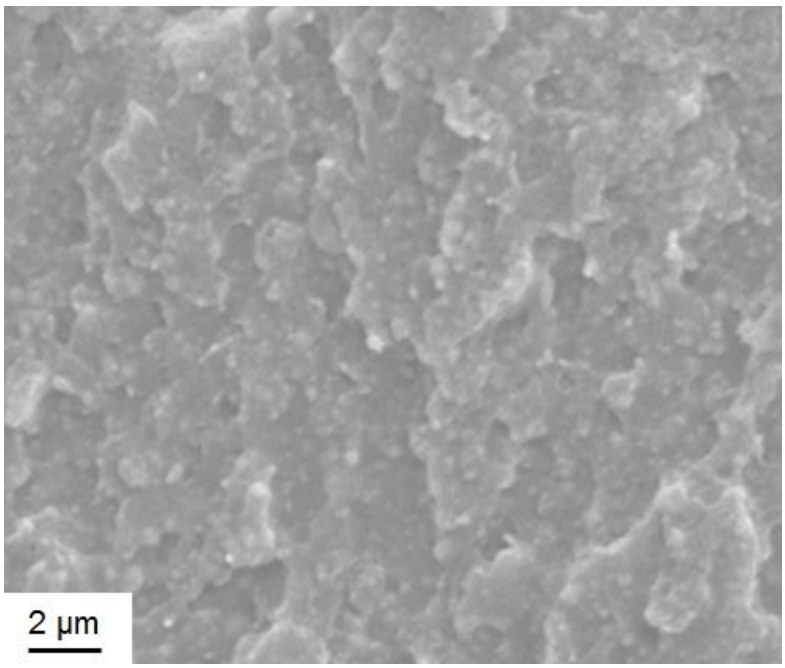

(b) Crosslinking density: 2490 mol/m^3

Fig. 4.4 Fracture surfaces observed with SEM.

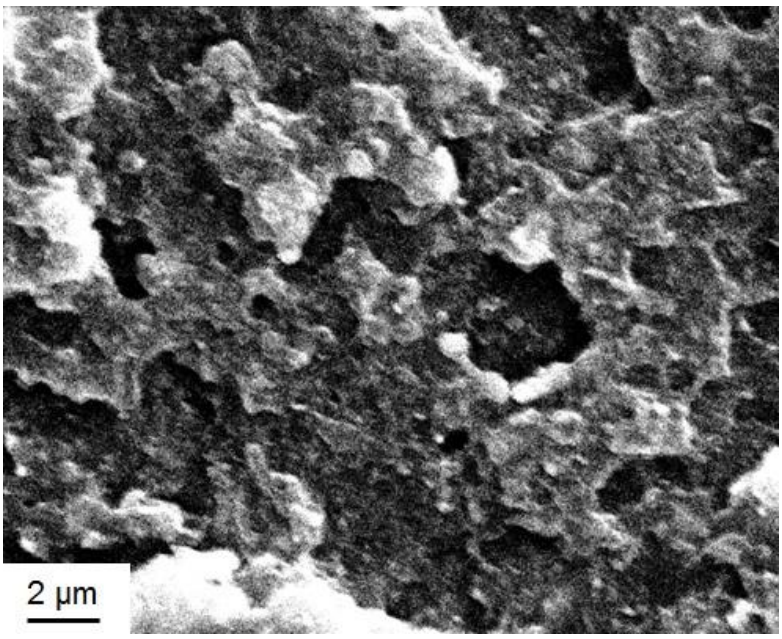

(c) Crosslinking density: 2030 mol/m^3

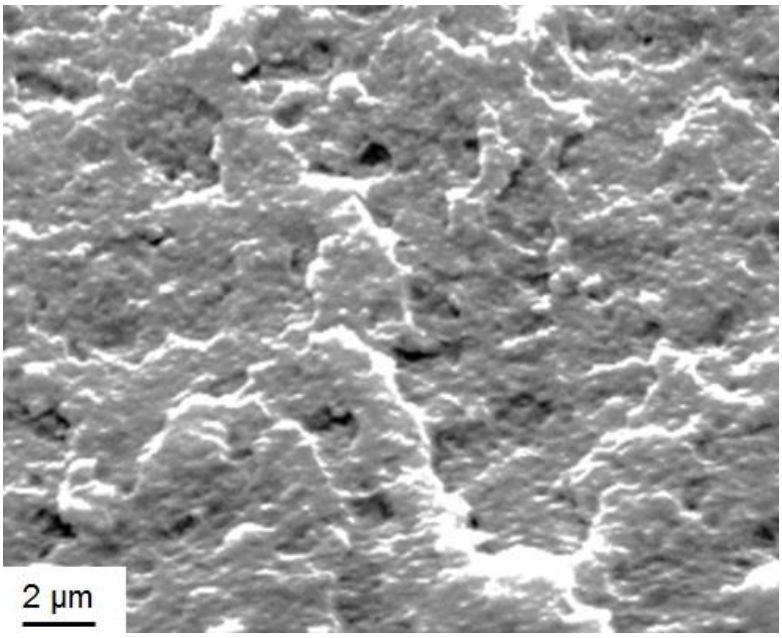

(d) Crosslinking density: 1550 mol/m^3

Fig. 4.4 Fracture surfaces observed with SEM. *(Continued)*

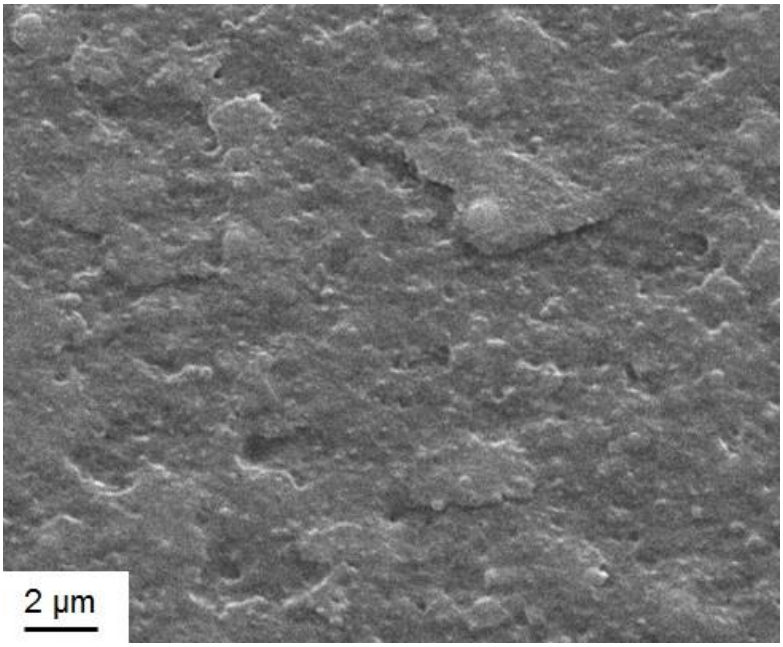

(e) Crosslinking density: 910 mol/m^3

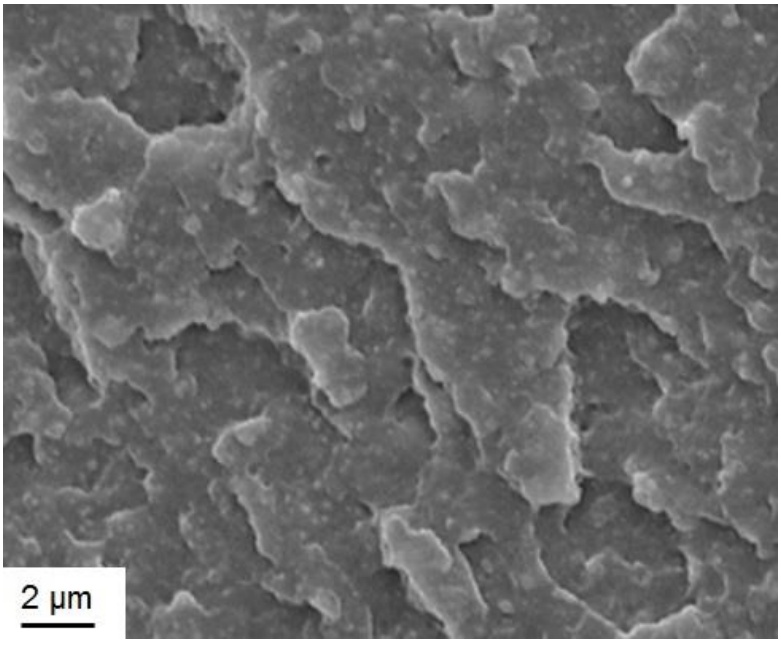

(f) Crosslinking density: 490 mol/m^3

Fig. 4.4 Fracture surfaces observed with SEM. *(Continued)*

4.4.3. Fracture toughness and bending strength

Figure 4.5 plots the fracture toughness and bending strength for neat epoxy resins and composites. The open circles and triangles are averages of the bending strength and fracture toughness calculated from more than five experimental results. The error bars indicate the standard deviations for the experiment data and the solid lines are the fitting curves.

Within the crosslinking density decreasing from stoichiometric condition (2740 mol/m^3) to 1500 mol/m^3 in Fig. 4.5(a), the fracture toughness of the neat epoxy resins suddenly increased and reached 1.7 MPa $m^{1/2}$, whereas the bending strength was constant at 150 MPa, which was approximately the same as that for the stoichiometrically cured epoxy resin. Below the crosslinking density of 1500 mol/m^3, the fracture toughness moderately decreased although the bending strengths suddenly decreased from 150 to 100 MPa.

In Fig. 4.5(b), the fracture toughness of the composites drastically increased and reached 2.3 MPa $m^{1/2}$, which was 30 % more than that for the stoichiometrically cured composites. After that, the fracture toughness reduced below that for the stoichiometrically cured neat epoxy resins. The bending strength was constant from the stoichiometric condition and decreased similarly to the tendency in Fig. 4.4(b). The rate of decrease for the bending strength was larger than that for the neat epoxy resin.

The results in Fig. 4.5 can be summarized as follows. The non-stoichiometric curing of the neat epoxy resins, i.e., the rough network structure of the resins increased fracture toughness, especially for resins with low crosslinking density. The composites with slightly smaller crosslinking density than that of the stoichiometric condition were clarified to greatly improve the fracture toughness due to the large interactive effect between the nano-particles and slightly incomplete network structures in the resins. However, the nano-particles in composites having lower crosslinking densities severely reduced below the fracture toughness of the neat epoxy resins. Therefore, the nano-particles were found to reinforce the fracture toughness for stoichiomerically cured or slightly non-stoichiometrically cured composites, and the particles seriously reduced the fracture toughness as defects. The interactive effects of nano-silica particles and non-stiochiometrically cured epoxy resins on mechanical properties are examined in the next section.

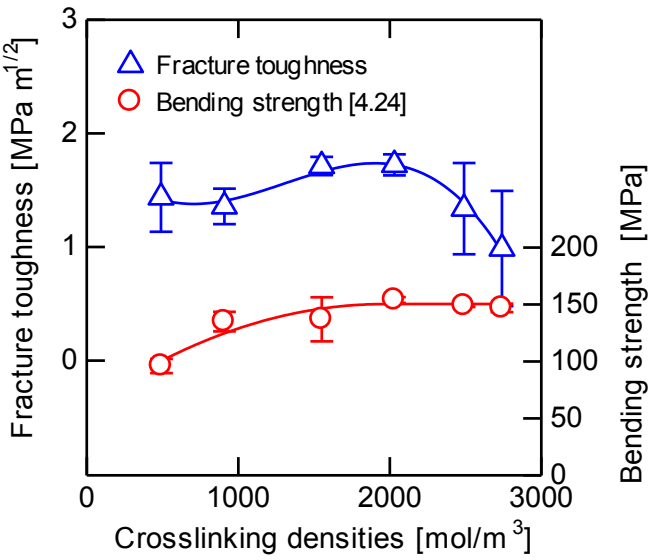

(a) Neat epoxy resins

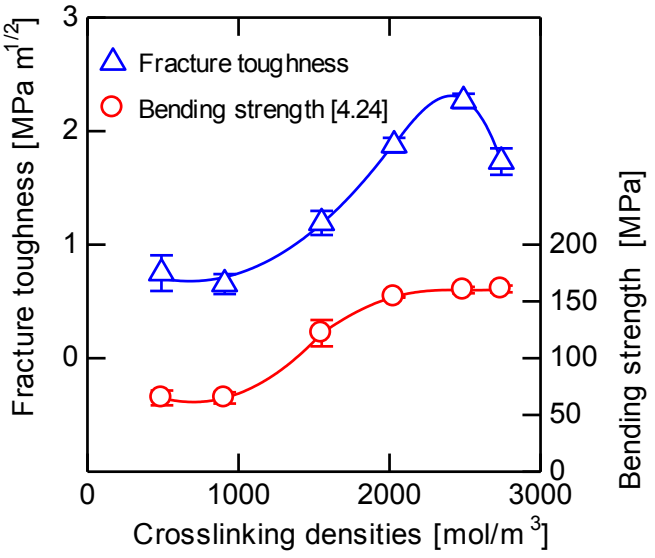

(b) Composites

Fig. 4.5 Fracture toughness and bending strength.

4.5. Discussion

Figure 4.6 plots the ratios between bending strength and the fracture toughness for the neat epoxy resins and composites. The fracture toughness of the neat epoxy resins is not clearly correlated with the bending strength in Fig. 4.6(a). However, the fracture toughness of the composites is correlated with the bending strength in Fig. 4.6(b). It was difficult to consider the interaction between the nano-silica particles and the network structures in the epoxy resins on the basis of Fig. 4.6 because the relations between composites had different correlations from those of neat epoxy resins.

The fracture toughness and the bending strength of all composites were normalized to clearly express reinforced of the nano-silica particles by using two definitions:

Normalized fracture toughness: $K_N = \frac{K_{COMP} - K_{EPOXY}}{K_{EPOXY}}$ and (4.3)

Normalized bending strength: $\sigma_N = \frac{\sigma_{COMP} - \sigma_{EPOXY}}{\sigma_{EPOXY}}$, (4.4)

where K_{COMP} and σ_{COMP} are the fracture toughness and the bending strength of the composite. K_{EPOXY} and σ_{EPOXY} are the fracture toughness and the bending strength of neat epoxy resins with the same crosslinking density as that in the matrix resins of the composites. The normalized properties mean improvements to neat epoxy resins due to the addition of the nano-silica particles. If the normalized values were positive, the epoxy resin matrixes were considered to be reinforced with filling particles.

Figure 4.7 plots variations in the normalized fracture toughness and bending strength of composites with the crosslinking density of the matrix resins. In No Fig. 4.7(a) given, the normalized fracture toughness is positive within the crosslinking densities that range from stoichiometric conditions of 2740 mol/m^3 to approximately 2000 mol/m^3, and negative below the crosslinking density of 2000 mol/m^3. Especially, the composite with crosslinking density of 2490 mol/m^3, which was slighly lower than that with stoichiometric curing, had maximum fracture toughness. In No Fig. 4.7(b) given, the normalized bending strength was slightly positive in the same region of crosslinking density, from 2740 to 2000 mol/m^3, and negative below the other region. Therefore, the epoxy resin was reinforced by adding nano-silica particles to the fine network structures of matrix resins having high crosslinking densities near the stoichiometric conditions of 2740 to 2000 mol/m^3, and the particles reduced the fracture toughness and strength of matrix resins having rough networks below 2000 mol/m^3.

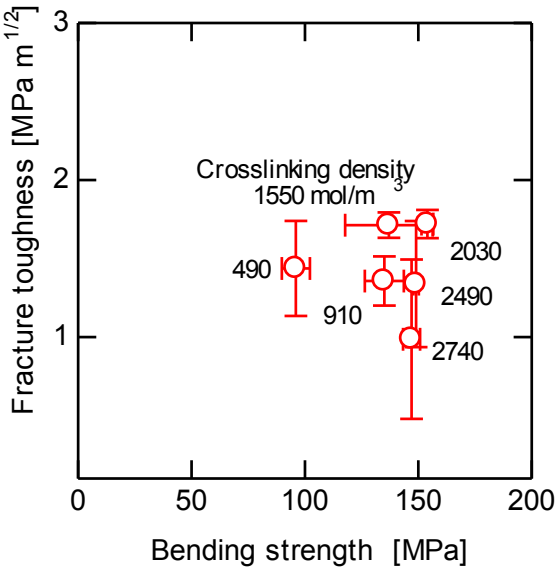

(a) Neat epoxy resins

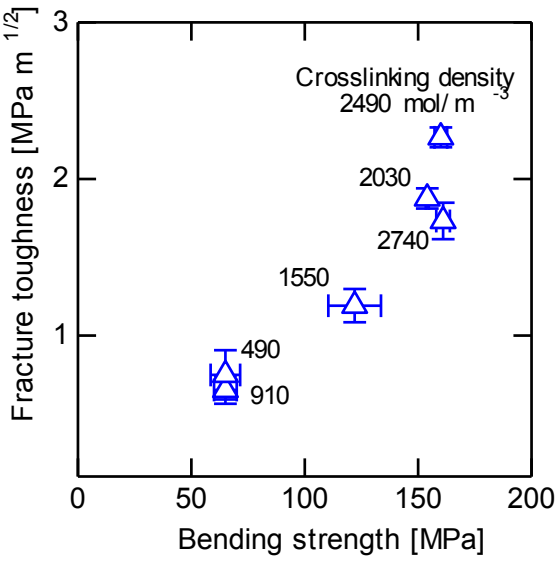

(b) Composites

Fig. 4.6 Relations between fracture toughness and bending strength.

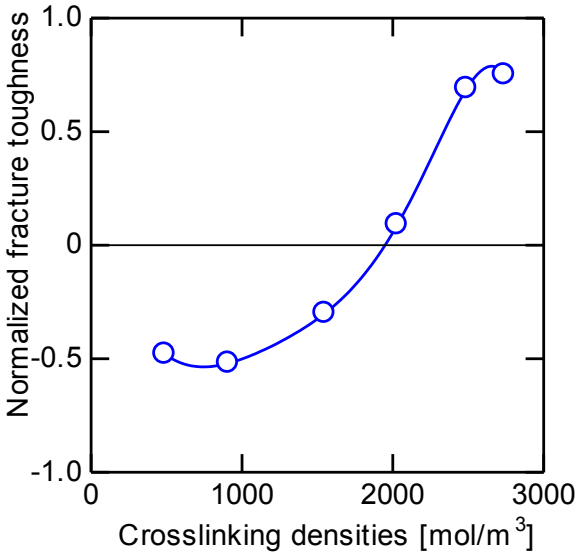

(a) Normalized fracture toughness

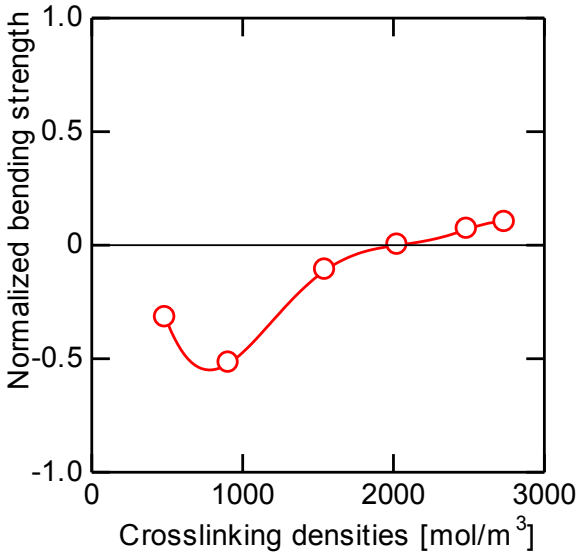

(b) Normalized bending strength.

Fig. 4.7 Normalized fracture toughness and bending strength of composites with crosslinking density of the matrix resins.

Figure 4.8 plots the relation between normalized fracture toughness and bending strength of composites to clarify the sensitivity of properties to the crosslinking densities. In the region of high crosslinking densities, the normalized fracture toughness was extremely sensitive to the crosslinking density although the bending strength was approximately constant. In the region of low crosslinking densities, the normalized fracture toughness was constant and the normalized bending strength was drastically varied, however, adding nano-silica particles had negative effects on both properties.

The results can be summarized as follows. The improved effects of fracture toughness and bending strength could not be explained on the basis of reduced stress concentration near the particles or simple mixing of particles and matrix resin because the normalized fracture toughness and bending strength of composites with different crosslinking densities were not constant under fixed volume fractions of particles in Fig. 4.7. The crosslinking densities in the matrix resins greatly contributed to fracture toughness due to stronger interaction between the matrix resins and nano-silica particles due to slightly incomplete network structures in the matrix resins. This is because cracks in the fracture tests propagated in the matrix resins, as observed in Fig. 4.4. In contrast, the interactive effect between the particles and network structures in the matrix resins on bending strength of composites was relative small and the strength of the matrix resins mainly affected the strength of the composites because fractures in bending tests propagated in the matrix resins [4.17]. Therefore, the interaction between the particles and matrix resins played an important role in the fracture toughness of the composites. The fracture toughness of the composite was predicted to be controlled by the particles size because the interactive effect changed.

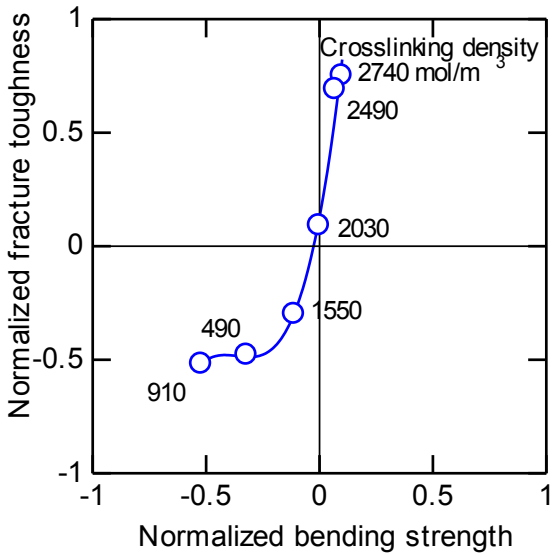

Fig. 4.8 Relation between normalized fracture toughness and bending strength.

4.6. Conclusion

The fracture toughness of nano-silica particulate-reinforced epoxy composites with different crosslinking densities was experimentally investigated to take into consideration the interactive effects between nano-particles and the network structures in matrix resins. The composite materials were prepared by adding silica particles that were 240 nm in median diameter to bisphenol A type epoxy resins with the particles volume fraction of 0.2. The neat epoxy resins and the composites were cured non-stoichiometrically to change the crosslinking densities of the neat epoxy resins and the matrix resins of the composites within 2740 to 490 mol/m^3.

The fracture toughnesses and the bending strengths of nano-silica particulate-reinforced epoxy composites and the neat epoxy resin strongly depended on the crosslinking densities in the resins. Although the fracture toughness decreased monotonously from that of the stoichiometically cured resins as the crosslinking density decreased, the fracture toughness of the composites was maximum at a sligthly lower crosslinking density of approximately 2490 mol/m^3 from the stoichiometric condition, i.e., 2740 mol/m^3. The dependence of fracture toughness on the crosslinking density of composites differed greatly from that for neat epoxy resins.

Fracture toughness and bending strength were improved from these of neat epoxy resins by adding particles to achieve crosslinking densities higher than 2000 mol/m^3. At crosslinking densities lower than 2000 mol/m^3, the particles worked against mechanical properties as defects in matrix resins. The improvements to toughness were more sensitive to crosslinking density than those of bending strength.

4.7. References

[4.1] Spanoudakis J., Young R. J., Crack propagation in a glass particle-filled epoxy resin. Part 1: Effect of particle volume fraction and size, *Journal of Materials Science*, Vol. 19, pp. 473-486, 1984.

[4.2] Spanoudakis J., Young R. J., Crack propagation in a glass particle-filled epoxy resin. Part 2: Effect of particle-matrix adhesion, *Journal of Materials Science*, Vol. 19, pp. 487-496, 1984.

[4.3] Moloney A. C., Kausch H. H., Kaiser T., Beer H. R., Review parameters determining the strength and toughness of particulate filled epoxide resins, *Journal of Materials Science*, Vol. 22, pp. 381-393, 1987.

[4.4] Nakamura Y., Okabe S., Iida T., Effect of particle size on the fracture toughness of epoxy resin filled with spherical silica, *Polymer*, Vol. 33, No. 16, pp. 3415-3426, 1992..

[4.5] Nakamura Y., Okabe S., Iida T., Effects of particle shape, size and interfacial adhesion on the fracture strength of silica-filled epoxy resin, *Polymers and Polymer Composites*, Vol. 7, No. 3, pp. 177-186, 1997.

[4.6] Adachi T, Araki W, Nakahara T, Yamaji A, Gamou M, Fracture toughness of silica particulate-filled epoxy composite, *Journal of Applied Polymers Science, Vol.* 86, pp. 2261-2265, 2002.

[4.7] Preghenella M., Pegoretti A., Migliaresi C., Atomic force acoustic microscopy analysis of epoxy-silica nanocomposites, *Polymer Testing*, Vol. 25, pp. 443-451, 2006.

[4.8] Kitey R., Tippur H. V., Dynamic crack growth in particulate bimaterials having discrete and diffuse interfaces: Role of microstructure, *Engineering Fracture Mechanics*, Vol. 72, pp. 2721-2743, 2005.

[4.9] Butcher RJ, Rousseau CE, Tippur HV. A functionally graded particulate composite: preparation, measurements and failure analysis. *Acta Materialia*, Vol. 47(1), pp. 259–68, 1999.

[4.10] Kwon S. Ch., Adachi T., Araki W., Yamaji A., Effect of particle size on fracture toughness of spherical silica particles filled epoxy composite, *Key Engineering Materials*, Vol. 297-300, pp. 207-212, 2005.

[4.11] Kwon S. Ch., Adachi T., Araki W., Yamaji A., Thermo-viscoelastic properties of silica particulate reinforced epoxy composites: considered in terms of particle packing model, *Acta Materialia*, Vol. 54, pp. 3369-3374, 2006.

[4.12] Kwon, S. Ch. and Adachi, T., Strength and fracture toughness of nano and micron-silica particles bidispersed epoxy composites: evaluated by fragility parameter, *Journal of Materials Science*, Vol. 42, pp. 5516-5523, 2007.

[4.13] Kwon, S.Ch., Adachi, T., Araki, W., Yamaji, A., Mechanical properties of nano/micro-silica particles bidispersed epoxy composites, *Key Engineering Materials*, Vol. 345-346, pp. 1507–1510, 2007.

[4.14] Kwon, S.Ch., Adachi, T., Araki, W., Temperature dependence of fracture toughness of silica/epoxy composites: related to microstructure of nano- and micro-particles packing, *Composites Part B*, Vol. 39, pp. 773–781, 2008.

[4.15] Kwon SCh, Adachi T, Araki W, Yamaji A, Effect of composing particle of two sizes on mechanical properties of spherical-silica-particulate-reinforced epoxy composite, *Composites Part B*, Vol.39, pp. 740-746, 2008.

[4.16] Adachi T, Osaki M, Araki W, Kwon SCh, Fracture toughness of nano- and micro-spherical silica-particle-filled epoxy composite, *Acta Materialia*, Vol. 56, pp. 2101-2109, 2008.

[4.17] Adachi T, Araki W, Higuchi M, Mixture law including particle-size effect on fracture toughness of nano- and micro-spherical particle-filled composites, *Acta Mechanic*, Vol. 214, pp. 61–69, 2010.

[4.18] Adachi T., Imai Y., Higuchi M., Fracture Energy of Nano- and Micro-Silica Particle-Filled Epoxy Composites, *International Journal of Theoretical and Applied Multiscale Mechanics*, Vol. 2, No.1, pp.82-94, 2011.

[4.19] Rong M. Z., Zhang M. Q., Pan S. L., Lehmann B., Friedrich K., Analysis of the interfacial interactions in polypropylene/silica nanocomposites, *Polymer International*, Vol. 53, pp. 176-183, 2004.

[4.20] Brechet Y., Cavaille J. YY., Chabert E., Chazeau L., Dendievel R., Flandin L., Gauthier C., Polymer based nanocomposites: effect of filler-filler and filler-matrix interactions, *Advanced Engineering Materials*, Vol. 3, pp. 571-577, 2001.

[4.21] Kovacevic V., Lucic S., Leskovac M., Morphology and failure in nanocomposites Part I: structural and mechanical properties, *Journal of Adhesion Science and Technology*, Vol. 16, pp. 1343-1365, 2002.

[4.22] Adachi T, Oishi K, Higuchi M, Umboh MK, Major Z, Non-stoichiometric curing effect in dynamic mechanic properties of bisphenol A –type epoxy resin, *Journal of the Japanese Society for Experimental Mechanics*, Vol. 13, pp.148-154, 2013.

[4.23] Umboh MK, Adachi T, Oishi K, Higuchi M, Major Z. Effect of non-stoichiometric curing on dynamic compression properties of epoxy composites filled with nano-silica particles, *Abstracts Book of 8th Inter Symposium Impact Engineering*, p. 97, 2013.

[4.24] Umboh M.K., Adachi T., Oishi K., Higuchi M., Major Z., Mechanical properties of nano-silica particulate-reinforced epoxy composites considered in terms of crosslinking effect in matrix resins, *Journal of Materials Science*, Vol. 48, pp. 5148-5156, 2013.

[4.25] Bignotti F., Pandini S., Baldi F., De Santis R., Effect of the resin/hardener ratio on curing, structure and glass transition temperature of nanofilled epoxies, *Polymer Composites*, Vol. 32, pp. 1034-1048, 2011.

[4.26] Ward I.M., *Mechanical properties of solid polymers*, Second ed., New York, Wiley, 1990.

CHAPTER 5

CONCLUSIONS

5.1. Summary

This study proposed the different network structure by non-stoichiometric curing effects in matrix resin to explain the interaction effects between the particles and matrixes because the properties of micro- or nano-particles-reinforced epoxy composites are considerably dependent not only on the particle size effect but also on the interaction of particles and matrix resins. The main objectives of this study are to clarify experimentally the interaction effects between nano-particles and different network structure in matrix resins on the mechanical properties of nano-silica particulate reinforced epoxy composites. The mechanical properties: thermo-viscoelastic, elasticity, bending strength, compressive yield stress and fracture toughness are clarified by using different crosslinking density in matrix resin in order to elucidate the influences of the interactions between nano-silica particles and the matrix resins.

The matrixes were prepared by curing with an excessive mixture of diglycidyl ether of bisphenol A type epoxy resin to the curing agent (methyl-tetrahydro-phthalic anhydride) for the stoichiometric condition. The matrix resin was a blend of the diglycidyl ether of bisphenol A type epoxy resin, with methyl-tetrahydro-phthalic anhydride as the curing agent and 2,4,6-tris (dimethyl aminomethyl) phenol as the accelerator. The mixture ratio of the epoxide resin and the curing agent was changed to consider the interaction between the silica particles and the network structures in the matrix resin. The changed mixture ratio is hereafter expressed as the epoxy-equivalent-weight ratio (EEWR) defined by the epoxide resin weight over the stoichiometric epoxide resin weight in the mixture. In the research, the EEWR ranged from 1.0 to 3.2. Silica particles with a median diameter of 240 nm were used as the filler of the composite. The volume fraction of the silica particles was 0.2 for every composite. The surfaces of the particles were not chemically coated. The conclusion obtained in each chapter is summarized in Fig. 5.1.

In chapter 2, "*Thermo-viscoelastic and bending behaviors*", the interaction effects between nano-silica particles and epoxy network structures on thermo-viscoelastic and bending properties of epoxy composites were investigated by non-stoichiometric curing effects in matrix resin. The network structures of each neat epoxy resin and composite were appreciated by crosslinking densities of matrix resins and were characterized from the dynamic storage moduli of neat epoxy resins in a rubbery state. The glass transition temperatures of the neat epoxy resins and the composites were determined

from the temperature dependence of the loss tangents. It was found that the crosslinking densities of the matrix resins was from 2740 (stoichiometric condition) to 490 mol/m^3 and the glass transition temperatures of the neat epoxy resins decreased linearly as the crosslinking densities decreased from the stoichiometric condition. The interaction effects between nano-particles and network structures in matrix resin reduced the glass transition temperatures of the composite lower than those of the neat epoxy resins because the chain entanglement of the molecules in the matrix resin was considered to be encumbered by the particles. Both the bending moduli and the dynamic storage moduli in the glassy state of the composites were larger than those of the neat epoxy resins and decreased slightly as the crosslinking densities decreased from the stoichiometric condition. The interaction effects between the silica particles and the polymer network structure in the matrix resins did not affect either the bending moduli or the dynamic storage moduli in the glassy state of the composite because an elastic modulus is typically insensitive to microstructures in a material. The mobility of the molecules in the matrix resins became active above the glass transition temperature, and the interaction increased, so the dynamic storage moduli could not be predicted by the mixture law. The bending strengths were very sensitive to the microstructures, and the strengths for the composites were more sensitive than those of the neat epoxy resins because the existence of the nano-silica particles encumbered the entanglements of the molecular chains in the matrix resins having rough network structures with low crosslinking densities.

In chapter 3, "*Compression behavior*", the interaction effects between nano-silica particles and epoxy network structures on static and dynamic compression behaviors were discussed by non-stoichiometric curing effects in matrix resin using a material testing machine and a split Hopkinson pressure bar (SHPB) machine. The network structures of each neat epoxy resin and composite were appreciated by crosslinking densities of matrix resins where were obtained in Chapter 2. The static and dynamic compression tests were performed by using a universal material testing machine and a split Hopkinson pressure bar testing machine, where the strain rates were 3.3×10^{-3} to 1500 1/s. The compressive yield stresses of the composites and the neat epoxy resins having high crosslinking densities were larger than those having low crosslinking densities, although the strain rate effect on the compressive yield stresses of the neat epoxy resins were not affected by the crosslinking densities. The existence of nano-silica particles in the matrix resins prevented the yielding due to the interaction of the

particles and the network structures of the matrix resin. Although the strain softening of the neat epoxy resins after the yielding was larger for high strain rates, the strain softening of the composites after the yielding was not much larger even for higher strain rates because the existence of the nano-silica particles disturbed the release of the entanglements.

In chapter 4, "*Fracture toughness behavior"*, the interaction effects between nano-silica particles and epoxy network structures on Mode I fracture toughness was investigated and discussed by non-stoichiometric curing effects in matrix resin. The non-stoichiometric curing produced the different crosslinking densities in matrix resins where was obtained in Chapter 2. The fracture toughness of the composites and the neat epoxy resins were performed at room temperature to measure mode I fracture and were compared with the bending strength result in Chapter 2. Although the fracture toughness decreased monotonously from that of the stoichiometically cured resins as the crosslinking density decreased, the fracture toughness of the composites was maximum at a sligthly lower crosslinking density of approximately 2490 mol/m^3 from the stoichiometric condition, i.e., 2740 mol/m^3. The dependence of fracture toughness on the crosslinking density of composites differed greatly from that for neat epoxy resins. Fracture toughness and bending strength were improved from these of neat epoxy resins by adding particles to achieve crosslinking densities higher than 2000 mol/m^3. At crosslinking densities lower than 2000 mol/m^3, the particles worked against mechanical properties as defects in matrix resins. The improvements to toughness were more sensitive to crosslinking density than those of bending strength.

As summarizing the results in the dissertation, the interaction effects between nano-silica particles and network structures using non-stoichiometric curing process to produce different crosslinking density in matrix resin was effective to change the mechanical properties of nano-silica particulate-reinforced epoxy composites. The results show that the thermo-viscoelastic properties, bending properties, compression properties, and fracture properties were strongly dependent on interactions between nano-silica particles and network structures in matrix resins. The measured bending elastic moduli and dynamic storage moduli at glassy state of the composites agreed well with the results calculated from the experimental results of the neat epoxy resins with mixture law. This corresponds to the fact that an elastic modulus is generally insensitive to micro-structure in a material and tends to have average properties. The observed denoted improvements in bending strength, fracture toughness, and

compressive yield stress of composites compared with neat epoxy resins at high crosslinking densities in matrix resins where the improvements to toughness were more sensitive to crosslinking density than those of bending strength. The fracture toughness and the bending strength were improved for crosslinking densities higher than 2000 mol/m^3 by adding particles. At crosslinking density lower than 2000 mol/m^3, the particles worked against the mechanical properties as defects in matrix resins. Otherwise, in consideration to practically produce the epoxy composites with high strength and fracture toughness through non-stoichiometic curing process, the maximum fracture toughness of the composites can be resulted with crosslinking density approximately 2490 mol/m^3 from the stoichiometric condition, i.e., 2740 mol/m^3. Moreover, the interaction between the particles and matrix resins played an important role in mechanical properties of the composites

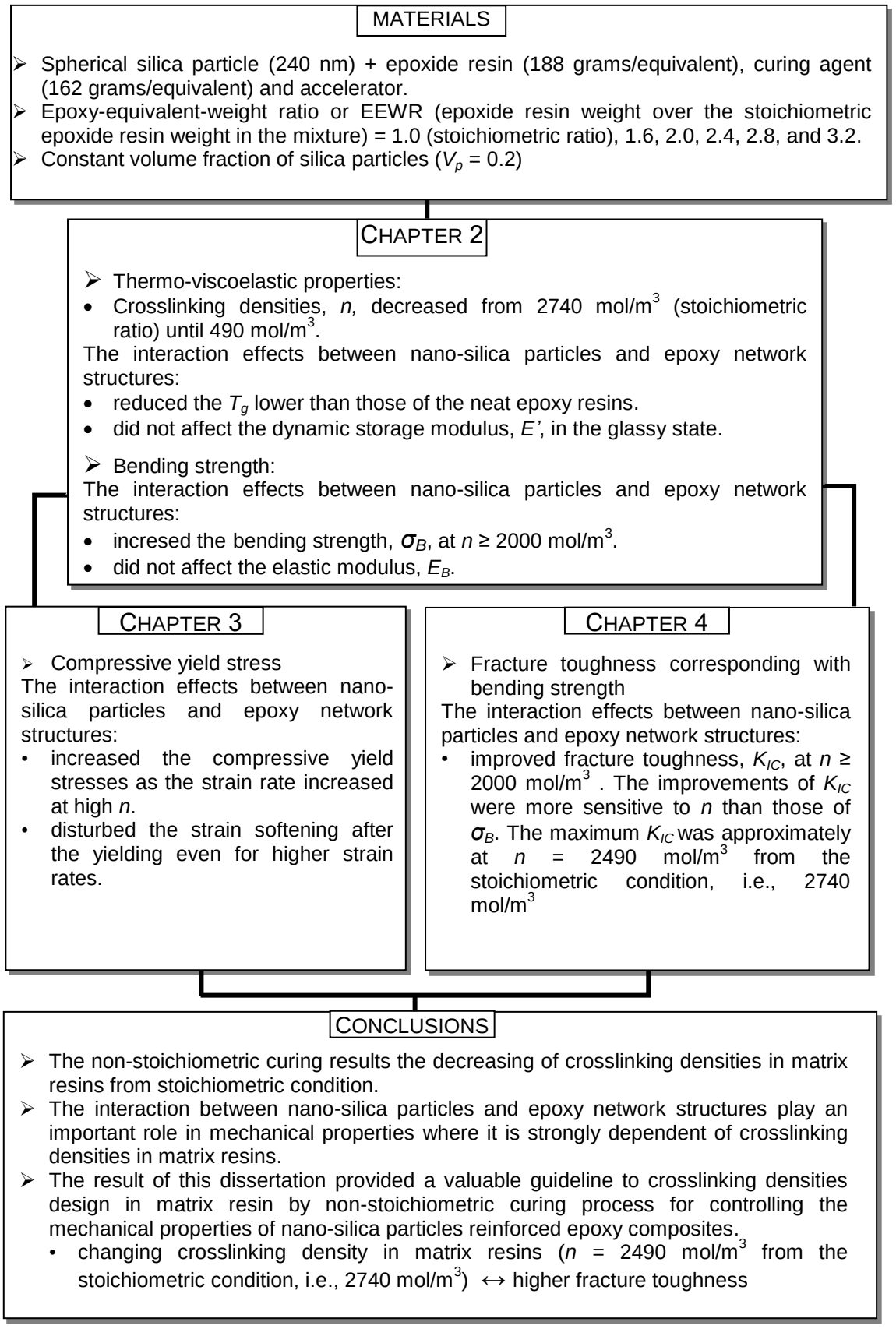

Fig. 5.1 Summary of conclusion

As the extended summary, the interactions between nano-silica particle and epoxy network structures on mechanical properties can be clarified by the relation between the normalized properties and the crosslinking density as shown in Fig. 5.2. This result shows that the bending elastic moduli did not have correlation with the interaction effects because the normalized properties of them were approximately constant to crosslinking densities. Moreover, the interaction effects on fracture toughness were more sensitive than those of bending strength in high crosslinking densities. The interaction effects of fracture toughness and bending strength could not be explained on the basis of reduced stress concentration near the particles or simple mixing of particles and matrix resin because the interaction effect on fracture toughness and bending strength with different crosslinking densities were not constant under fixed volume fractions of particles. To comprehend the interaction effects in nanocomposites, the illustration of the relation between nano-silica particles with different network structures of epoxy resin using non-stoichiometric curing process to produce incomplete network structures in matrix resins are shown in Fig. 5.3. There are four categories of the network structures: very fine, fine, rough and very rough network structures. This illustration can be used to understand the improvement on fracture toughness or bending strength of the composites to correlate with the interaction effects between nano-silica particle and different network structures in matrix resins as shown in in Fig. 5.4. This result shows that the composites with slightly smaller crosslinking density than that of the stoichiometric condition were clarified to greatly improve the fracture toughness due to the large interactive effect between the nano-particles and slightly incomplete network structures in the resins. The crosslinking densities in the matrix resins greatly contributed to fracture toughness due to stronger interaction between the matrix resins and nano-silica particles due to slightly incomplete network structures in the matrix resins. In contrast, the interactive effect between the particles and network structures in the matrix resins on bending strength of composites was relative small and the strength of the matrix resins mainly affected the strength of the composites. These results provided a valuable guideline to crosslinking densities design in matrix resin by non-stoichiometric curing process for controlling the mechanical properties of nano-silica particles reinforced epoxy composites due to interaction effect of particles and matrixes.

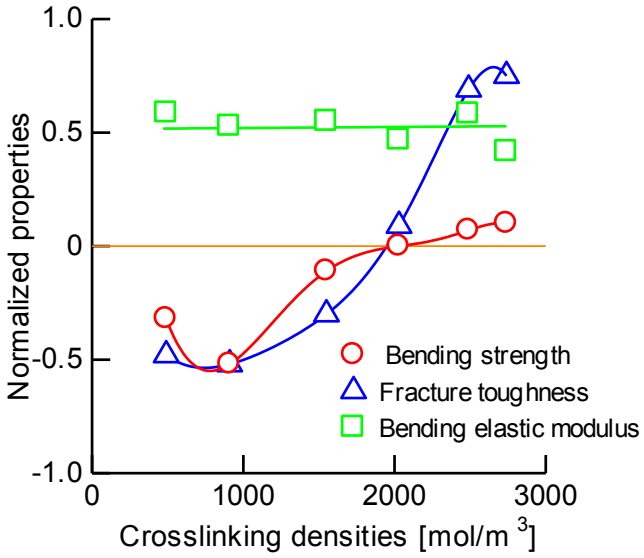

Fig. 5.2 Relation between normalized properties and crosslinking densities.

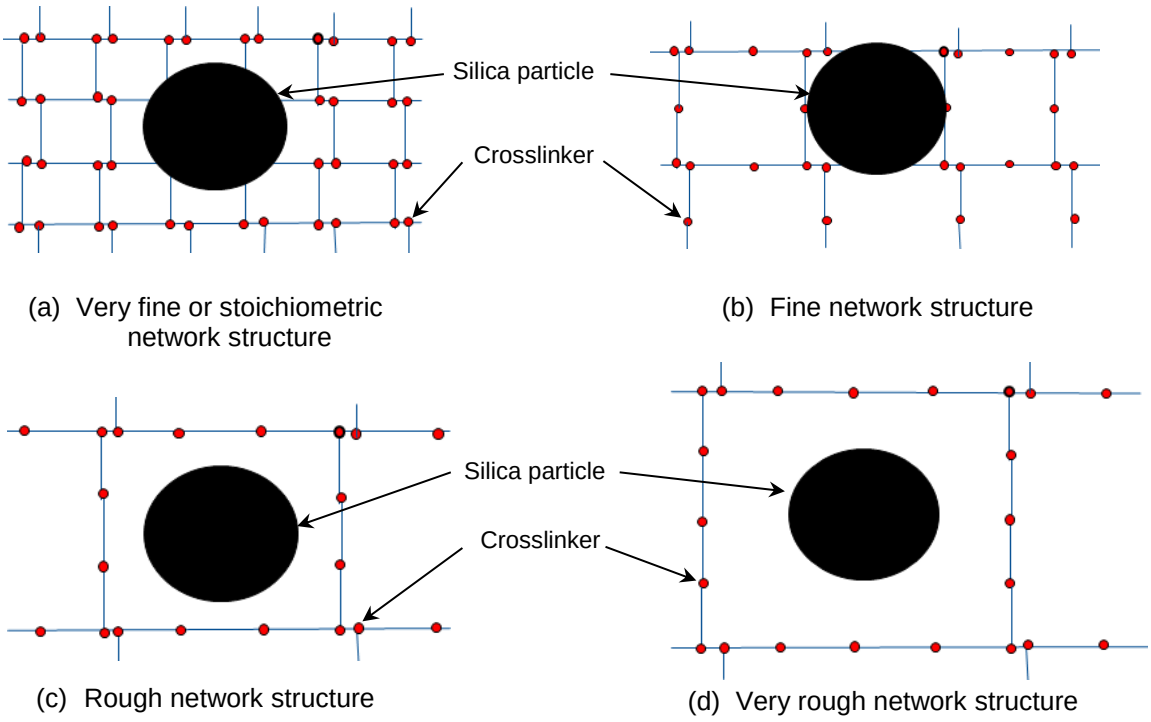

Fig. 5.3 Illustrations of the relation between nano-silica particles with different network structures of epoxy resin.

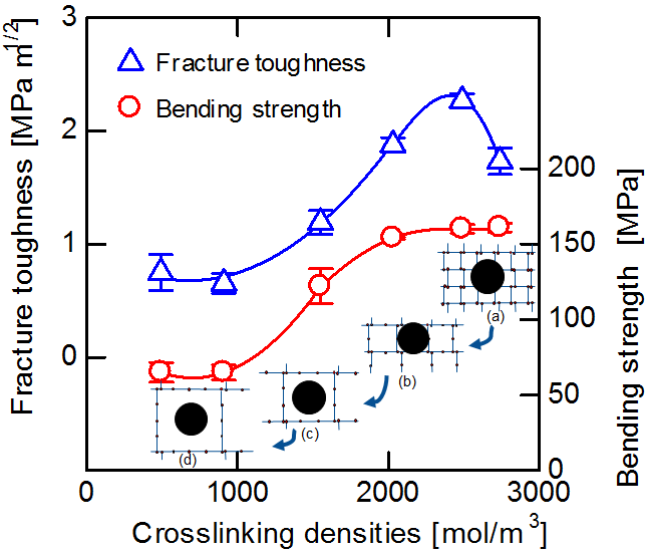

Fig. 5.4 Bending strength and fracture toughness of composites to correlate with the interaction effects between nano-silica particle and different network structures in matrix resins.

5.2. Future Works

The application and compatibility of silica particles reinforced epoxy composites, in terms of practicality and multi-functionality can be substantially improved by interaction between silica particles and epoxy network structures using non-stoichiometric curing process. For instances, this composite can be used in the structural materials for mobile phone, portable computer and batteries, also in high performance materials for nanoelectronic-devices and micro-sized sensor, etc.

Based on this research, the interactions between the particles and matrix resins played an important role to characterize the mechanical properties of nano-silica particles reinforced epoxy composites with various crosslinking densities in matrix resins. The non-stoichiometric curing process was designed to get the easy modification of network structures in the matrix resins without modification of the chemical nature of epoxy chains. Therefore, based on the discussions in this study, it could be interesting to study the mechanical behavior of the epoxy composites at various crosslinking densities with various particle sizes or various particle volume fractions to complete the clarification of interaction effects between nano-silica particles and epoxy network structures.

This research could be used as basis for developing multi-functional composites by controlling the crosslinking densities in matrix resins to clarify the interaction effects between the particles and matrix resins using non-stoichiometric curing process. Furthermore, in view of the fact that the most important industry sectors are conspicuously changed by the development and the application of new feature-rich nanocomposites, hence, the experimental results in this study can be used to improve the properties of nano-silica particles reinforced epoxy composite.

APPENDIXES

A. Properties of silica particles

The one of the most abundant materials in the earth crust is silicon, which especially in the crystalline form of quartzite, tridymite and cristobalite, and in an amorphous form of silica (or silicon dioxide) being synthesized industrially. Table A.1 summarized the physical, mechanical, thermal and electrical properties of the common silica.

Synthetic fused silica (amorphous silicon dioxide) is formed by chemical combination of silicon and oxygen, SiO_2 which is around 99.4 – 99.9 % purity of grade. Mostly fused silica is produced by reacting powdered crude metal with a gaseous flame mixture of hydrogen and hydrogen chloride in a fluidized bed. The initial product $SiHCl_3$ is fractionally distilled then reduced by hydrogen. Finally, it is deposited on a presilicon filament, which is heated to approximately between 1200 and 1500 °C then further purification is done by refining process [A.1].

Fused silica particle is primarily used to the electronic industry (around 70 % of the total market) as filler in electronic encapsulation materials, because a number of advantages [A.2–A.4]:

1. Excellent electrical insulation up to approximately 1000 °C
2. Low dielectric constant and loss
3. Extremely low coefficient of thermal expansion, which provides stability and resistance to thermal shock over large temperature
4. Wider thermal operating range
5. Increasing hardness and resistance to scratching
6. Extremely higher resistance to radiation darkening from ultraviolet, X-rays, gamma rays, and neutrons

Table A.1 Physical, mechanical, thermal and electrical properties of common silicon [A.4]

	Crystal structure			Amorphous structure
	Quartzite	Tridymite	Cristobalite	Fused silica
Density [kg/m^3]	2650	2300	2200	2200
Thermal conductivity [Wm^{-1}K]	1.3			1.4
Thermal expansion coeff. [10^{-6} K^{-1}]	12.3	21	10.3	0.4
Tensile strength [MPa]	55			110
Compressive strength [MPa]	2070			690 ~ 1380
Poisson's ratio	0.17			0.165
Fracture toughness [MPa]	-			0.79
Melting point [°C]	1830			1830
Modulus of elasticity [GPa]	70			73
Thermal shock resistance	High			High
Permittivity [ε'][A]	3.8 ~ 5.4			3.8
Loss factor [ε"][A]	0.0015			-
Tan δ [$\times 10^4$] [A]	3			-
Dielectric field strength [kV/mm] [A]	15 ~ 25			15 ~ 40
Resistivity [Ωm]	10^{12} ~ 10^{16}			> 10^{18}

[A] Dielectric properties at 1 MHz, 25°C

B. Non-stoichiometric calculation

The stoichiometric proportions of the curing agent (anhydride) and epoxide resin (DGEBA) are for ensuring maximum stability of the product but in many cases, the non-stoichiometric mixture ratio of epoxide resin to curing agent with or without fillers can result better mechanical properties as compared to stoichiometric mixture ratio of epoxide resin to curing agent. According to stoichiometric mixture ratio, the amount of anhydride used per hundred grams of DGEBA (phr) is calculated as follows [A.5]:

$$\text{Anhydride(phr)} = \frac{\alpha\beta}{\gamma} \times 100. \quad \text{(A.1)}$$

α is the constant for epoxy/anhydride system with value of 0.915 – 1.0 [A.6], β is the acid anhydride equivalent weight, and γ is the epoxy equivalent weight. The stoichiometric calculation in this research is shown below. The material specifications of epoxy resin and curing agent used in the calculations are listed in Table A.2. Regarding the accelerator, it is usually added at relatively low levels (0 to 5 parts per hundred of resin, phr).

Table A.2 Material specifications.

	Epoxy equivalent weight (grams/equivalent)
Epoxide Monomers	188
Curing Agent	162

Stoichiometric calculation (Epoxy-equivalent-weight ratio (EEWR) = 1.0):

α = 1.0

β = 162 grams/equivalent

γ = 188 grams/equivalent

Amount of anhydride used per one hundred grams of epoxide monomers is 86 grams. The percentage connection of epoxide monomers with curing agent in the epoxy system is (86/86)*100% = 100%

Non-stoichiometric calculation for EEWR = 1.6:

α = 1.0

β = 162 grams/equivalent

γ = 188 grams/equivalent

Amount of anhydride used per one hundred sixty grams of the blend is 138 grams. The amount of anhydride reserved of the blend is only 86 grams so the percentage connection of epoxide monomers with curing agent in the epoxy system is (86/138)*100% ≈ 60%

The percentage connections of epoxide monomers with curing agent for neat epoxy resins and composites at EEWR ranged from 1.0 to 3.2 are listed in Table A.3.

Table A.3 Percentage connection of stoichiometric and non-stoichiometric curing epoxide monomers with curing agent.

Materials	Matrix (weight ratio)			Epoxy-equivalent-weight ratio	Volume fraction of silica particles	Connection epoxide monomers with curing agent (%)
	Epoxide resin	Curing agent	Accelerator			
Neat epoxy resin	100	86	0.5	1.0	-	100
	160	86	0.5	1.6	-	60
	200	86	0.5	2.0	-	50
	240	86	0.5	2.4	-	40
	280	86	0.5	2.8	-	35
	320	86	0.5	3.2	-	30
Composite	100	86	0.5	1.0	0.2	100
	160	86	0.5	1.6	0.2	60
	200	86	0.5	2.0	0.2	50
	240	86	0.5	2.4	0.2	40
	280	86	0.5	2.8	0.2	35
	320	86	0.5	3.2	0.2	30

C. Dynamic mechanical analysis principle

Dynamic mechanical testers apply a periodic stress or strain to a sample and measure the resulting strain or stress response. Due to the time-dependent properties of polymers the resultant response is out-of-phase with the applied stimulus. As shown in Fig. A.1, when a sinusoidal stress, $\sigma(t)$ with amplitude σ_o is applied at some frequency, *f*, polymers will behave neither as a perfectly elastic nor as a perfectly viscous, and the strain, $\varepsilon(t)$, will lag behind excitation, namely phase lag δ will occur. Therefore, by using strain amplitude, ε_o, a complex dynamic modulus, *E** is defined as [A.5, A.7],

$$E^* = \frac{\sigma(t)}{\varepsilon(t)} = \frac{\sigma_o}{\varepsilon_o}\exp(i\delta) \tag{A.2}$$

where *t* is the time, and *i* = $\sqrt{-1}$.

The *E** is the instantaneous ratio of the stress amplitude to the strain amplitude. It can be resolved into a real component denoted as storage modulus, *E'*, and an imaginary component denoted as loss modulus, *E"*;

$$E^* = E' + E'' \tag{A.3}$$

where

$$E' = \frac{\sigma_o}{\varepsilon_o}\cos\delta, \quad E'' = \frac{\sigma_o}{\varepsilon_o}\sin\delta.$$

The *E'* is the in-phase or elastic response (this being the recoverable or stored energy), but the *E"* is the imaginary or viscous response (this being proportional to the irrecoverable or dissipated energy). The tan δ is proportional to the ratio of energy dissipated to energy stored. This is called the loss tangent or damping factor.

$$\tan\delta = \frac{E''}{E'}. \tag{A.4}$$

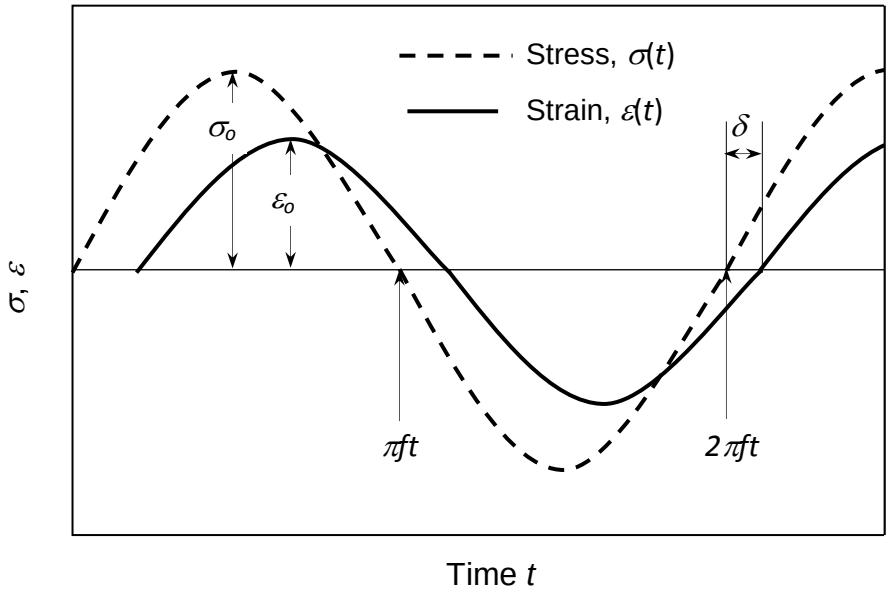

Fig. A.1 Sinusoidal oscillation and response of viscoelastic material.

References

[A.1] Kwon S.Ch., *Mechanical behaviors of nano- and micro-silica particles reinforced epoxy composites*, Doctorial Thesis, Tokyo Institute of Technology, 2006.

[A.2] Ke Y.C., Stroeve P., *Polymer-layered silicate and silica nanocomposites*, Elsevier Science, Amsterdam, 2005.

[A.3] Otterstedt J-E., Brandreth D.A., *Small particles technology*, Plenum Press, New York, 1998.

[A.4] Devine R.A.D., Duraud J-P., Dooryhee E., *Structure and imperfections in amorphous and crystalline silicon dioxide*, John Wiley & Sons, New York, 2000.

[A.5] Haris A., *Mechanical properties of blended epoxy resins containing two monomers with different molecular weights*, Doctorial Thesis, Tokyo Institute of Technology, 2008.

[A.6] Shimbo, M., Basic properties of cured material. In *Handbook of Epoxy Resin*, Shimbo, Nikkan Kogyo Shinbunsha, Tokyo, 1987. (in Japanese).

[A.7] Nielsen L.E., *Mechanical properties of polymers and composites*. Marcell Dekker, New York, 1994.